**Climate Change Effects on the Sacramento Basin's Flood Control Projects**

By

ANN DENISE FISSEKIS
B.A. (University of Southern California) 2002

THESIS

Submitted in partial satisfaction of the requirements for the degree of

MASTER OF SCIENCE

in

Civil and Environmental Engineering

in the

OFFICE OF GRADUATE STUDIES

of the

UNIVERSITY OF CALIFORNIA

DAVIS

Approved:

______________________________________

______________________________________

______________________________________

Committee in Charge

2008

Table of Contents

**Abstract**

Increasing temperatures are likely to affect flood control operations in the Sacramento Valley. Snowpack storage will decrease and the fraction of rain in storm events will increase. Reservoirs with flood control objectives manage floods using static rule curves that define how much water can be stored and the rate at which it can be released from the dam. Studying the effect of climate change, and, in particular, increasing temperatures, on the Shasta, Oroville and New Bullards Bar dams' flood control operations illustrates that static flood control curves perform poorly in changing climates. Two reservoirs, Shasta and Oroville, have dynamic curves that improve each dam's flood control and storage abilities. The existing flood control rule curves are based on historic data from the first half of the 20th century and should be updated to account for past and projected changes to the hydrologic regime.

## Chapter I. Introduction

When dams with flood control objectives are built, a flood control operations curve is created to guide (or often restrict) water managers' flood operations at any time during the year. These flood control curves, or rule curves, define the maximum allowable reservoir pool elevation against day of the year and represent the balance between flood control and water supply objectives for each dam. The maximum allowable pool elevation is established using the historical hydrologic record; physical constraints, such as downstream channel capacity; and functional constraints, such as the water supply, hydropower and other dam objectives. Because most of California's dams were built in the mid-1900s, the historical record used to create rule curves includes only the first half of the 20th century (Townsley, personal communication, 2007). While hydrologic trends have changed since that period (Collins and Whitin 2004, Saunders et al. 2008), the rule curves have not been updated to reflect this new hydrology (Countryman, personal communication, 2007). And while the existing rule curves may accommodate past changes, climate change projections provide an additional challenge for the 20th century technology. In most of the West, especially Washington, Oregon and California, snow is the largest component of seasonal water storage, making the West's water storage vulnerable to climatic variations and changes that influence fractions of snow in winter precipitation (Barnett et al. 2008, Regonda et al. 2005) and spring snowpack volumes and runoff timing (Mote et al. 2005). The West is being affected by climate change more than other parts of the United States outside of Alaska (Saunders et al. 2008). Several studies have identified the watersheds in the Northern Sierra Nevada as the most sensitive to short-term climate change and warming temperatures (Cayan et al. 1993, Knowles et al. 2006, Medellin et al. 2008, Mote et al. 2005, Regonda et al. 2005, Saunders et al. 2008). As California receives little runoff between June and October, adapting to changes in peak flow timing and snowmelt runoff is not only crucial to reserve an adequate supply of water into the summer and fall, but also to ensure adequate flood storage. The combination of a greater flood risk with reduced natural storage threatens to exacerbate the tension between flood control and storage priorities for many western reservoir managers (Knowles et al. 2006). This study explores the effects of climate change on flood control operations for three basins in the Northern Sierra Nevada: the Upper Sacramento River above Shasta Dam, the Feather River above

Oroville Dam, and the North Yuba River above New Bullards Bar Dam. Existing rule curves for these dams will be tested against a range of climate change scenarios projected for the study basins to assess the ability of existing rule curves and reservoirs to accommodate or adapt to a warmer climate.

## Chapter II. Background

*Basin hydrology*

The Upper Sacramento River above Shasta Dam, the Feather River above Oroville Dam, and the North Yuba River above New Bullards Bar Dam are in the northern part of California's Central Valley (Figure 1). While the size and elevation range varies for each basin, their general hydrologic characteristics are similar (Table 1). The climate in these study areas is distinct from winter to summer. Winters are wet, with 90 percent of the total annual precipitation occurring in 2 to 3 months during the period between November and April. While some snow accumulates at elevations above 5,000 ft (1524 m) during the wet months, storms predominately consist of rain as winter temperatures occur near or above the freezing point. If warm temperatures accompany a storm, rain can occur at the highest elevations. Likewise, if temperatures are cold, snow can fall on the valley floor (USACE 1977, USACE 2004, USACE 2005). The areas above Shasta, Oroville and New Bullards Bar are studied because their relatively low elevation distributions, illustrated by area elevation curves, make them sensitive to small climate shifts (Figure 2). The amount and timing of runoff are influenced by climatic variables, such as precipitation and temperature, as well as nonclimatic factors, such as lithology, soil and vegetative conditions (Aguado et al. 1992). In this study, only past and projected changes pertaining to temperature and precipitation are examined. Other changes, such as past and projected land use trends, are neglected.


**Figure 1. Major watersheds that drain the western slope of the Sierra Nevada into the Sacramento-San Joaquin Valley.** The polka-dotted areas indicate elevations above 5000ft, a crude estimate of the rain-snow boundary elevation. If warm temperatures accompany a storm, rain can occur at the highest elevations. Likewise, if temperatures are cold, snow can fall on the valley floor. The Upper Sacramento and Feather rivers are the most northern basins on the map. New Bullards Bar is located within the Yuba River watershed and abuts the southern boundary of the Feather River watershed (Figure taken from Collins and Whitin 2004).

| Characteristic | Outlet point and basin characteristics | | |
|---|---|---|---|
| Site name | 1. Sacramento River at Shasta | 2. Feather River at Oroville | 3. North Yuba River at New Bullards Bar |
| Latitude | $40^{o}43'$N | $39^{o}22'$N | $39^{o}23'$N |
| Longitude | $122^{o}25'$W | $121^{o}39'$W | $121^{o}08'$W |
| Drainage area ($mi^2$) | 6421 | 3611 | 489 |
| Mean basin elevation (ft) | 4576 | 5030 | 4898 |
| Max basin elevation (ft) | 14116 | 10,466 | 8500 |
| Min basin elevation (ft) | 587 | 900 | 1825 |
| Mean annual runoff (Thousand Acre Feet) | 5737 | 4547 | 1258 |
| Gross reservoir storage capacity (TAF) | 4552 | 3538 | 966 |

**Table 1. General basin characteristics for the watersheds above the study reservoirs (USACE 1977, USACE 2004, USACE 2005).**

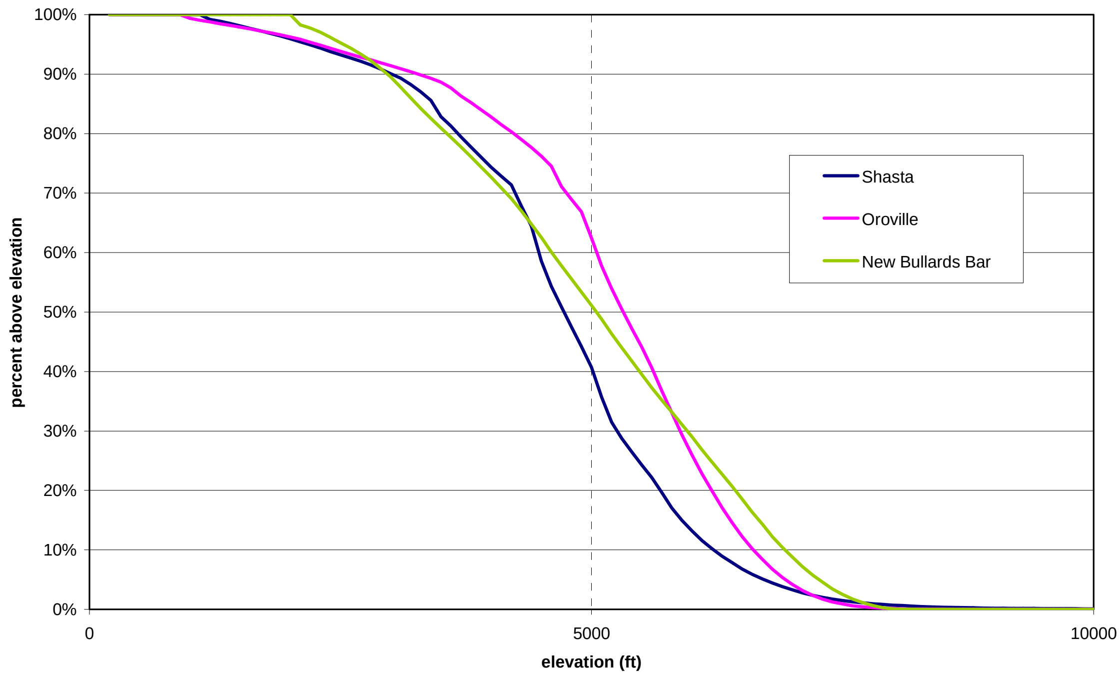


**Figure 2. Area elevation curves for the three study basins.** Precipitation that falls in elevations above 5000 ft. generally falls as snow; precipitation that falls in areas below 5000 ft. generally consist of rain.

*Basin rule curves*

Two key components of a basin's flow regime that help define its rule curve are the timing and magnitude of seasonal runoff. The rule curve illustrated in Figure 3 describes the flood control requirements for Oroville Dam. The negatively sloped segment indicates the early period of the flood season when water managers must prepare for large inflows by increasing the flood control space reserved in the dam. The horizontal section of the curve indicates the flood season when frequent storm events could potentially cause flooding. The positively sloped section defines the transition from the flood season to the conservation season. During this period, water managers can allow the reservoir to fill and store water for use during the dry season from late summer through autumn.

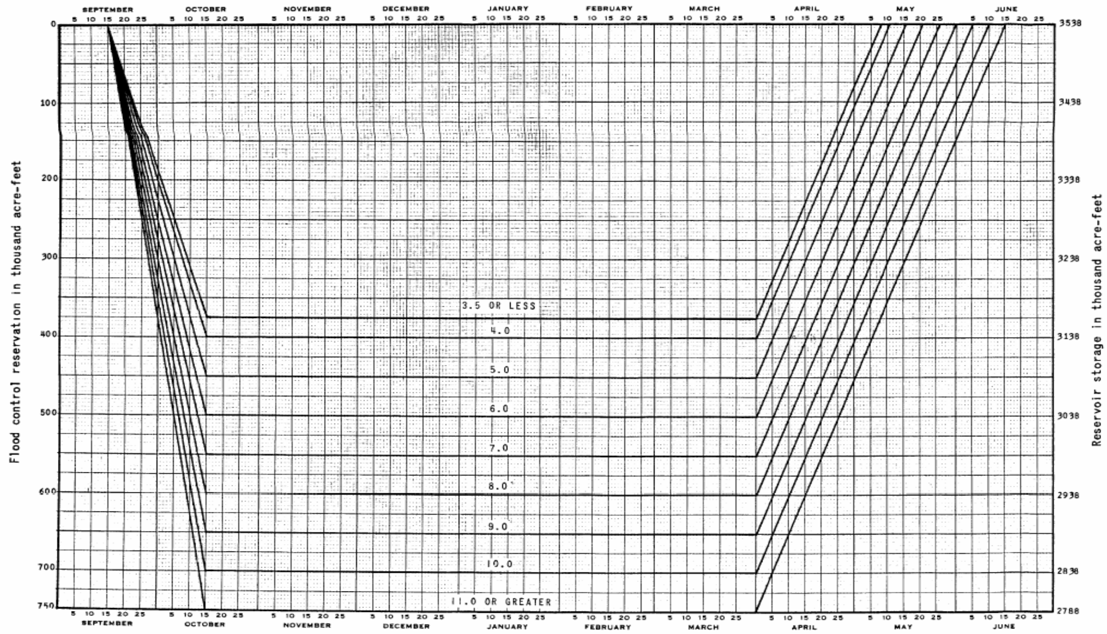


**Figure 3. The flood control diagram for Oroville Dam.** Each line represents allowable storage requirements based on seasonal precipitation. In this diagram, the alternative curves allow water managers some flexibility in the release volumes, but no flexibility for refill timing (USACE 2005).

Each rule curve was developed as each dam was constructed and was based on the basin's hydrologic record; physical constraints, such as downstream channel and outlet works capacity; and functional constraints, such as the water supply, hydropower and other dam objectives. The method originally used to create rule curves is best described as trial and modify. After the Corps gained some experience creating rule curves, a master manual providing an overview of reservoir regulation was published (USACE 1959). Combining the trial and modify approach with the guidelines described in the master manual, some flood control curves were updated. The flood rules were scheduled to be reviewed and updated if necessary on a three- to five-year cycle. In the 1990s, a lawsuit prevented the Corps from updating the Oroville rule curve without developing a National Environmental Policy Act document to support the revision. This ruling also applied to all reservoirs that reserve federal flood space, whether they are owned by the Corps or not. This NEPA documentation proved to be costly and beyond the scheduled funding established for updating the manuals. Hence, flood rule curves have not been updated for at least 15 years (Countryman, personal communication, 2008).

Oroville Dam's rule curve was last updated in 1971 and includes a state parameter that allows water managers to store more water in the reservoir during dry years; the reservoir pool elevation must be drawn down further during wetter years. This state parameter is determined by the basin's geomorphology and directly relates to seasonal inflow volumes. Oroville Dam's state parameter is based on each season's observed precipitation. Parameters are computed daily from the weighted accumulation of season basin mean precipitation by multiplying the preceding day's parameter by 0.97 and adding the current day's precipitation (USACE 1971). For example, if the computed parameter is 3.5 inches or less, reservoir needs to be drawn down to the volume defined by the top line on the chart. While the magnitude of releases varies, the start date when spring refill begins does not. Unfortunately, the current curve reflects a refill schedule that coincides with historical snow-melt timing; Oroville is a rain-flood dominated basin with relatively little snowpack. The refill period does not take advantage of the rainfall runoff characteristics of the basin. Furthermore, the rate of refill does not vary – in years with little precipitation, the reservoir must be filled at the same rate as in years with above-normal precipitation. Finally, the likelihood of forecasted precipitation is not considered (USACE 2005).

Shasta Dam's rule curve also incorporates a state parameter, though its parameter is not based on precipitation as Oroville Dam's curve is (Figure 4). Shasta Dam's state parameter is based on cumulative seasonal inflow to the reservoir. Also, while Oroville Dam's curve provides flexibility in the initial draw down volume, Shasta Dam's curve does not. Shasta's curve requires that the flood control pool be drained to allow 1.3 MAF of flood pool space each December. However, some flexibility is incorporated into the refill schedule. Shasta Dam's water managers may begin refilling the conservation pool as early as December 25. This refill schedule better reflects the rain-flood dominated hydrology of this basin (Countryman, personal communication, 2007) as it allows water managers to fill the conservation pool using winter rainfall runoff rather than waiting for the spring snowmelt runoff. Finally, the rate of refill varies depending on the seasonal inflow volume. When inflow volumes are low, water managers can refill the conservation pool at a faster rate than if inflow volumes are high. Similarly to Oroville Dam's rule curve, no climate forecasts are considered. Shasta Dam's curve was last revised in 1977 (USACE 1977).

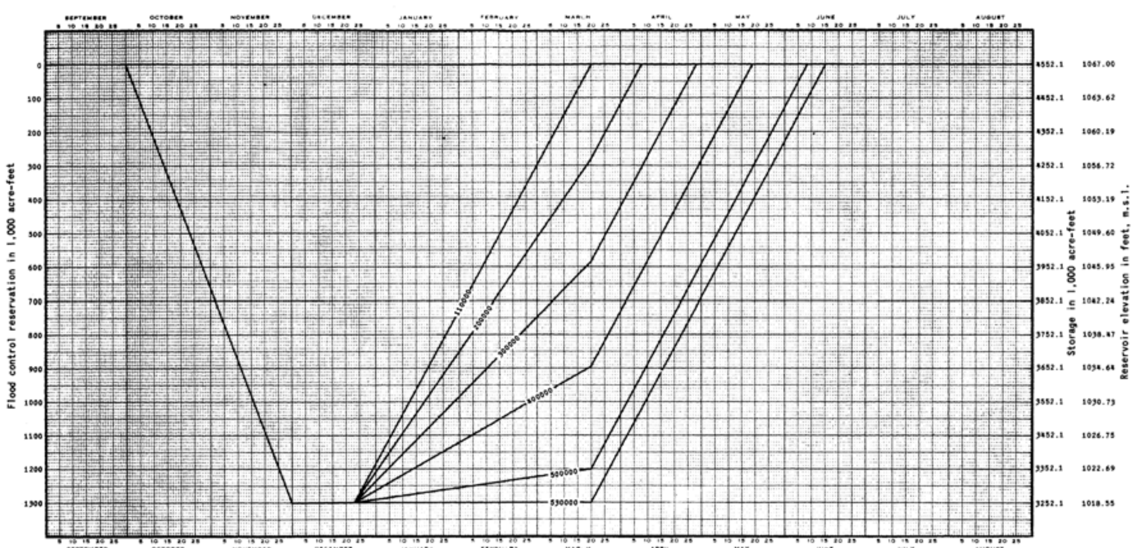


**Figure 4. The flood control rule curve for Shasta Dam on the Upper Sacramento River.** This rule curve requires the reservoir to draw down to the same level ever year. However, the refill schedule begins during the rainflood season, when the majority of basin runoff occurs. Rates of refill vary depending on the volume of seasonal inflows (USACE 1977).

New Bullards Bar Dam's rule curve provides no flexibility in either its release or refill requirements (Figure 5). No state parameter is incorporated into the curve – the same pool elevation must be maintained regardless of whether the season is wet or dry. Also, the rate of refill is fixed. Again, the likelihood of future precipitation events is not considered. Finally, the refill schedule begins during typical snow-melt periods and does not take advantage of the rainflood runoffs characteristics that are similar to the Feather River.

One unusual feature of the flood control operations described in the New Bullards Bar water control manual is that they are linked to the operation of Marysville Dam. For example, the downstream channel capacity constraints take into consideration how the Marysville Dam would also affect channel flow volumes. Marysville Dam was never built; the flood control operations of New Bullards Bar Dam are partially defined by another major flood control project that does not exist. The original curve created for New Bullards Bar, which accounts for the construction of Marysville Dam, was approved in 1978 and is still operational (USACE 2004).

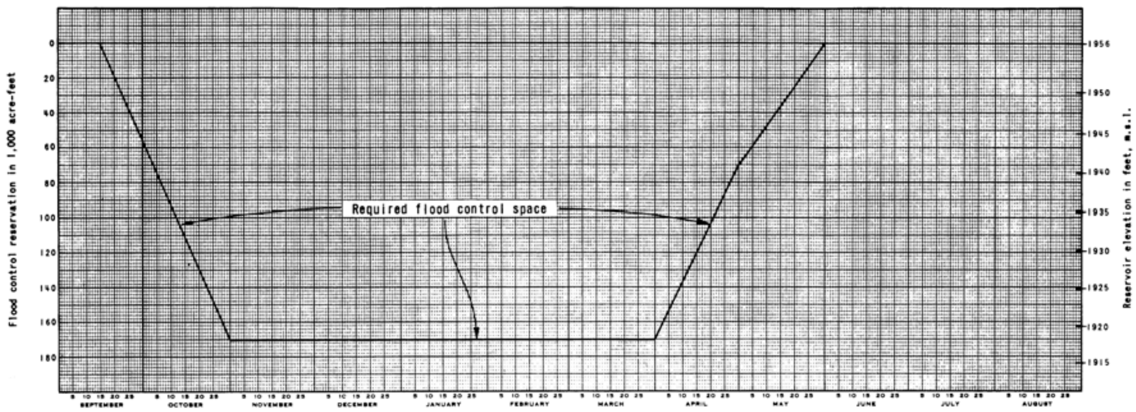


**Figure 5. New Bullards Bar flood control rule curve.** This basic curve does not include any state parameters that could add flexibility to the release and refill schedule (USACE 2004).

## Chapter III. Climate Change

Currently observed global hydrologic trends include a shift in overall hydrologic conditions since the mid-20th century with significant effects on flood management (IPCC 2007). To examine how global trends correlate to regional trends, several studies focusing on the western United States and the Northern Sierra Nevada have evaluated past and projected climate change patterns and how those patterns affect hydrologic regimes (Barnett et al. 2008, Bonfils et al. 2006, Collins et al. 2004, Kim et al. 1998, Knowles et al. 2006, McCabe and Clark 2005, Miller et al. 2003, Mote et al. 2005, Mote 2003, Regonda et al. 2005, Saunders et al. 2008, Zhu et al. 2007). These studies focus on temperature, precipitation and flow regime changes.

### *Temperature Literature Review*

Temperature trends that exceed the boundaries of natural variability are frequently used as evidence of climate change. Floods are sensitive to temperature changes as they affect fractions of rain versus snow in precipitation composition and the timing of snowmelt runoff. Given that the sensitivity of flooding to temperature variations is potentially different for basins with different temperature regimes, the mid to low elevation basins in the West are recognized as the areas most sensitive to initial shifts in baseline temperatures (Lettenmaier and Gan 1990; Hamlet and Lettenmaier 2007, Knowles et al. 2006, McCabe and Clark 2005, Mote 2003). Understanding the reasons for the Sacramento River basins' sensitivity and the magnitude of these changes explains why the study basins can provide a useful glimpse into the short term response of mid to low elevation basins to small temperature shifts.

When compared to the $20^{th}$ century average, the West has experienced an increase in average temperature during the last five years that is 70 percent greater than the global trend (Saunders et al. 2006). While five years may be too short a period over which to identify long-term trends, analyses of longer periods of record yield similar results. Trends in temperature are “overwhelmingly” positive for the period between 1950 and 1997, increasing at a rate of $3^{o}$F/century ($1.6^{o}$C/century) (Mote et al. 2005). Hamlet and Lettenmaier (2007) examined areas including the Pacific Northwest, California and Nevada and compared the rate of temperature increase from 1916 to 2003 to the rate of temperature increase from 1947 to 2003. The rate during the last half of the century is roughly double that of the longer period, indicating that trends over the past few decades are diverging from long-term signals.

But these temperature changes are not detected uniformly. Rather, the changes are specific to region, elevations and ranges of temperature (Maurer 2007, Knowles and Cayan 2004). Minimum temperatures have increased more than maximum temperatures for the same basins from 1949 to 2004: minimum temperatures have increased an average of $2.5^{o}$F ($1.4^{o}$C) compared to $1.8^{o}$F ($1.0^{o}$C) for maximum temperatures (Knowles et al. 2006). Higher minimum temperatures mean that critical freezing temperatures are most affected by regional warming. Trends are strongest in the Northern Sierra Nevada and Pacific Northwest, where winter temperatures are closer to the melting point. In these regions in particular, modest shifts in temperature can force large shifts in a basin’s hydrologic response (Knowles et al. 2006, Regonda et al. 2005, Saunders et al. 2008).

Increasing temperatures directly affect some key hydrologic characteristics. Regional trends in surface temperature modify the volume, intensity or type of precipitation and seasonal timing of streamflow (Regonda et al. 2005). Rising temperatures raise the elevation of the snowline; snow that used to accumulate at lower elevations becomes rainfall runoff, resulting in less long-term snowpack storage and increased runoff volumes (Kim et al. 1998, Droz et al. 2002). In the West, warming has already reduced the fraction of precipitation falling as snow from 1949 to 2004 and, consequently, increased the fraction falling as rain and reduced volumes naturally stored in the snowpack (Knowles et al. 2006). Temperatures also affect the duration of water storage in the snowpack. Warming produces lower snow-water equivalents (SWE), largely by increasing the frequency of melt events, not by simply enhancing the fraction of rain versus snow (Mote et al. 2005). As temperatures increase, melted snow is stored unfrozen in the pores of the snowpack. When the pores in the snowpack are saturated, the snowpack is “ripe.” High temperatures also cause the snowpack to ripen more quickly and run off faster than low temperatures (Mount 1995). Much of California’s warming has occurred during the winter, though, and so more of an effect is expected in the ratio of rain to snow and less effect is expected from early snowmelt (Regonda et al. 2005, Knowles et al. 2006).

Some debate exists over the correct attribution of the observed temperature increases. Some researchers suggest that the consistency of spatial patterns with climate trends and the elevational dependence of trends with declining snowpack trends are climate related (Mote et al. 2005). However, whether the changing climate trends are greenhouse gas-driven or fall within the range of natural variability is still debated (Mote et al. 2005, Barnett et al. 2008, Mote 2003, McCabe and Clark 2005). Even the question of whether natural variability is static or shifting is debated (Milly et al. 2008). Milly et al. (2008) argue that natural variability may not be limited to a static range of possible trends. The range of possible trends may change naturally over time. However, even if climate change is driven by "shifting" natural variability, rule curves are not designed to accommodate these shifts. While increasing temperatures trends may not persist, static rule curves are not designed to address any temperature trend changes. No matter the cause of temperature increases, changes in water management practices are needed to adapt to the altered hydrologic regime (Barnett et al. 2008, Regonda et al. 2005).

*Precipitation Literature Review*

While significant agreement exists that observed and projected temperature trends are increasing for the Northern Sierra Nevada, far less is known about changes to precipitation. Current climate models disagree about whether overall precipitation levels in the West are likely to increase or decrease (IPCC 2007, Saunders et al. 2008, Vanrheenen 2004). Where changes have been identified, trends have all fallen within the bounds of natural variability (Barnett et al. 2008, Hamlet and Lettenmaier 2007). Furthermore, even if precipitation increases, those changes may not be enough to overcome temperature-driven effects such as decreased snow-water equivalents (SWE) (Mote et al. 2005, Mote 2003, Regonda et al. 2005). Precipitation changes are expected to be uniform across elevation bands in each basin (Mote 2003, Regonda et al. 2005, Saunders et al. 2008).

Although changes in the overall amount of precipitation are currently uncertain, general agreement exists over the change in precipitation composition (i.e. snow vs. rain) as well as the understanding that those changes are temperature-driven. Between 1950 and 1999, the character of mountain precipitation shifted, with more winter precipitation falling as rain instead of snow (Barnett et al. 2008, Regonda et al. 2005). The shift towards more rainfall runoff has been accompanied by consistent declines in monthly SWE, with the largest declines in the Cascades and the northern Sierra Nevada (Mote et al. 2005, Regonda et al. 2005).

*Hydrology Literature Review*

The effects of past temperature and temperature-driven precipitation changes have affected the timing and magnitude of river flows. These runoff pattern changes are symptoms of decreased snowpack, increased frequency of winter flooding, reduced summer baseflows, and increased competition for over-allocated water resources (IPCC 2007, Regonda et al. 2005). Runoff patterns have changed suddenly, as a step change rather than gradually, indicating that periodic reviews of the curves to adapt to sudden changes may be worth considering (McCabe and Clark 2005). Until the late 20$^{th}$ century, flood control curves were scheduled for review on a three- to five-year cycle.

In the Northern Sierra Nevada, the average amount of water stored on April 1 as snow that ultimately drains towards the Sacramento-San Joaquin River system is about 10.1 MAF, more than twice the total capacity of Lake Shasta (4.6 MAF), the largest man-made reservoir in California (Maurer 2007). While total annual runoff has not changed, shifts in the timing of snowmelt and the magnitude of winter storm runoff have occurred. However, runoff pattern changes differ depending on the basin elevation. Above 8200 ft

(2500 m), snowmelt timing has shifted approximately 10 to 20 days earlier for many rivers in the western U.S. (McCabe and Clark 2005, Saunders et al. 2008) and runoff volumes between April and July have decreased (Cayan et al. 1993, Collins 2004, McCabe and Clark 2005, Peterson et al. 1999, Regonda et al. 2005). Below 8200 ft (2500 m), little change in snowmelt timing is evident (Regonda et al. 2005), but SWE have declined between 50 and 75 percent since 1950 (Mote 2005, Saunders et al. 2008). The strongest shift is observed in the Sierra Nevada, where half of the snow-covered regions have elevations between 4500 ft (1371 m) and 6000 ft (1829 m) (Cayan et al. 1993, Peterson et al. 1999).

*Water Management Literature Review*

Some efforts have been made to create reservoir rule curves that can adapt to changing and unpredictable conditions. Research efforts have focused on incorporating short and long-term forecasts into operational procedures, integrating all dam objectives into a comprehensive decision-making paradigm, and optimizing curves based on water supply goals at the end of the flood season. Each of these efforts identifies different ways to revise rule curves for dams in California and the Pacific Northwest that yield improvements over the existing operation methods. Regardless of their recommendations, all researchers agree that the existing static rule curves will not adapt well to changing hydrologic conditions (Medellin et al. 2008).

One improvement incorporates global climate model (GCM) forecasts into the management of Folsom Dam on the American River in the Sacramento Basin. Results show a variable gain in management benefits when GCM data is incorporated into operational forecast scenarios. Benefits from including GCM data in reservoir operations resulted mainly during high flow periods (Carpenter and Georgakakos 2001). However, forecasts alone do not result in improved reservoir management – forecasts must be used in conjunction with dynamic operational practices (Yao and Georgakakos 2001). Yao and Georgakakos (2001) looked at the value of using both the existing rule curve and a dynamic, adaptive management rule curve for Folsom Dam. Reservoir performance substantially benefits from adaptive management decisions rather than the existing static curves.

Going beyond the operation of a single dam, Georgakakos et al. (2005) developed the Integrated Forecast and Reservoir Management (INFORM) project that integrated system operations for primary reservoirs in Northern California, including Folsom, Oroville and Shasta dams, and added climate model forecasts to the operational data. Average energy production increases up to 15 to 18 percent and unnecessary spillage decreases by 50 percent without increasing flood damage; the amount of water supply available for agricultural, municipal and environmental uses also increases with the incorporation of GCM forecasting to integrated reservoir management. Existing rule curves need to be replaced with a more dynamic system. Without updating rule curves to incorporate more flexibility, including GCM forecasts in water management operations will not improve reservoir management and will increase the risk of costly failure (Georgakakos et al. 2005).

Replacing all existing rule curves with a dynamic, integrated system may not be realistic for all agencies involved in water management. Lee et al. (2006) explored possible improvements for existing rule curves by optimizing their refill schedules and drawdown volumes for floods and water supply. Flood rule curves are optimized for the Columbia River Basin given a 2$^{o}$C step increase to the basin's historical temperature record. Existing curves do not adapt to the shift in flow timing due to increased winter rainstorm runoff and earlier spring snowmelt. However, when curves are updated to address the changed flow regime, there is a robust decrease in storage deficits without increased flood risk (Lee et al. 2006).

## Chapter IV. Data and Methods

The goal of this study is to test flood control rule curves for Shasta, Oroville and New Bullards Bar dams against a range of climate change scenarios projected for those regions. Details regarding the models and data used to accomplish that goal are discussed in the sections below; an overview is provided here (Figure 6).

Regional climate change projections for the three study basins are determined based on downscaled and bias-corrected global climate model (GCM) projections. A likely range of temperature and precipitation changes projected for the year 2025 is determined statistically to provide a possible range of climate changes against which to test reservoir operations. As this work mainly focuses on the basins' sensitivity to climate change, quantifying exact climate projections for the study basins is unnecessary. The statistically determined climate changes are applied to forty-year records of observed temperature and precipitation for the study basins. Once the historical temperature and precipitation records are perturbed, they are input to the National Weather Service River Forecast System (NWS-RFS) to model reservoir inflows over the forty-year period given different climate scenarios. These inflows are then used to test each reservoir's rule curve using the Hydrologic Engineering Center Reservoir Simulation (ResSim) model.

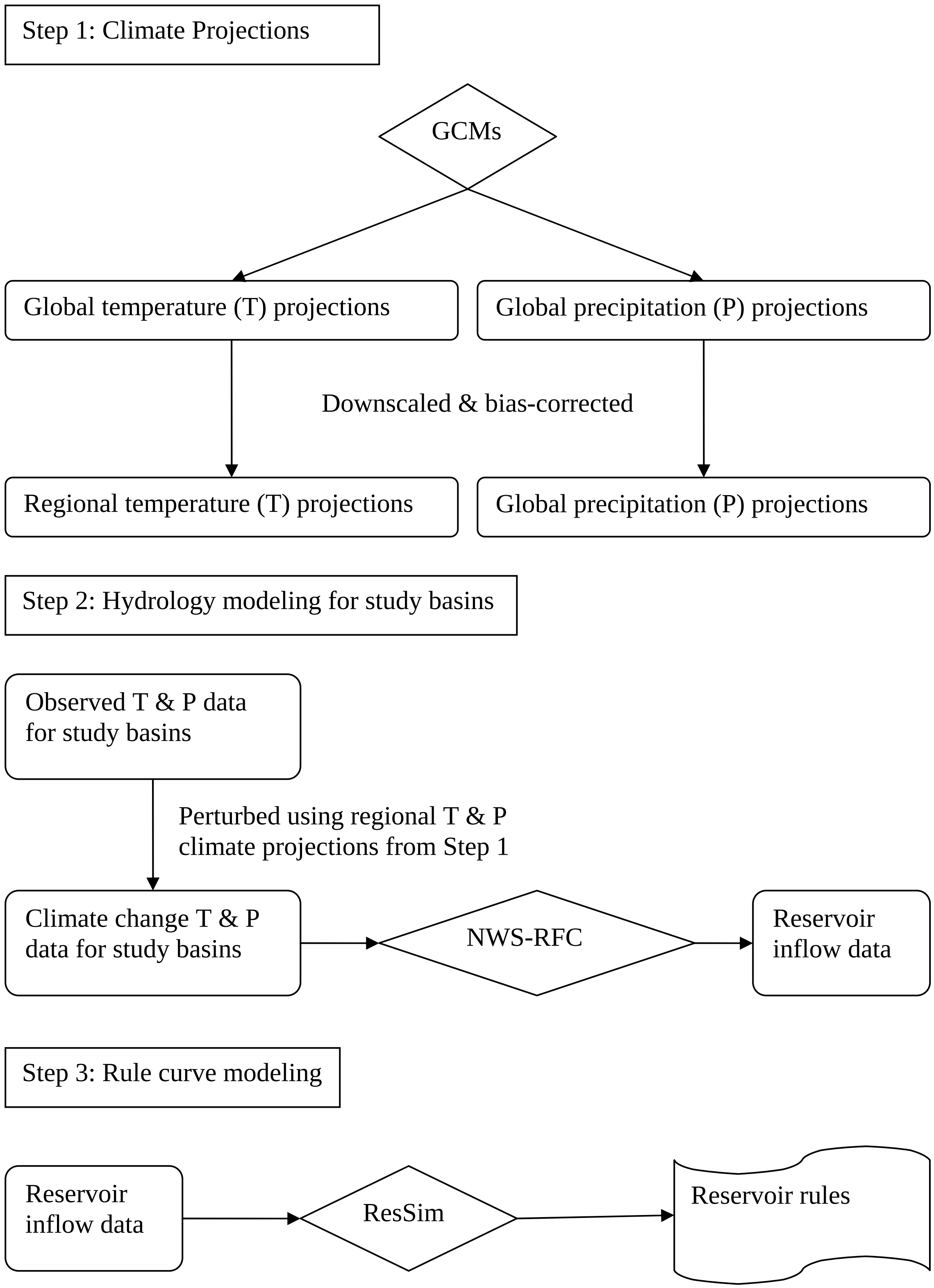


**Figure 6. A schematic overview of the modeling process.** Models are represented with diamonds. Data inputs and outputs are represented with rounded rectangles. Details of the modeling process are described below.

*Global Circulation Models*

Global Circulation Models use mathematics to describe how climate behaves. Two key structural features of GCMs are the forcing factors used to influence climate and the gridded resolution of the results. Forcing factors are components of the climate system that affect its energy balance. They affect the balance of incoming versus outgoing radiation, or Earth's energy flux (U.S. EPA 2006). Change in the radiation flux influences global surface temperatures and is the fundamental idea behind the science of climate change. Some forcing factors that directly affect Earth's radiation flux include amounts of greenhouse gases and aerosols; other indirect factors include land use practices.

Areas of the globe are represented in GCMs using a grid (Figure 7). The grid cell size defines a model's resolution. High resolution models have small-celled grids, and finer detailed results. Low resolution models use large-celled grids. Typical surface area grid sizes for GCMs are two to five degrees; for latitudes and longitudes in the Sacramento basin, two to five degree grids would cover areas from 175 $mi^2$ to 430 $mi^2$. Vertically, grids are divided into 15 to 50 sections. Horizontal degrees correspond to latitude and longitude. Thus two-degree resolution corresponds to two longitudinal and latitudinal degrees on a map. Vertical resolution determines how many vertical boxes divide the space between the earth's surface and top of the atmosphere (IPCC 2007). High resolution models give finely detailed results, which provide a breakdown of regional climate change. However, those projections are widely variable. Low resolution results illustrate broader trends in climate change and are less variable, but they provide less information about how specific regions will be affected.

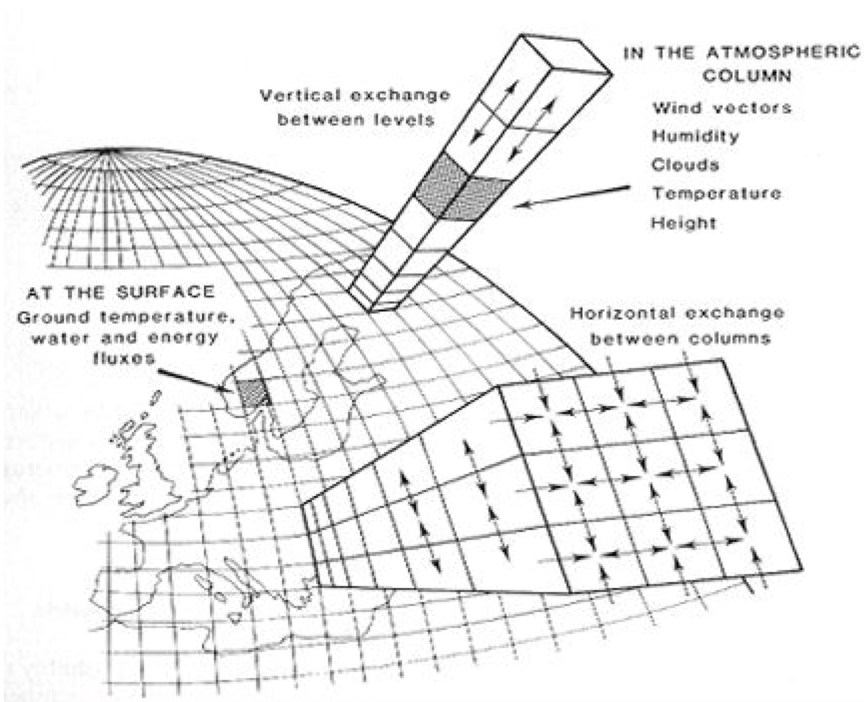


**Figure 7. An example of vertical and horizontal grids that define the resolution of a Global Circulation Model (Smith and Smith 2006).**

*Climate Change Data*

The likely range of temperature and precipitation changes in each study basin is generated using 11 GCMs identified in the IPCC Fourth Assessment Report (2007) that project the most likely climate changes (Table 2). Each GCM includes the same 11 forcing factors, however, for each GCM, the forcing factors are represented at different levels of detail (Table 3). Shaded boxes in Table 3 indicate that both interannual and seasonal patterns are represented. Unshaded boxes indicate that only seasonal patterns are represented (Karl et al. 2006).

| Modeling group, country | IPCC model ID | Abbreviation | Primary reference |
|---|---|---|---|
| Météo-France / Centre National de Recherches Météorologiques, France | CNRM-CM3 | Cnrm | Salas-Mélia et al. 2005 |
| CSIRO Atmospheric Research, Australia | CSIRO-Mk3.0 | Csiro | Gordon et al. 2002 |
| US Dept. of Commerce / NOAA / Geophysical Fluid Dynamics Laboratory, USA | GFDL-CM2.0 | Gfdl | Delworth et al. 2005 |
| NASA / Goddard Institute for Space Studies, USA | GISS-ER | Giss | Russell et al. 1995, 2000 |
| Institute for Numerical Mathematics, Russia | INM-CM3.0 | Inmcm | Diansky and Volodin 2002 |
| Institut Pierre Simon Laplace, France | IPSL-CM4 | Ipsl | IPSL 2005 |
| Center for Climate System Research (The University of Tokyo), National Institute for Environmental Studies, and Frontier Research Center for Global Change (JAMSTEC), Japan | MIROC3.2 (medres) | Miroc | K-1 model developers 2004 |
| Max Planck Institute for Meteorology, Germany | ECHAM5/ MPI-OM | Mpi | Jungclaus et al. 2006 |
| Meteorological Research Institute, Japan | MRI-CGCM2.3.2 | Mri | Yukimoto et al. 2001 |
| National Center for Atmospheric Research, USA | PCM | Pcm | Washington et al. 2000 |
| Hadley Centre for Climate Prediction and Research / Met Office, UK | UKMO-HadCM3 | hadcm3 | Gordon et al. 2000 |

**Table 2. Global Climate Models used to generate climate change projections forced by two emissions scenarios, A2 and B1.** These results were bias corrected and downscaled for the three study basins (Maurer 2007).

| Model ID | Vintage | Forcing Factors: Greenhouse Gases | Ozone | Sulfate aerosols, Direct effect | Sulfate Aerosols, Indirect effects | Black Carbon Aerosol | Organic Carbon Aerosol | Mineral Dust | Sea Salt | Land Use | Solar Irradiance | Volcanic Aerosols |
|---|---|---|---|---|---|---|---|---|---|---|---|---|
| CNRM-CM3 | 2004 | ■ | ■ | ■ | | ■ | | | | | | |
| CSIRO-MK3.0 | 2001 | ■ | | ■ | | | | | | | | |
| ECHAM5/MPI-OM | 2005 | ■ | ■ | ■ | ■ | | | | | | | |
| GFDL-CM2.0 | 2005 | ■ | ■ | ■ | | ■ | ■ | | | ■ | ■ | ■ |
| GISS-ER | 2004 | ■ | ■ | ■ | ■ | ■ | ■ | ■ | ■ | ■ | ■ | ■ |
| INM-CM3.0 | 2004 | ■ | | ■ | | | | | | | ■ | |
| IPSL-CM4 | 2005 | ■ | | ■ | ■ | | | | | | | |
| MIROC3.2 | 2004 | ■ | ■ | ■ | | ■ | ■ | ■ | ■ | ■ | ■ | ■ |
| MRI-CGCM2.3.2 | 2003 | ■ | | ■ | | | | | | | ■ | |
| PCM | 1998 | ■ | ■ | ■ | | | | | | | ■ | ■ |
| UKMO-HadCM3 | 1997 | ■ | ■ | ■ | ■ | | | | | | | |

**Table 3. Overview of the 11 climate change models and the detail with which they represent forcing factors.** Shaded boxes indicate that the model looks at both interannual and seasonal trends. Unshaded boxes indicate that only seasonal trends are accounted for.

Using these 11 GCMs, climate projections are determined given two different emissions scenarios described by the IPCC (2007): the higher emission scenario A2 and lower emission scenario B1. Details of these emissions scenarios are described in Nakicenovic et al. (2000), where each scenario is built on a storyline that relates emissions to driving forces. A2 describes a world in which the economy is regionally based, technological change is fragmented, and population growth is high. B1 describes a world in which the economy is more globally based and focuses on service and information, with relatively rapid introduction of clean and resource-efficient technologies. Though A2 does not represent the "worst-case" scenario for future emissions, it is generally regarded as the upper bound scenario for climate change studies; B1 generally represents the best-case future emissions scenario. Running GCMs using different emissions scenarios allows comparisons across a range of different potential futures, preventing the pitfall of planning for one possible but not guaranteed future (Maurer 2007). Eleven GCMs run for each emission scenario yields 22 different climate scenario results.

These GCMs provide global projections that are downscaled and bias-corrected from $2^o$ resolution to $1/8^o$ resolution. Wood et al. (2002) developed the downscaling and bias-correcting techniques for using global model forecast output for long-range streamflow forecasting (Maurer 2007). Downscaling provides regional data for each subbasin within the three study areas (Figure 8). These subbasin borders correspond to the basin configuration represented in the National Weather Service River Forecast System (NWS-RFS), the hydrologic model used to simulate climate change hydrology for the three study basins. The NWS-RFS is discussed in more detail later in this paper. Subbasins that comprise each study basin are listed in Table 4.

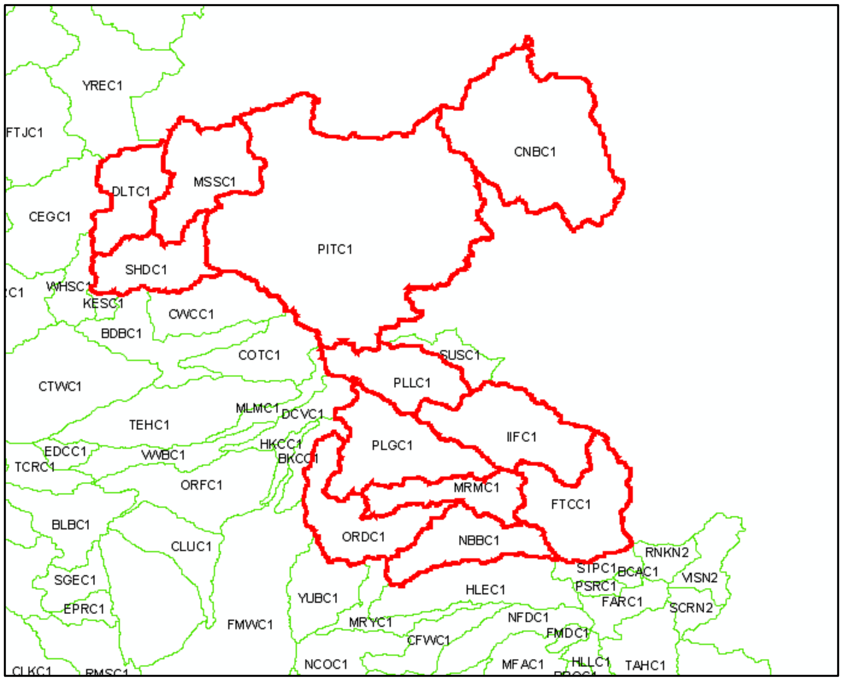


**Figure 8. Subbasin borders within each of the three study areas are outlined in red.** Downscaling detail corresponds to the subbasin borders used in the National Weather Service River Forecast System hydrologic model. The NWS-RFC was used to simulate climate change hydrology for the three study basins. The basin above Shasta Dam contains five subbasins: cnbc1, pitc1, mssc1, dltc1, and shdc1. The basin above Oroville Dam contains six subbasins: pllc1, plgc1, iifc1, ordc1, mrmc1, and ftcc1. The basin above New Bullards Bar Dam contains one subbasin: nbbc1. Projected temperature and precipitation changes were analyzed for each subbasin.

| BASIN | SUBBASIN |
|---|---|
| Shasta | CNBC1 |
| | PITC1 |
| | MSSC1 |
| | DLTC1 |
| | SHDC1 |
| Oroville | PLLC1 |
| | PLGC1 |
| | IIFC1 |
| | FTCC1 |
| | MRMC1 |
| | ORDC1 |
| New Bullards Bar | NBBC1 |

**Table 4. Each of the three study basins is divided into subbasins according to the basin boundaries in the National Weather Service River Forecast System hydrologic model.**

Six hour time series temperature and precipitation data from October 1960 through September 1990, provided by the California-Nevada River Forecast Center (CN-RFC) is used as a baseline against which to compare the data from the GCM projections for the period 2010-2040. Projected changes for the year 2025 relative to the year 1975 are determined using the monthly average value of temperature and precipitation from 1960 to 1990 (30 years centered on 1975) and from 2010 to 2040 (30 years centered on 2025). The ratio-minus-one value of the 2025 average over the 1975 average determines the percent increase of 2025 from 1975, or the percent change across 50 years (Equation 1).

$$\frac{AVG_{2025}}{AVG_{1975}} - 1 = \text{\% change across 50 years}$$

**Equation 1. Equation to determine percent of temperature and precipitation changes across a given 50-year period.** The 2025 average is determined using the monthly temperature and precipitation averages from 2010-2040. The 1975 average is determined using monthly temperature and precipitation averages from 1960-1990.

Finally, the 10th, median, and 90th percentile values of the 22 model range are determined, yielding the range of possible temperature and precipitation changes for the year 2025 (Faber, personal communication, 2008). The 90th, median and 10th percentile values are used to include 80 percent of the likely range of future climate projections, neglecting the least likely extremes. Values for the increases to the temperature record and percentage change for precipitation can be found in Table 5.

| | Percentile | | |
|---|---|---|---|
| | **10th** | **50th** | **90th** |
| **Δ Temperature** | +0.8°F | +1.8°F | +2.5°F |
| **Δ Precipitation** | -6.6% | +4.5% | +16.8% |

**Table 5. Temperature and precipitation projections used to perturb the observed record for the three study basins.** The 10th and 90th percentile values were chosen to include 80 percent of the projected climate change scenarios while neglecting the most unlikely extremes. These values represent the average changes expected over the three study basins. Projected temperature increases for each subbasin vary within 0.1°F. Projected precipitation changes vary within 3% for each subbasin except for the 90th percentile values, which vary more than 7%. A single value is applied to each subbasin for each percentile increase to illustrate the sensitivity of the basin to temperature and precipitation changes, but not to determine quantitative changes due to temperature and precipitation changes.

Climate scenarios are identified by the temperature and precipitation perturbations they represent. For example, T+1.8, P-6.6% refers to the climate scenario in which the historical temperature record is increased by 1.8°F and the historical precipitation record is decreased by 6.6%.

Although temperature and precipitation projections are available for each subbasin within the three main watersheds, basin average values are used. This was done because little variability exists between each subbasin's projected temperature changes. Precipitation changes are widely variable, however, as this work examines the sensitivity of basins to climate change and does not try to quantify future changes, a single, average percentile value is applied across all three study basins. A single value reflects expectations that precipitation changes will be similar across elevation bands (Mote 2003, Regonda et al. 2005, Saunders et al. 2008). These step changes are used to perturb observed temperature and precipitation data for the three study basins. The observed, six-hour time step record ranges from October 1, 1960 to September 30, 1999.

*National Weather Service River Forecast System*

The National Weather Service River Forecast System is a robust river and hydrologic forecast system. River Forecast Centers around the country, including the California-Nevada office, use the NWS-RFS to make both short-term (a day to a week in advance) and long-term (a week to months in advance) forecasts. However, this model is also used for operations planning, policy, and research.

Among the types of operations modeled by the NWS-RFS are snowmelt and rainfall runoff procedures, temporal distributions of runoff, channel losses or gains, routing models, baseflow, reservoir regulation, stage/discharge conversions, time series manipulations, statistical functions and water balance. The system uses observed and forecast point data for meteorological components such as temperature and precipitation and generates information about predicted river stage and discharge at selected forecast points. The RFS also stores information about the hydrologic conditions of a basin including snow cover, soil moisture and channel storage given a time series input (NOAA 2008).

One important process simulated by the NWS-RFS is infiltration. Infiltration processes are represented using soil “tanks” that fill at a rate determined by transpiration, horizontal drainage and vertical percolation processes. A schematic of the NWS-RFS model’s soil tanks is illustrated in Figure 9. Soil processes are represented by upper and lower tanks. Rainfall is first routed through the upper tank. The upper tank models vertical percolation, horizontal drainage, transpiration and soil absorption processes. If the precipitation rate exceeds the percolation and drainage rate, the upper zone becomes saturated and further precipitation is routed as surface flow. If dry periods occur, percolation rates increase. After the water is routed through the upper zone, the percolated water is routed to the lower zone, where groundwater processes are modeled such as water table storage and subsurface and base flows. As this work examines runoff volume changes during flood events, the basin conditions that precede each flood event play an important role in defining how climate change affects hydrology.

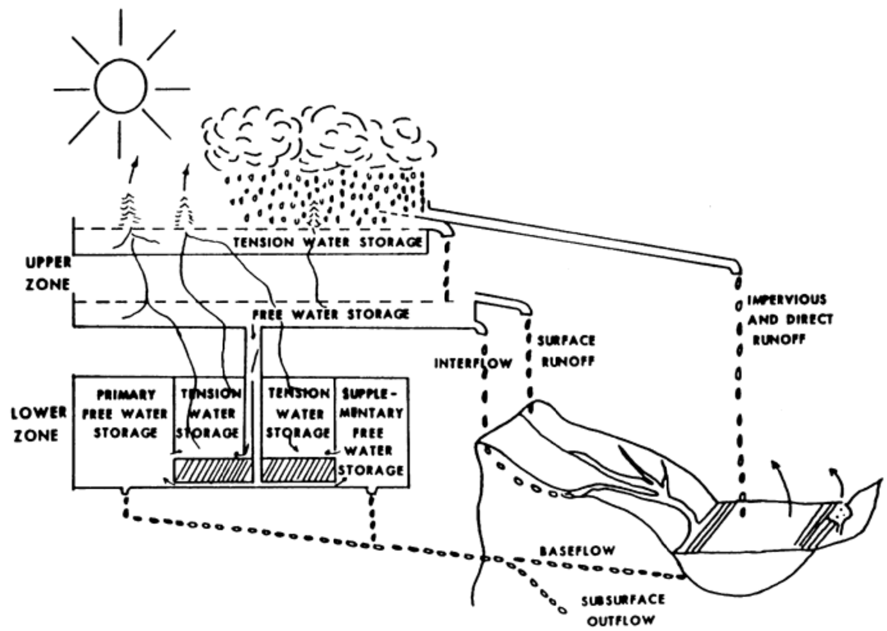


**Figure 9. A schematic of the soil drainage processes represented in the NWS-RFS model.** The soil mantle is divided into an upper and lower zone. The upper zone simulates horizontal and vertical flow processes and determines whether rainfall drains vertically into the lower zone, which contains the water table, or moves as intersurface or surface runoff, which affects the volume of surface flow during rain events (Figure taken from NOAA 2002).

*Hydrology Data*

Hydrology data is generated using the perturbed temperature and precipitation files to calculate the resultant runoff using the National Weather Service River Forecast System (NWS-RFS). Six hour time-step temperature and precipitation data for the period October 1, 1960 to September 30, 1999 for each subbasin in the three basins is used. Shasta has five subbasins, Oroville six subbasins, and New Bullards Bar one subbasin. Each observed temperature and precipitation file is perturbed by the amounts determined by the statistical analysis of the downscaled subbasin data. Each temperature scenario, including the observed record, is combined with each precipitation scenario. Including the observed record, 16 unique climate scenarios are explored for each basin.

These temperature and precipitation records serve as the inputs to the NWS-RFS model. Six hour time step inflows to Shasta, Oroville and New Bullards Bar reservoirs are the outputs. Results of this modeling are analyzed later in this work.

*ResSim*

The Hydrologic Engineering Center-Reservoir Simulation (ResSim) model is software developed by the Corps of Engineers to route reservoir inflows and releases based on watershed characteristics and dam operating parameters. This model is used by the Corps of Engineers to assess release objectives during flood events and can also be used for planning, policy, and research.

Inputs to this model are the six-hour time series runoff hydrology results generated by the NWS-RFS. In this project, only reservoir releases are accounted for in the basin model. Local flows at downstream points are neglected as data for each downstream inflow site is unavailable. One limitation imposed by this model is that it can only apply one rule curve per simulation. Without further scripting, the model cannot incorporate dynamic rule curves such as the ones used at Oroville and Shasta dams. To overcome this limitation, simulations are repeated for Shasta and Oroville basins using alternate curves defined in their flood control manuals.

Flood events are sampled to reflect a range of storm timings, intensities and rain to snow ratios (Table 6). Events during which temperatures in the upper basin elevations are at and below freezing are called cold events. Cold events include January 1969, January 1980, December 1982, March 1983 and March 1995. Average temperatures during some of the cold events are above freezing in some of the study basins but below freezing in others; however, snowpacks for all cold years are some of the largest on record (Rizzardo, personal communication, 2008; Roos, personal communication, 2008). Therefore, while the isolated events may not show a strong response to temperature increases, the effect of increasing temperatures over the season is significant. Events during which temperatures are above freezing in the upper basin elevations are called warm events. Warm events are January 1960, December 1964, February 1986 and January 1997. Some events occur within days of smaller precipitation events; events that follow an antecedent event are indicated on the table.

| **Sample storm events to test reservoir rule curve operations** | | | | |
|---|---|---|---|---|
| **Name** | **Event Type** | **Antecedent event?** | **Duration (hrs)** | **Flood volumes (TAF) (% of study basins' mean annual flow)** |
| January 1963 | Warm | No | 144 | 1734 (15) |
| December 1964 | Warm | No | 312 | 4587 (39) |
| January 1969 | Cold | Yes | 498 | 2660 (23) |
| January 1980 | Cold | Yes | 330 | 2348 (20) |
| December 1982 | Cold | No | 144 | 878 (7) |
| March 1983 | Cold | Yes | 570 | 4785 (41) |
| February 1986 | Warm | Yes | 402 | 4834 (41) |
| March 1995 | Cold | No | 522 | 4405 (38) |
| January 1997 | Warm | Yes | 408 | 4402 (38) |

**Table 6. Sample storm events that illustrate the effect of temperature and precipitation changes on a given storm.** Each event varies in intensity, timing and duration. Figures illustrating the runoff trends for each event can be found in Appendix A.

Some climate change scenarios are excluded from the analysis due to missing data. For the Oroville watershed, hydrologic data describing the T+0.8$^{o}$F, P-6.6% is unavailable, however, results are available for the other three scenarios representing precipitation intensities decreased by 6.6%. Trends across the available data are consistent with trends across the complete data sets available for Shasta and New

Bullards Bar, implying that Oroville's basin response can be inferred. Data describing the T+2.5°F, P-6.6% scenario in the Shasta watershed is also unavailable. As such, the analysis for Shasta Dam does not include the worst case scenario representing the highest temperatures combined with the lowest precipitation intensities. However, as this study looks at basin sensitivity and does not quantify the hydrologic response due to climate change, the general trends of the hydrologic response to temperature and precipitation changes are examined for consistency with the other two study basins.

## Chapter V. Results

*Effects of Climate Change on Storms*

Across the three study basins, storms' responses to changes in temperature and precipitation regimes are broadly similar. Discharge from warm events responds strongly to changes in precipitation intensities, but weakly to temperature changes because of the original precipitation composition of the warm storms.  Temperatures during warm events are above freezing and therefore contain a small fraction of snow in the overall precipitation composition. When temperatures increase, the precipitation is already warmed and does not change its physical state. For cold events, discharge volumes respond strongly to both temperature and precipitation changes. Temperatures during cold events are at or below freezing; small temperature increases raise temperatures above freezing. The warmer temperatures generate inflow changes consistent with those expected from higher fractions of rain and wetter basin conditions. Figures illustrating each storm's runoff patterns in each of the three study basins can be found in Appendices A, B and C.

| Event | Event type | Shasta | | Percent change in inflow volumes | | |
|---|---|---|---|---|---|---|
| | | Average upper basin temp | Average lower basin temp | T+0.8 | T+1.8 | T+2.5 |
| Jan-63 | warm | 42.9 | 46.6 | -0.3 | -0.7 | -1.2 |
| Dec-64 | warm | 44.3 | 49.6 | 3.2 | 7.3 | 10.0 |
| Feb-86 | warm | 37.2 | 41.3 | 1.0 | 2.0 | 2.6 |
| Jan-97 | warm | 39.0 | 43.8 | 0.3 | 0.9 | 1.4 |
| Jan-69 | cold | 25.0 | 29.9 | 10.5 | 20.3 | 25.6 |
| Jan-80 | cold | 34.2 | 38.6 | -0.7 | -1.9 | -2.1 |
| Dec-82 | cold | 25.3 | 28.7 | 6.4 | 12.0 | 14.1 |
| Mar-83 | cold | 35.6 | 38.8 | 0.8 | 2.8 | 4.2 |
| Mar-95 | cold | 38.7 | 42.4 | -0.5 | -1.0 | -0.2 |

**Table 7.  Average temperatures and inflow volume changes in the Shasta basin given temperature increases.**

| Event | Event type | Oroville | | Percent change in inflow volumes | | |
|---|---|---|---|---|---|---|
| | | Average upper basin temp | Average lower basin temp | T+0.8 | T+1.8 | T+2.5 |
| Jan-63 | warm | 39.9 | 43.3 | 1.1 | 0.2 | 0.7 |
| Dec-64 | warm | 41.1 | 46.2 | 6.2 | 14.9 | 20.5 |
| Feb-86 | warm | 36.8 | 41.0 | 5.4 | 11.3 | 15.4 |
| Jan-97 | warm | 37.3 | 42.8 | 4.6 | 9.7 | 13.1 |
| Jan-69 | cold | 26.9 | 32.2 | 14.1 | 33.0 | 43.6 |
| Jan-80 | cold | 37.3 | 41.3 | 5.4 | 10.1 | 13.4 |
| Dec-82 | cold | 27.4 | 30.9 | 13.3 | 29.3 | 40.1 |
| Mar-83 | cold | 34.7 | 37.7 | 6.8 | 15.4 | 22.8 |
| Mar-95 | cold | 37.1 | 40.4 | 4.6 | 8.0 | 13.1 |

**Table 8. Average temperatures and inflow volume changes in the Oroville basin given temperature increases.**

| Event | Event type | New Bullards Bar | | Percent change in inflow volumes | | |
|---|---|---|---|---|---|---|
| | | Average upper basin temperatures | Average lower basin temperatures | T+0.8 | T+1.8 | T+2.5 |
| Jan-63 | warm | 40.5 | 48.5 | 0.4 | 1.0 | 1.6 |
| Dec-64 | warm | 51.6 | 51.6 | 4.5 | 8.6 | 10.3 |
| Feb-86 | warm | 34.6 | 44.3 | 8.4 | 18.6 | 24.9 |
| Jan-97 | warm | 35.1 | 45.4 | 3.7 | 6.7 | 7.2 |
| Jan-69 | cold | 28.8 | 38.7 | 9.4 | 21.8 | 29.9 |
| Jan-80 | cold | 37.9 | 45.3 | 6.2 | 12.7 | 16.3 |
| Dec-82 | cold | 29.1 | 37.3 | 6.9 | 17.0 | 24.7 |
| Mar-83 | cold | 33.4 | 42.7 | 9.6 | 22.9 | 32.2 |
| Mar-95 | cold | 32.4 | 42.8 | 10.0 | 20.9 | 27.3 |

**Table 9. Average temperatures and inflow volume changes in the New Bullards Bar basin given temperature increases.**

To illustrate the broad trends observed across all three study basins, results from New Bullards Bar basin are presented. Temperature trends during each event are plotted to help define the event as warm or cold. Mean area temperatures are given for elevations above and below 5000 ft, the general elevation of the snow-rain boundary. Mean area temperatures for elevations below 5000 ft. in the New Bullards Bar basin are illustrated by the dark blue line. Mean area temperatures for elevations above 5000 ft are illustrated by the pink line. The freezing point (32$^{o}$F) is illustrated by the thick black line. A hydrograph that plots inflows for climate scenarios that perturb temperature illustrates how warm and cold events respond differently to temperature increases. The same data format conventions are used for all temperature charts presented in this work.

The effects of temperature on storm runoff are more pronounced in cold events than in warm events. The hydrograph and temperature trends for the January 1997 event illustrate how a warm event is affected from increasing temperatures (Figures 10-13). Figure 10 illustrates the observed temperature record during the January 1997 event. Except for Day 10 during the event (hours 216-240), temperatures throughout the storm are above freezing for several hours during each day. Preceding the peak flow for several days and during the peak flow (hours 144-168), temperatures are well above freezing (Figure 10).

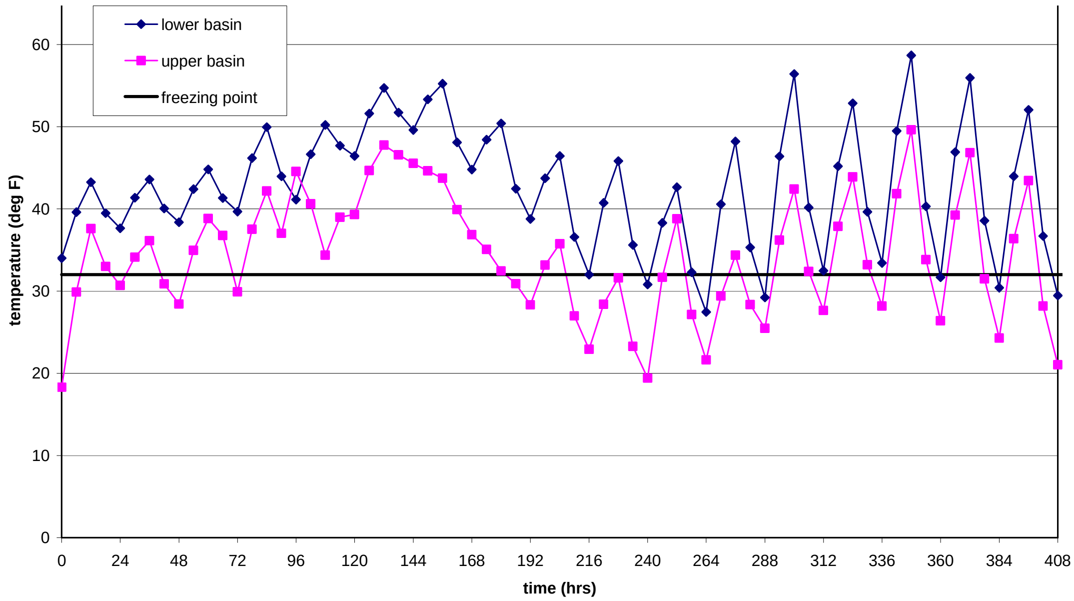


**Figure 10. Observed temperatures before, during, and after the January 1997 rain event in the New Bullards Bar basin.** The storm event occurs during hours 144-216 and peaks near hour 168. By the time temperatures drop near and below freezing, the storm event has passed. The dark blue line shows mean area temperatures for elevations below 5000 ft. The pink line shows mean area temperatures for elevations above 5000 ft. The freezing point, 32°F, is illustrated by the thick black line. Because temperatures are generally above freezing during the storm event, this event is categorized as warm.

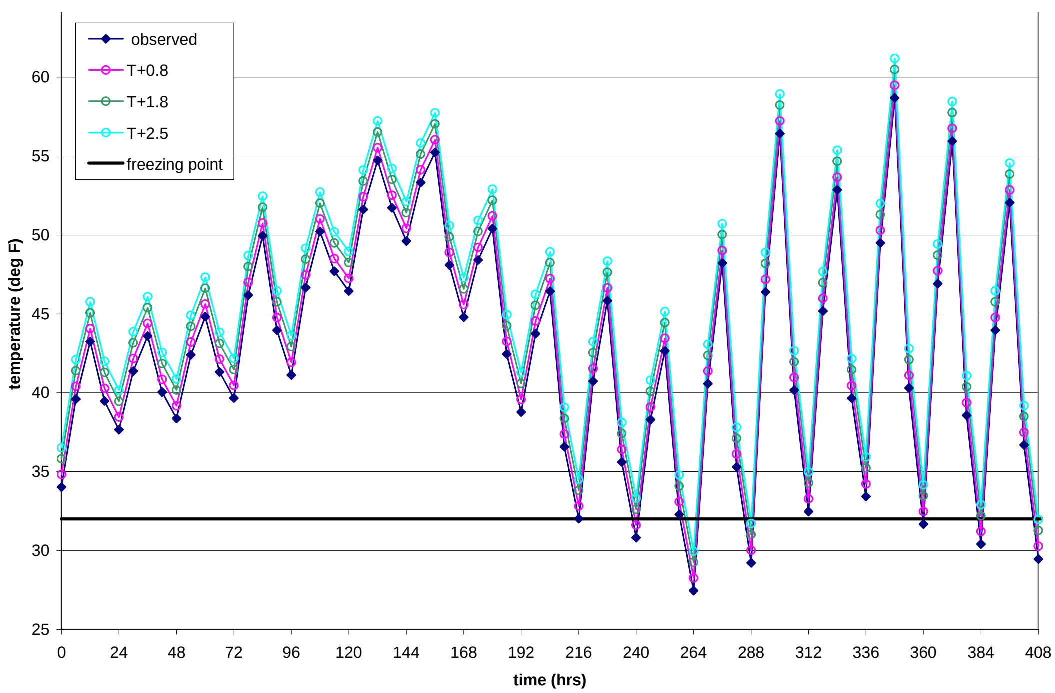


**Figure 11. Temperature shifts for the January 1997 rain event in the New Bullards Bar basin below 5000 ft.** Each line represents a different temperature regime used to model the January 1997 flood event. The solid blue line illustrates the observed temperatures in the lower basin. Each line with hollow data points illustrates the perturbed temperature scenarios. Temperatures during the observed event (hours 144-216), especially during the peak (hour 168) are well above freezing. During this period, precipitation is composed of rain. Increasing temperatures do not change the physical state of the precipitation; therefore, this event is not sensitive to temperature increases.

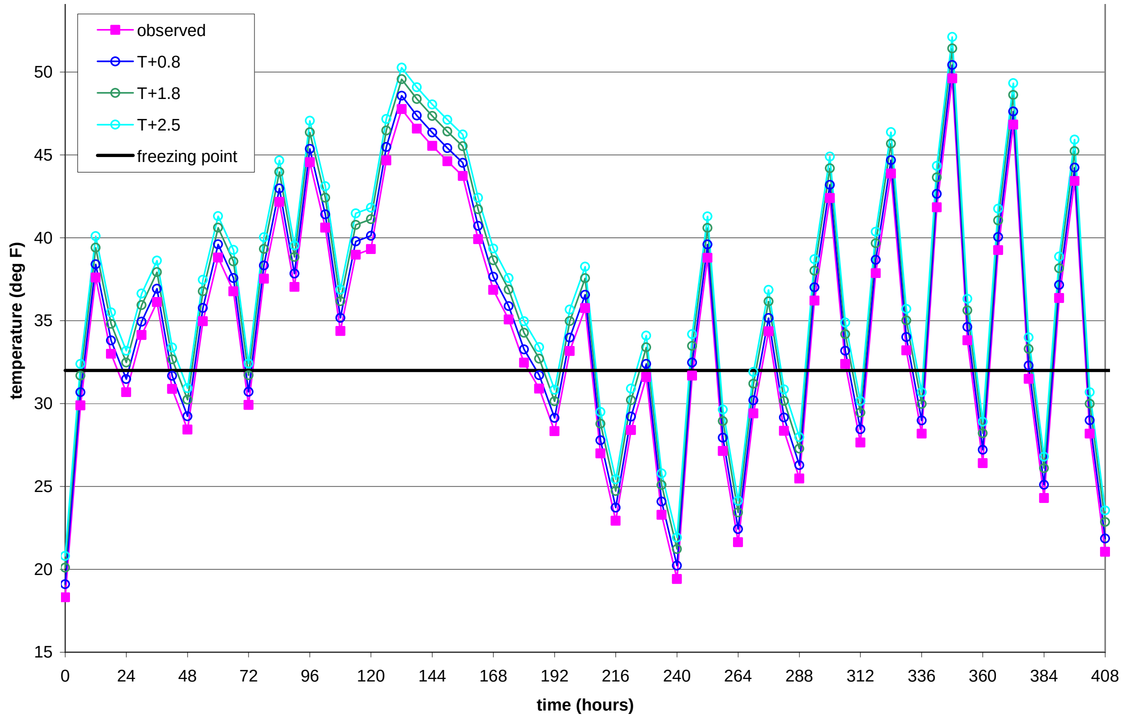


**Figure 12. Temperature shifts for the January 1997 rain event in the New Bullards Bar basin above 5000 ft.** Each line represents a different temperature regime used to model the January 1997 flood event. The solid blue line illustrates the observed temperatures in the lower basin. Each line with hollow data points illustrates the perturbed temperature scenarios. Temperatures during the observed event (hours 144-216), especially during the peak (hour 168) are well above freezing. During this period, precipitation is composed of rain. Increasing temperatures do not change the physical state of the precipitation; therefore, this event is not sensitive to temperature increases.

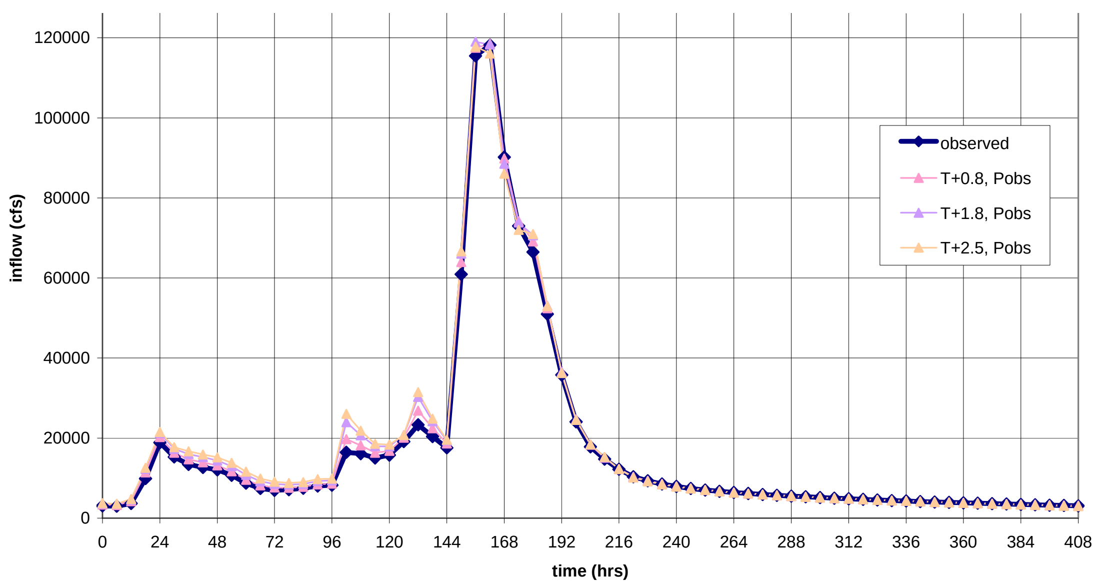


**Figure 13. Runoff trends for the January 1997 rain event in the New Bullards Bar basin for the four different temperature scenarios.** As the runoff patterns for each temperature scenario generally overlap the observed record, the results indicate that runoff from warm events does not respond strongly to increasing temperatures.

The hydrograph for the January 1997 event illustrates the runoff rates for the observed and perturbed temperature scenarios with no significant change in precipitation intensities (Figure 13). The hydrographs for each scenario generally overlap; the magnitude and timing of warm event inflows are not affected by increasing temperatures. For the warmest temperature scenario, T+2.5$^{o}$F, overall discharge volumes increase only seven percent from the observed runoff. The precipitation composition of warm events does not change when temperatures increase because temperatures are already above freezing. On the other hand, cold events respond more to increasing temperatures.

Two events are presented to illustrate how a cold event responds to increasing temperatures. The March 1983 snow event has observed temperatures that fluctuate around the freezing point (32$^{o}$F) for most of the event (Figure 14-15). Because temperatures are close to freezing, small shifts in temperature significantly affect overall discharge. Such strong effects are illustrated in the March 1983 hydrograph for New Bullards Bar (Figure 16).

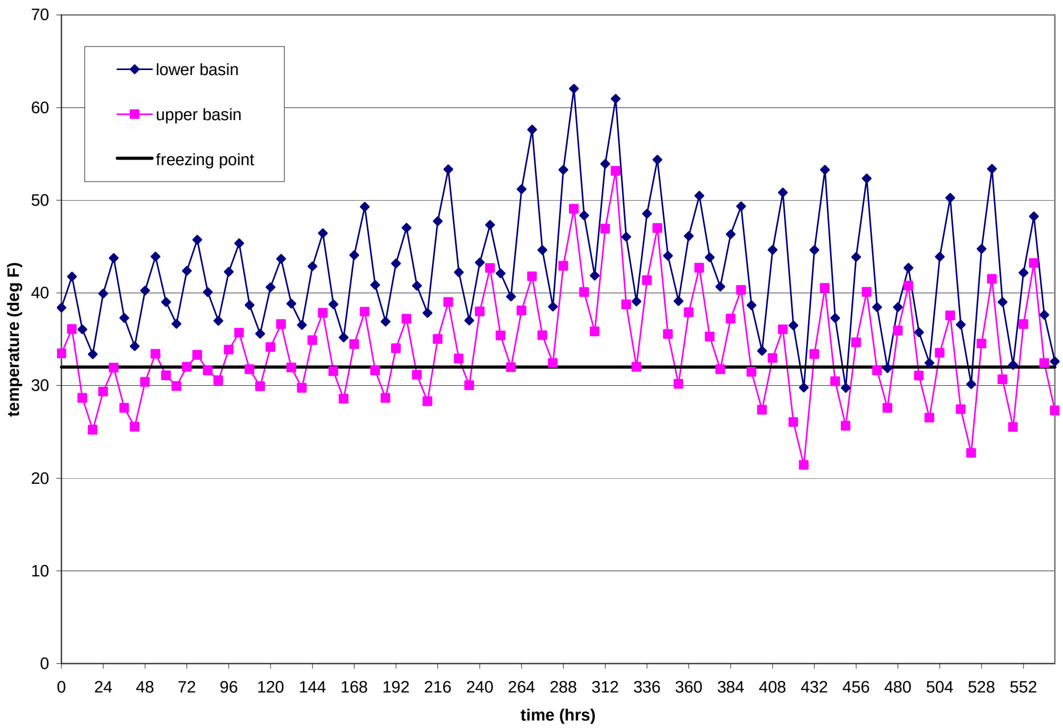


**Figure 14. Observed temperature record for the March 1983 snow event in the New Bullards Bar basin.** The same data format is used in Figure 8. The March 1983 event illustrates how cold events, during which temperatures are close to freezing, respond to temperature increases. The flood event occurs between hours 384 and 456, when temperatures are near and below freezing. An earlier, smaller event occurs during hours 72-144, when temperatures are near and below freezing in the upper basin. When temperatures are at and below freezing, precipitation is modeled as snow.

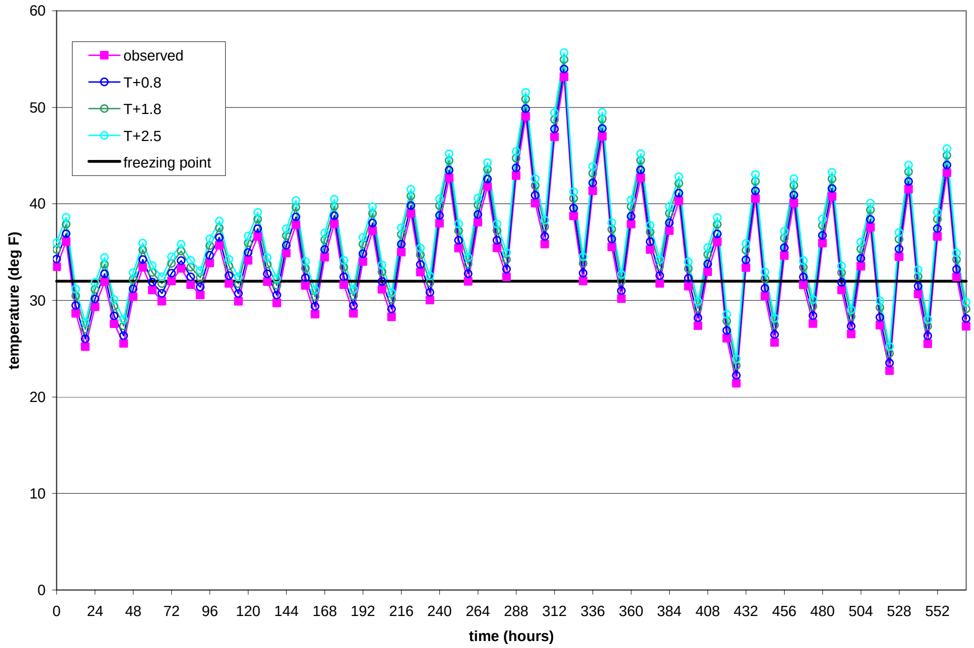


**Figure 15. Temperature shifts for the March 1983 snow event in the New Bullards Bar basin above 5000 ft.** Each line represents a different temperature regime used to model the March 1983 flood event. The solid pink line illustrates the observed temperatures in the upper basin. Each line with hollow data points illustrates the perturbed temperature scenarios. Temperatures during the observed event (hours 360-432), are near and below freezing. During this period, precipitation is composed of snow and rain. During the period of the observed event, temperatures are below freezing 17 times. When the climate scenario simulates the highest temperature increase (T+2.5), temperatures are below freezing 10 times. During the observed event peak, temperatures are below freezing (hour 384) in the observed climate scenario only. None of the climate scenarios simulating increased temperatures are below freezing during the event's peak. Increasing temperatures change the physical state of the precipitation from snow to rain as temperatures rise above freezing; therefore, this event is sensitive to temperature increases.

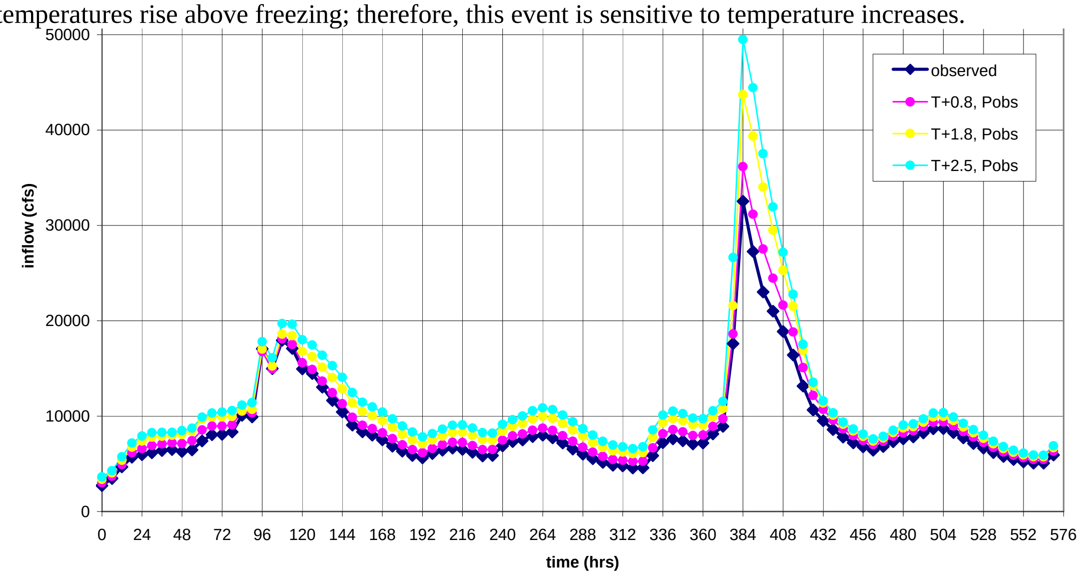


**Figure 16. Hydrograph patterns for the observed and perturbed temperature scenarios for the March 1983 event in the New Bullards Bar basin.** The observed hydrograph is illustrated by the dark blue line. A clear increase of discharge volume is evident from the smallest temperature increase, illustrated by the pink line; volumes continue to increase with each additional temperature increase, illustrated by the yellow and light blue lines, respectively. Unlike the hydrograph for the January 1997 rain event, small temperature shifts produce a noticeable shift to inflow patterns.

Changes in runoff rates are immediately caused by the smallest temperature increase, T+0.8°F, with no increase in precipitation intensities. Discharge volumes increase for the T+0.8°F, T+1.8°F, and T+2.5°F climate scenarios by 9.7 percent, 22.2 percent and 30.8 percent, respectively. During the main event peak for the T+0.8°F, T+1.8°F, and T+2.5°F climate scenarios, discharge volumes increased by 13 percent, 30 percent and 41 percent, respectively. This indicates that near-freezing events, which consist of more snowfall before temperature regimes are perturbed, are more sensitive to warming temperatures than warm events, which are predominately rain in the observed event. It also indicates that scenarios with observed temperatures close to freezing will be sensitive to small temperature increases.

Cold events, during which temperatures are significantly below freezing, are also analyzed. During the January 1969 snow event, temperatures are well below freezing over extended periods (Figure 17-18). For brief periods, temperatures are higher than the freezing point, but within several degrees of freezing.

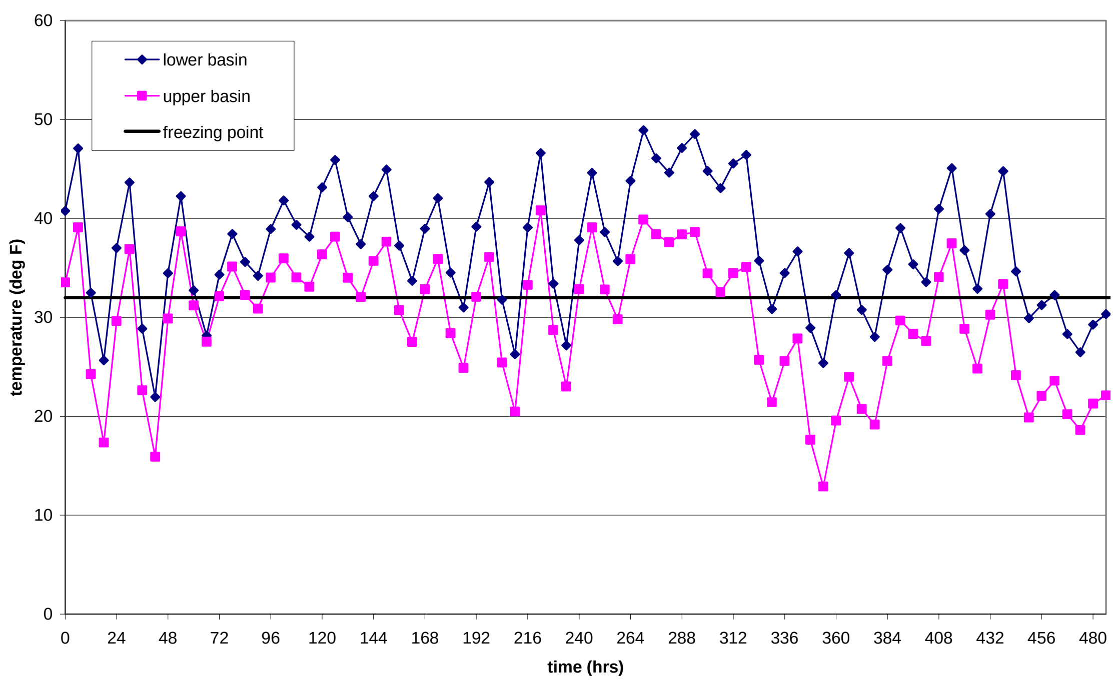


**Figure 17. Basin temperatures above and below the general snowline elevation for the January 1969 snow event in the New Bullards Bar basin.** Temperatures during a smaller event that precedes the main flood event are at and above freezing (hours 72-192). Temperatures during the main flood event begin above freezing, but drop well below the freezing point toward the end of the event (hours 264-384). Temperatures remain at or below the freezing point during another small event that followed the main flood event (hours 408-480).

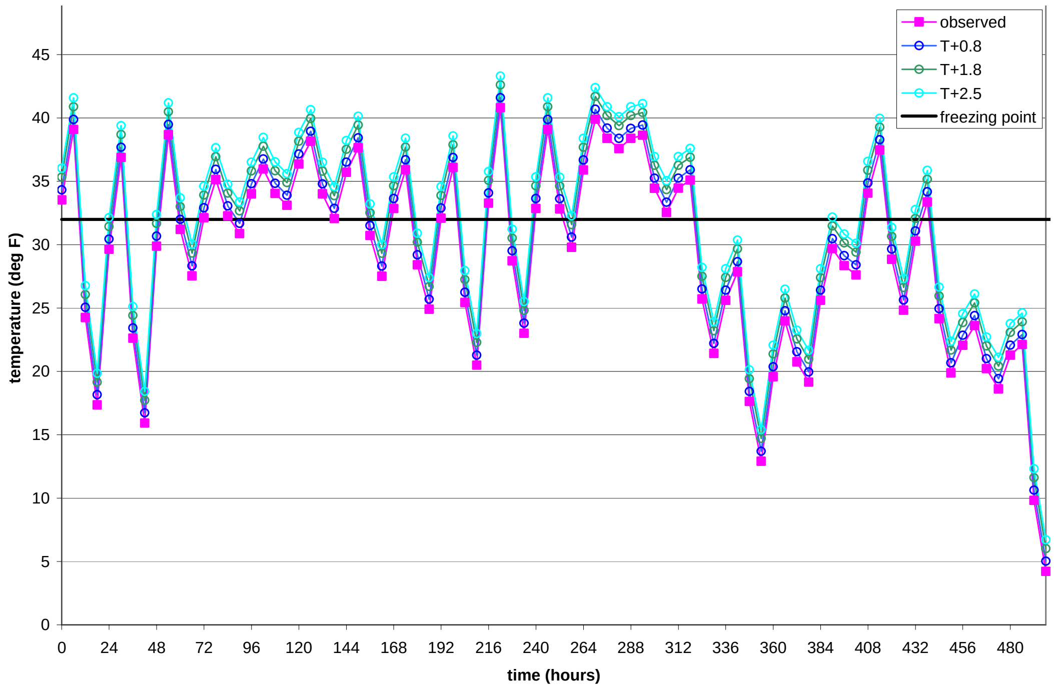


**Figure 18. Temperature shifts for the January 1969 snow event in the New Bullards Bar basin above 5000 ft.** Each line represents a different temperature regime used to model the January 1969 flood event. The solid pink line illustrates the observed temperatures in the upper basin. Each line with hollow data points illustrates the perturbed temperature scenarios. Temperatures during the observed event (hours 264-360), drop well below freezing. Except for the early period of the storm, precipitation is composed of snow. During the period of the observed event, temperatures are below freezing 7 times. When the climate scenario simulates the highest temperature increase (T+2.5), temperatures are below freezing 6 times. During the observed event peak, temperatures are above freezing (hours 288-312) in the observed and perturbed climate scenarios. After the peak and before the following, smaller event, temperatures during the observed and perturbed scenarios are all below freezing. This illustrates that cold events with temperatures several degrees below freezing will not be affected as strongly by temperature increases as events with temperatures near freezing.

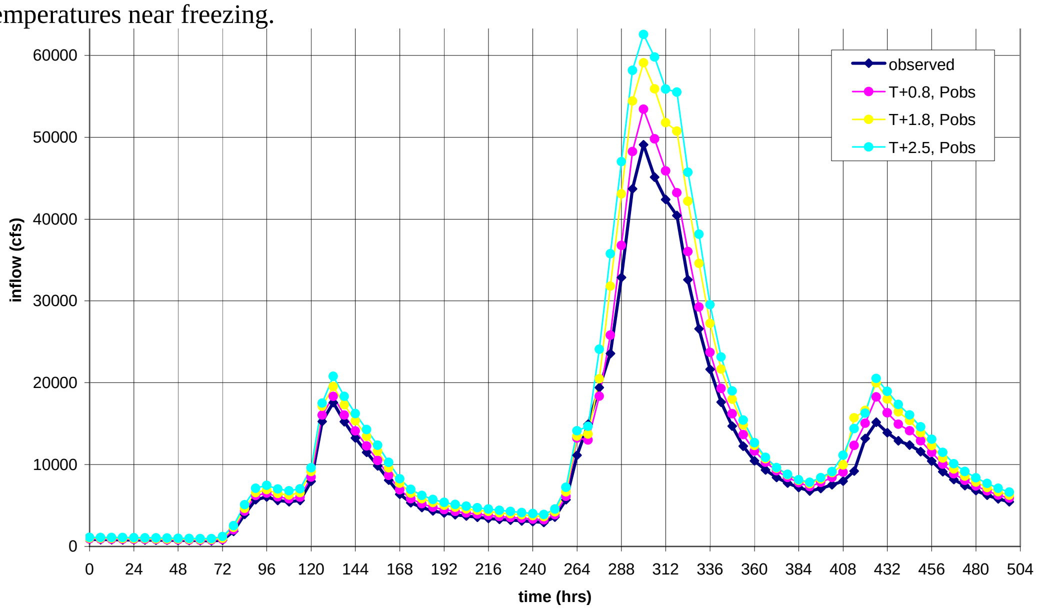


**Figure 19. Discharge patterns for the observed and perturbed temperature climate scenarios in the New Bullards Bar basin for the January 1969 event.** Though observed temperatures are sometimes well below freezing, inflows still respond to small temperature shifts.

Despite observed temperatures that are significantly below freezing, small temperature increases still affect discharge rates and volumes of the January 1969 event (Figure 19). Discharge volume increases for the T+0.8°F, T+1.8°F, and T+2.5°F climate scenarios by 9.4 percent, 20.6 percent and 29.1 percent, respectively, almost the same percentage increases shown in the cold event during which temperatures are closer to freezing. During the main event peak (hours 264-360), discharge volume increases for the T+0.8°F, T+1.8°F, and T+2.5°F climate scenarios increase 8.2 percent, 21.8 percent and 31.4 percent, respectively. This implies that for low elevation basins, cold events with temperatures below the freezing point will still be sensitive to small temperature increases, however, if cold events during which temperatures are several degrees below zero are less sensitive to temperature increases than events during which temperatures are near freezing.

Warmer temperature regimes can affect an event so strongly that runoff volumes increase in scenarios that simulate drier climates. In several of the sampled flood events, runoff volumes for cold storms sometimes exceed those in the observed event despite decreased storm intensities (the observed precipitation is decreased by 6.6%). These trends are also observed in all three basins. This phenomenon is explained by the antecedent basin conditions to each event. The cold January 1969 storm illustrates this concept.

One important characteristic of the January 1969 event is the antecedent event that peaks during a smaller event several days before the main storm peak. The peak from the antecedent event is illustrated below (Figure 20).

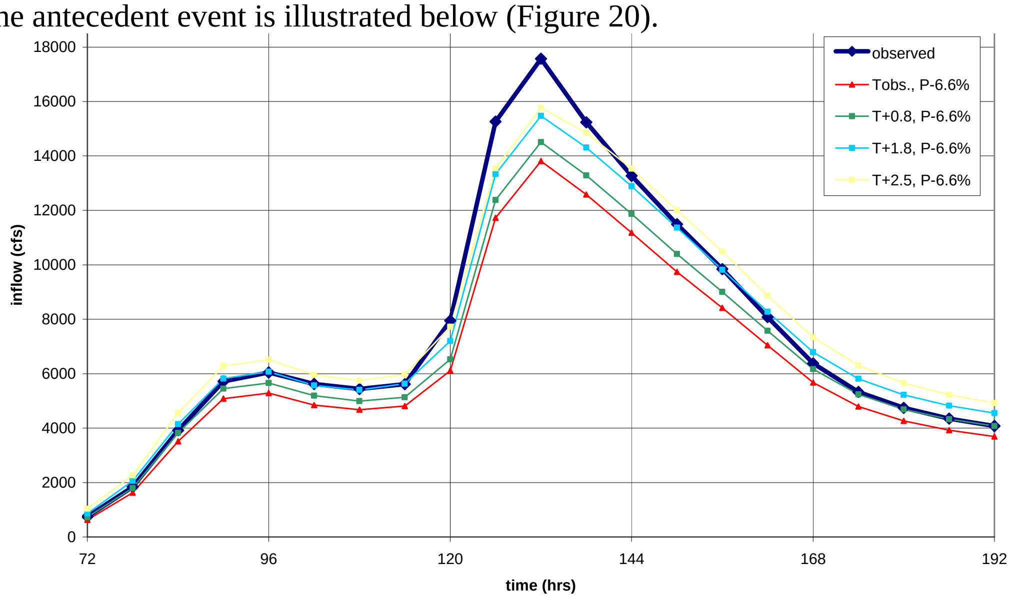


**Figure 20. The four lines below the observed record each represent decreased precipitation scenarios with various temperature increases.** The scenarios with the highest temperature increases, T+2.5°F and T+1.8°F, surpass the observed record's flow volume towards the end of the first peak. Inflows for the Tobs, P-6.6% scenario decrease more than 6.6% because of the effect of reduced precipitation intensity on infiltration. With less precipitation, the basin reaches its infiltration capacity later for two reasons. First, basin conditions are drier overall because the entire precipitation record is decreased by 6.6%. Less water is stored in the soil prior to the storm event, so more space exists for rainfall storage. Second, the decreased precipitation intensity causes less water to runoff at any given time. Therefore, infiltration saturation is reached slower than in the observed event, allowing more water to infiltrate and decreasing surface runoff rates.

The observed record is illustrated with the heavy, dark blue line that peaks above the others on day 6 (120-144 hours). The four lines below the observed record each simulate climates with the same precipitation intensity decrease (-6.6%) with four different temperature scenarios – the observed record and three temperature increases. Though each of the climate change scenarios peak below the observed record, runoff rates establish a different pattern. Inflows for the Tobs, P-6.6% scenario decrease more than 6.6% because of the effect of reduced precipitation intensity on infiltration. With less precipitation, the basin reaches its infiltration capacity later for two reasons. First, basin conditions are drier overall because the entire precipitation record is decreased by 6.6%. Less water is stored in the soil prior to the storm event, so more space exists for rainfall storage. Second, the decreased precipitation intensity causes less water to runoff at any given time. Therefore, infiltration saturation is reached slower than in the observed event, allowing more water to infiltrate and decreasing surface runoff rates.

Towards the end of the first peak, runoff rates from the T+2.5$^{o}$F and T+1.8$^{o}$F surpass the runoff rates from the observed event due to the increased fraction of rain that comprises the precipitation. Observed temperatures are at or below the freezing point eight times (Figure 21). During the T+1.8 and T+2.5 climate scenarios, temperatures are below freezing three times during the event and are above freezing during the first three days of the event. Therefore, for the first three days of the storm event for the T+1.8 and T+2.5 climate scenarios, all precipitation is modeled as rain. Infiltration saturation occurs faster, increasing the volume of surface runoff.

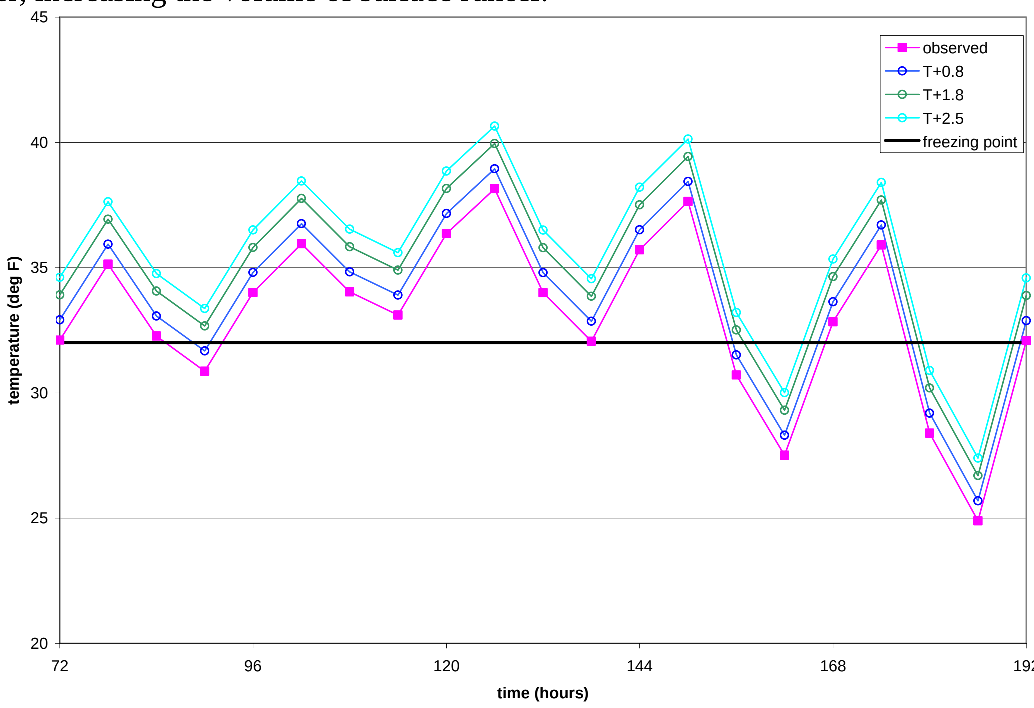


**Figure 21. Observed and perturbed temperatures during the first storm event during the January 1969 snow event in the New Bullards Bar basin above 5000 ft.** Observed temperatures are at or below the freezing point eight times. During the T+1.8 and T+2.5 climate scenarios, temperatures are below freezing three times during the event and are above freezing during the first three days of the event. Therefore, for the first three days of the storm event for the T+1.8 and T+2.5 climate scenarios, all precipitation is modeled as rain. Infiltration saturation occurs faster, increasing the volume of surface runoff.

The main storm peak further emphasizes the role of temperature and how it affects discharge (Figure 22). Three days after the antecedent event, the discharge from the main storm event begins. Now, the increased discharge from the two climate scenarios that increase temperatures and decrease storm intensities are more pronounced. Not only is the total volume discharge greater in the temperature-perturbed scenarios than in the observed event, but even the event peaks from the perturbed scenarios surpass the observed peak.

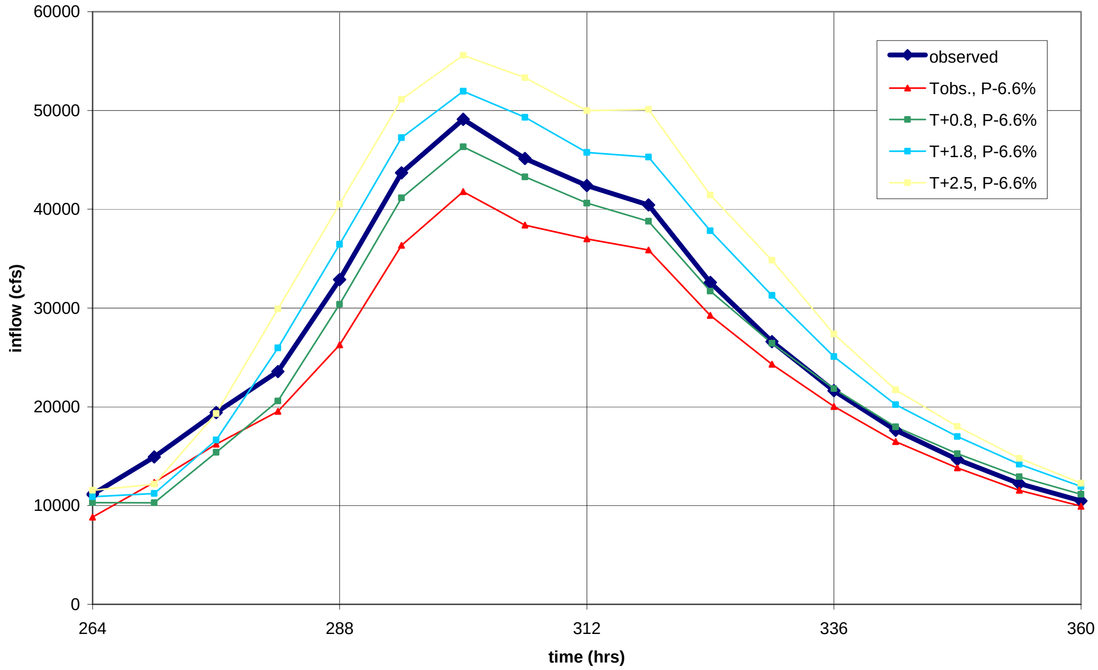


**Figure 22. Eleven days into the event, only two scenarios peak below the observed event – both simulate decreased precipitation and the two lowest temperature scenarios, Tobs and T+0.8°F.** However, towards the end of the second peak, flow volumes from the T+0.8 temperature scenario begin to surpass the observed event's flow volumes.

After the main storm event, another small event occurs within a few days (Figure 23). By now, even the climate scenario simulating the smallest temperature shift is generating discharge volumes greater than the observed event. The only climate scenario that yields less discharge than the observed event is the simulation of the observed temperature record with the decreased precipitation intensity.

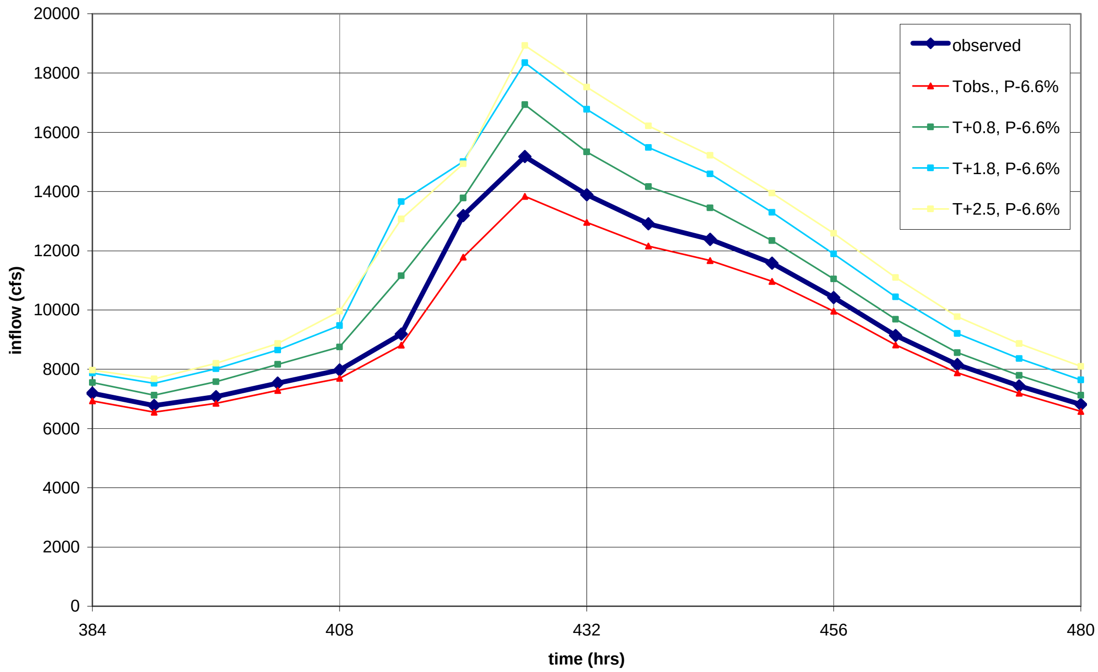


**Figure 23. By the end of the event, only one scenario – observed temperature combined with decreased precipitation – generates flow volumes below the observed event.**

The overall runoff volume and volume differences are illustrated below (Figures 24-25). The observed temperature record combined with decreased precipitation generates 11.5 percent less runoff than the observed event. While the scenario representing the smallest temperature increase (T+0.8°F) and decreased precipitation did not generate more runoff than the observed event, it still generated more runoff than the scenario combining observed temperatures with decreased precipitation. This implies that even with decreased precipitation intensities, increasing temperatures can still cause increased discharge volumes. This is due to the increasing basin wetness resulting from higher rain to snow ratios. Higher temperatures cause more of the storm to fall as rain rather than snow, increasing the volume of rainfall runoff despite the decreased precipitation intensity. This increased rainfall runoff saturates the basin more quickly than a storm with a greater snow to rain ratio. With more rainfall, the basin reaches its infiltration capacity more quickly. When storms occur within a few days of each other, as in the January 1969 event, more surface runoff is generated as a result of higher basin wetness and decreased snow to rain ratios.

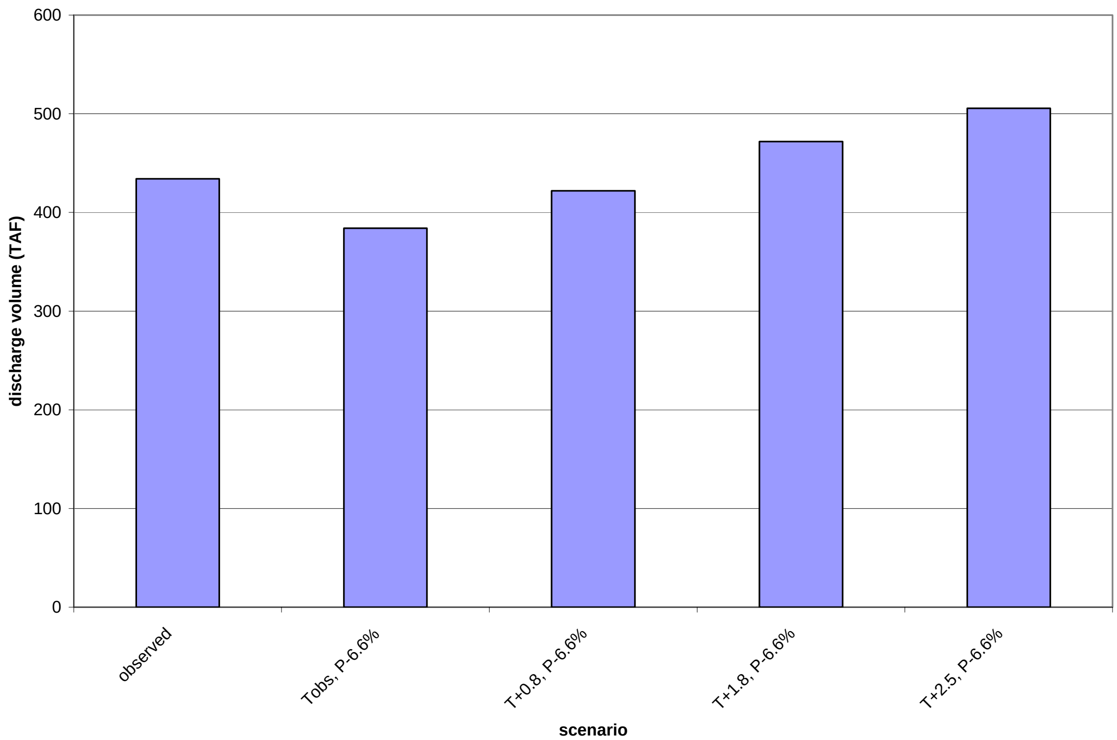


**Figure 24. Runoff volumes for the observed cold January 1969 event in the New Bullard's Bar basin and climate scenarios simulating decreased precipitation intensities with various temperature regimes.** When temperatures increase, runoff volumes also increase despite decreased precipitation intensities.

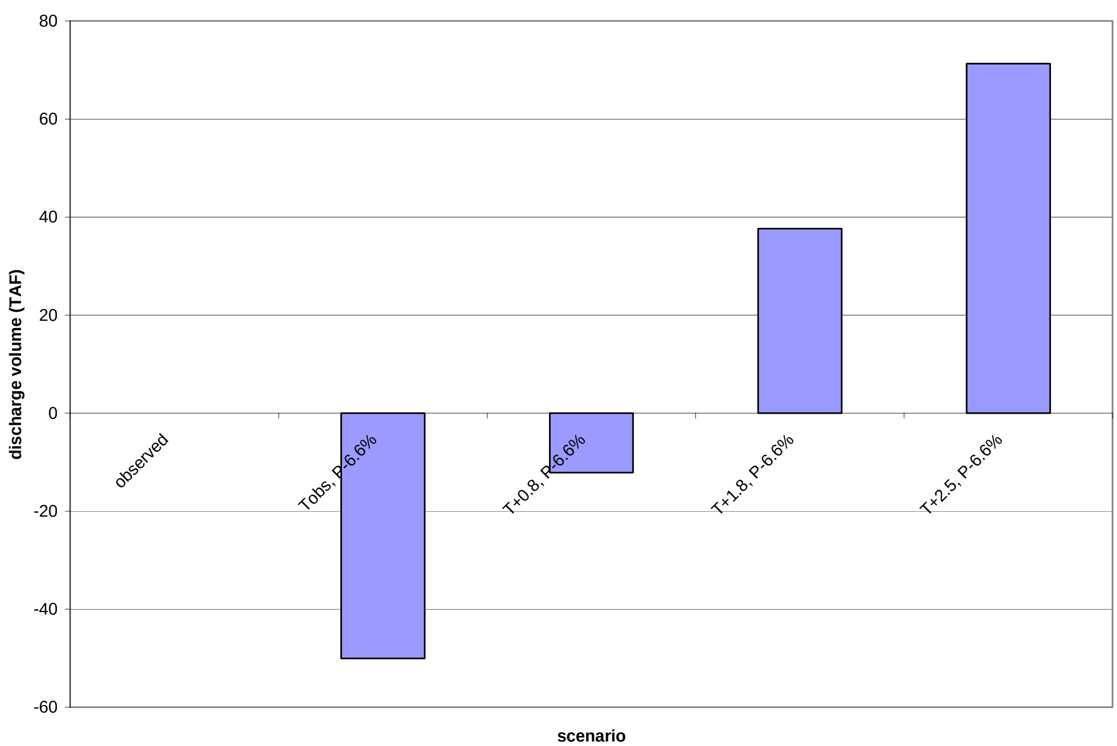


**Figure 25. Changes in runoff volume for the cold January 1969 event for New Bullards Bar.** Climate scenarios include decreased precipitation intensity scenarios with observed and perturbed temperatures.

*Effects of Climate Change on Reservoir Operations*

Although each of the three study basins displayed similar trends in their hydrologic response to temperature and precipitation perturbations, each basin reservoir is unique in its ability to control floods and provide a full conservation pool at the end of the flood season. Results ranged from dams that overtopped and provided consistently high conservation storage to dams that routed the largest inflows with room to spare and failed to fill the conservation pool more than a handful of years during the entire 40-year period of record. Results for each reservoir are presented below, though only figures for Shasta Dam's results are presented in the paper. Additional figures of results for Oroville and New Bullards Bar dams appear in the appendix.

Of the three reservoirs, Shasta Dam performed the best for flood control. For every sampled flood event and every climate change scenario, Shasta Dam's storage never exceeds the flood pool. Also, reservoir pool elevations are more sensitive to precipitation changes than temperature changes (Figures 26-27). The exceedence curves illustrate how the likelihood of exceeding each reservoir elevation changes with temperature and precipitation changes. As precipitation intensities increase, the exceedence curves shift to the right, indicating that the reservoir is more likely to contain larger volumes. On the other hand, exceedence values respond inversely to increasing temperatures. As the temperature regime warms, the exceedence curves shift left, reducing the likelihood that high storage volumes are reached. However, no matter what the climate regime, Shasta Dam performs poorly at filling its conservation pool at the end of the season when the rule curve limited the start date for refilling to March (Figure 28). When the conservation pool is full at the end of the refill period, the pool elevation reaches 1067.00 ft. When Shasta is forced to wait until March to begin refilling the reservoir, the conservation pool is filled less than 5 percent over the 40-year study period. When a rule curve that allows the refill to begin at the end of December is applied to the same climate scenarios and study period, Shasta Dam is 30 percent more likely to fill the conservation pool.

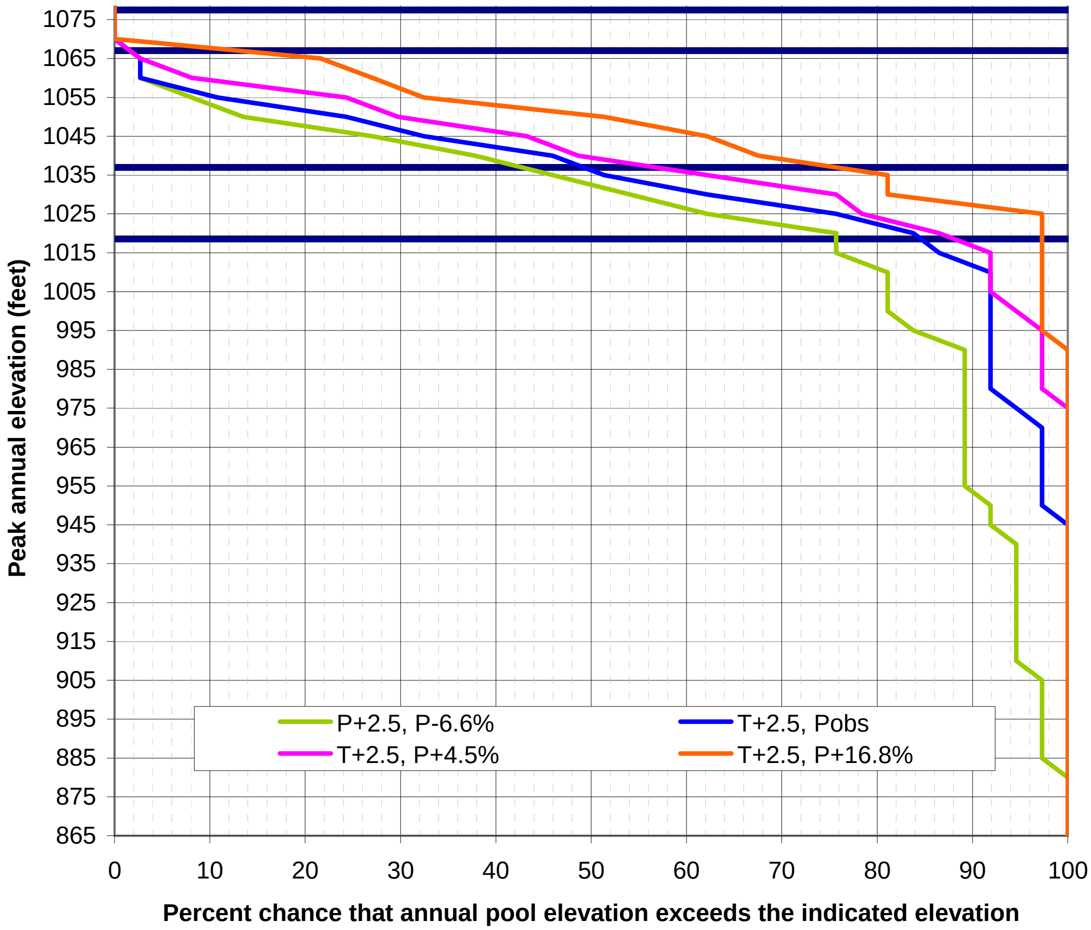


**Figure 26. Exceedence curves for Shasta Dam with increased temperatures (T+2.5$^{o}$F) and observed and perturbed precipitation records.** The four solid lines on the y-axis represent, from top to bottom, top of dam, gross pool, and spillway crest and bottom of flood control pool. The maximum allowable pool elevation at the end of the flood control season (i.e. the top of the conservation pool) is 1067.0 ft.

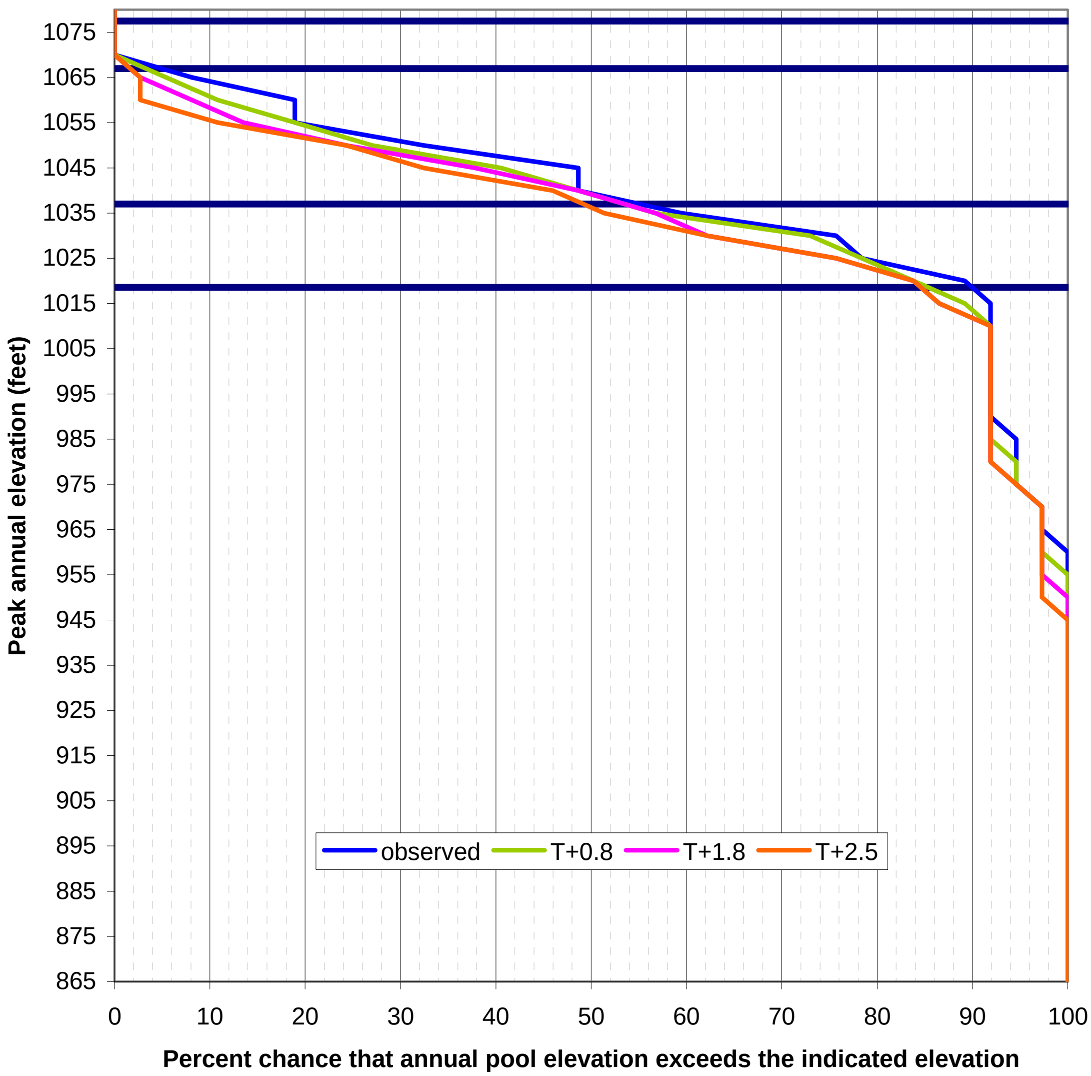


**Figure 27. Exceedence curves for Shasta Dam with the observed precipitation regime and observed and increased temperatures.** The four solid lines on the y-axis represent, from top to bottom, top of dam, gross pool, spillway crest and bottom of flood control pool. The maximum storage elevation at the end of the flood season (i.e. the top of the conservation pool) is 1067.0 ft.

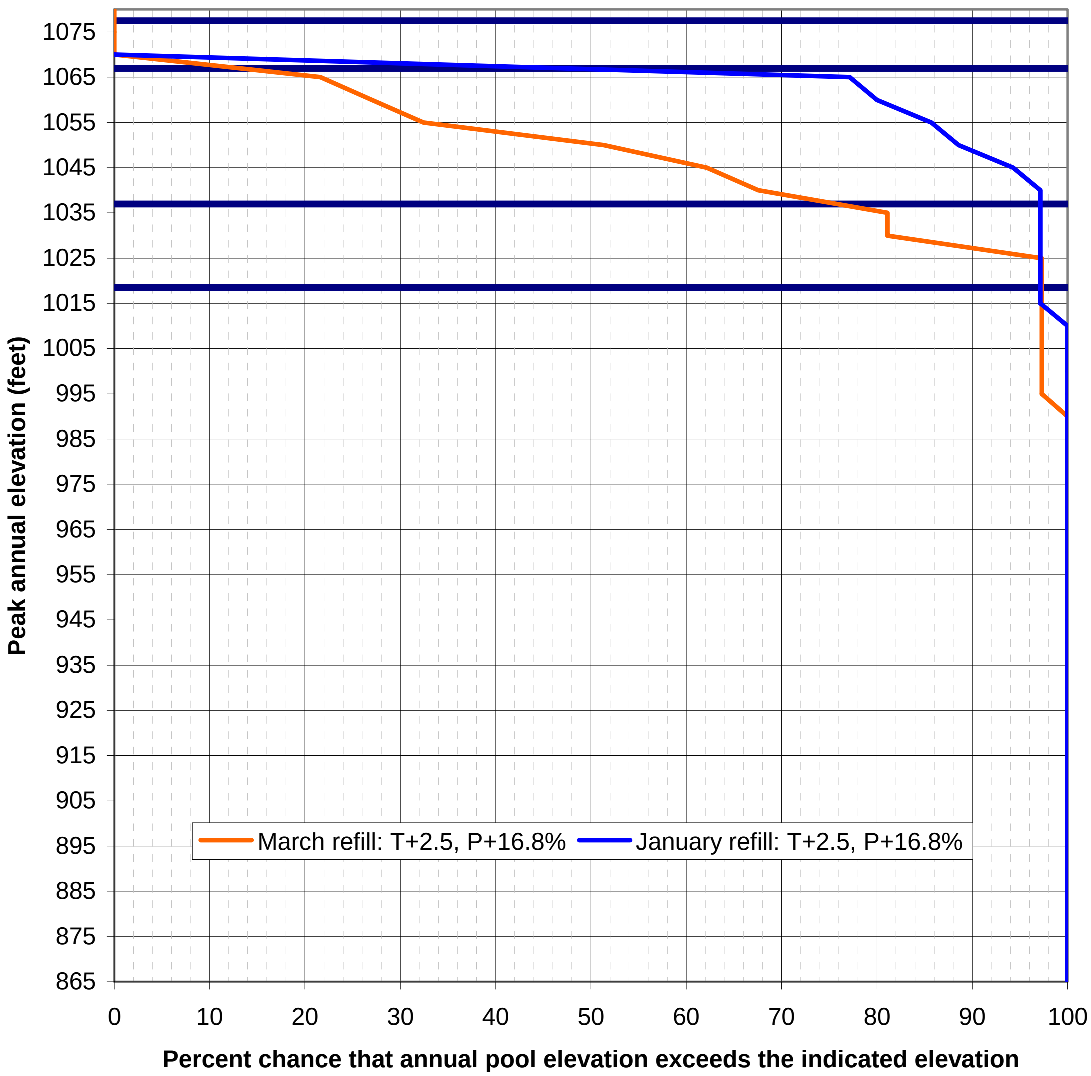


**Figure 28. Exceedence curves for the reservoir pool elevation in Shasta reservoir for two different refill schedules.** The orange line represents the latest possible refill schedule, which allows the reservoir to store more water beginning in March. The blue line represents the earliest possible refill schedule, when the reservoir begins storing floodwater beginning in January. The maximum allowable pool elevation at the end of the flood control season (i.e. the top of the conservation pool) is 1067.0 ft.

Oroville Dam performs the best at balancing flood control operations with water supply goals at the end of the flood period. Similarly to the model for Shasta Dam, the reservoir model for Oroville Dam applies a rule curve that requires a drawdown to 848.5 ft. (the deepest drawdown elevation indicated on the flood control diagram) and begins the refill period in April. Given that the reservoir is consistently drawn down to allow the maximum recommended flood control, some events still cause the reservoir pool elevation to rise into the surcharge pool, a zone above the flood pool and used to pass spillway flows.

For Oroville dam, for each climate scenario with increased precipitation intensity by 16.8 percent, one flood event causes the reservoir pool elevation to reach the surcharge zone. In the climate scenario that raises temperatures by 2.5°F and increases precipitation intensity by 16.8 percent, two of the flood events cause the reservoir pool elevation to reach the surcharge zone (Tables 10-11). During all other flood events, reservoir pool elevations never exceed the flood control zone. Also, despite requiring the deepest reservoir drawdown, Oroville successfully fills its conservation pool at the end of each flood season.

| Oroville Dam: Zone location of peak pool elevation for sampled flood events | | | | | | | | |
|---|---|---|---|---|---|---|---|---|
| event | scenario | | | | | | | |
| | observed | $T_{OBS}$, P-6.6% | $T_{OBS}$, P+4.5% | $T_{OBS}$, P+16.8% | T+0.8, P-6.6% | T+0.8, $P_{OBS}$ | T+0.8, P+4.5% | T+0.8, P+16.8% |
| Jan-63 | Flood | Flood | Flood | Flood | Flood | Flood | Flood | Flood |
| Dec-64 | Flood | Flood | Flood | Flood | Flood | Flood | Flood | Flood |
| Jan-69 | Flood | Flood | Flood | Flood | Flood | Flood | Flood | Flood |
| Jan-80 | Flood | Flood | Flood | Flood | Flood | Flood | Flood | Flood |
| Dec-82 | Flood | Flood | Flood | Flood | Flood | Flood | Flood | Flood |
| Mar-83 | Flood | Flood | Flood | Flood | Flood | Flood | Flood | Flood |
| Feb-86 | Flood | Flood | Flood | Top of Surcharge | Flood | Flood | Flood | Top of Sur-charge |
| Mar-95 | Flood | Flood | Flood | Flood | Flood | Flood | Flood | Flood |
| Jan-97 | Flood | Flood | Flood | Flood | Flood | Flood | Flood | Flood |

**Table 10. Location of peak pool elevations for sampled flood events in the Oroville basin.** Scenarios included in this table are the observed temperature regime and T+0.8°F regime combined with the observed and perturbed precipitation records. Highlighted areas indicate that the peak pool elevation exceeds the flood pool elevation.

| Oroville Dam: Location of peak pool elevation for sampled flood events | | | | | | | | |
|---|---|---|---|---|---|---|---|---|
| event | scenario | | | | | | | |
| | T+1.8, P-6.6% | T+1.8, $P_{OBS}$ | T+1.8, P+4.5% | T+1.8, P+16.8% | T+2.5, P-6.6% | T+2.5, $P_{OBS}$ | T+2.5, P+4.5% | T+2.5, P+16.8% |
| Jan-63 | Flood | Flood | Flood | Flood | Flood | Flood | Flood | Flood |
| Dec-64 | Flood | Flood | Flood | Flood | Flood | Flood | Flood | Flood |
| Jan-69 | Flood | Flood | Flood | Flood | Flood | Flood | Flood | Flood |
| Jan-80 | Flood | Flood | Flood | Flood | Flood | Flood | Flood | Flood |
| Dec-82 | Flood | Flood | Flood | Flood | Flood | Flood | Flood | Flood |
| Mar-83 | Flood | Flood | Flood | Flood | Flood | Flood | Flood | Flood |
| Feb-86 | Flood | Flood | Flood | Top of Surcharge | Flood | Flood | Top of Surcharge | Top of Surcharge |
| Mar-95 | Flood | Flood | Flood | Flood | Flood | Flood | Flood | Top of Surcharge |
| Jan-97 | Flood | Flood | Flood | Flood | Flood | Flood | Flood | Flood |

**Table 11. Location of peak pool elevations for sampled flood events in the Oroville basin.** Scenarios included in this table are the T+1.8°F and T+2.5°F temperature regimes combined with the observed and perturbed precipitation records. Highlighted areas indication that the peak pool elevation exceeds the flood pool elevation.

Exceedence curves for Oroville follow the same patterns as for Shasta. As precipitation intensities increase, the exceedence curve shifts to the right, indicating that the reservoir stores larger volumes of water more often. However, as temperatures increase, exceedence curves shift left, storing less water.

New Bullards Bar Dam performs the worst for flood protection under several climate change scenarios. Routing the observed record (i.e. no temperatures or precipitation perturbations), one flood event caused the reservoir pool to fill the surcharge zone. Both temperature and precipitation increases caused several flood events to fill the surcharge zone, reach the top of the dam and, in seven events, overtop the dam (Tables 12-13). These critical zone encroachments all occur during the rising limb of the main peak of the flood wave and last only a few hours. This indicates one drawback of ResSim – the model, unlike a reservoir operator, does not take forecasted flows into account. Instead, the model only takes observed flows into account, releasing only enough water to keep the reservoir under the rule curve reservoir pool elevation rather than releasing extra water in anticipation of future, larger flows. However, unlike the Shasta and Oroville simulations, no alternative curves are defined for New Bullards Bar that may allow additional flood control space. While flood control operations for New Bullards Bar Dam performed poorly, refill goals are met at the end of every flood season.

| New Bullards Bar Dam: Zone location of peak pool elevation for sampled flood events | | | | | | | | |
|---|---|---|---|---|---|---|---|---|
| event | scenario | | | | | | | |
| | observed | $T_{OBS}$, P-6.6% | $T_{OBS}$, P+4.5% | $T_{OBS}$, P+16.8% | T+0.8, P-6.6% | T+0.8, $P_{OBS}$ | T+0.8, P+4.5% | T+0.8, P+16.8% |
| Jan-63 | Flood | Flood | Flood | Flood | Flood | Flood | Flood | Flood |
| Dec-64 | Top of Surcharge | Flood | Top of Dam | Overtop | Flood | Top of Dam | Overtop | Overtop |
| Jan-69 | Flood | Flood | Flood | Flood | Flood | Flood | Flood | Flood |
| Jan-80 | Flood | Flood | Flood | Flood | Flood | Flood | Flood | Flood |
| Dec-82 | Flood | Flood | Flood | Flood | Flood | Flood | Flood | Flood |
| Mar-83 | Flood | Flood | Flood | Flood | Flood | Flood | Flood | Flood |
| Feb-86 | Flood | Flood | Flood | Flood | Flood | Flood | Flood | Flood |
| Mar-95 | Flood | Flood | Flood | Flood | Flood | Flood | Flood | Flood |
| Jan-97 | Flood | Flood | Flood | Top of Dam | Flood | Flood | Top of Surcharge | Top of Dam |

**Table 12. Location of peak pool elevations for sampled flood events in the New Bullards Bar basin.** Scenarios included in this table are the observed temperature regime and T+0.8$^{o}$F regime combined with the observed and perturbed precipitation records. Highlighted areas indicate that the peak pool elevation exceeds the flood pool elevation.

| New Bullards Bar Dam: Zone location of peak pool elevation for sampled flood events | | | | | | | | |
|---|---|---|---|---|---|---|---|---|
| event | scenario | | | | | | | |
| | T+1.8, P-6.6% | T+1.8, $P_{OBS}$ | T+1.8, P+4.5% | T+1.8, P+16.8% | T+2.5, P-6.6% | T+2.5, $P_{OBS}$ | T+2.5, P+4.5% | T+2.5, P+16.8% |
| Jan-63 | Flood | Flood | Flood | Flood | Flood | Flood | Flood | Flood |
| Dec-64 | Flood | Top of Dam | Overtop | Overtop | Flood | Top of Surcharge | Overtop | Overtop |
| Jan-69 | Flood | Flood | Flood | Flood | Flood | Flood | Flood | Flood |
| Jan-80 | Flood | Flood | Flood | Flood | Flood | Flood | Flood | Flood |
| Dec-82 | Flood | Flood | Flood | Flood | Flood | Flood | Flood | Flood |
| Mar-83 | Flood | Flood | Flood | Flood | Flood | Flood | Flood | Flood |
| Feb-86 | Flood | Flood | Flood | Top of Dam | Flood | Flood | Flood | Overtop |
| Mar-95 | Flood | Flood | Flood | Flood | Flood | Flood | Flood | Flood |
| Jan-97 | Flood | Flood | Top of Surcharge | Overtop | Flood | Flood | Top of Surcharge | Top of Dam |

**Table 13. Location of peak pool elevations for sampled flood events in the New Bullards Bar basin.** Scenarios included in this table are the T+1.8°F and T+2.5°F temperature regimes combined with the observed and perturbed precipitation records. Highlighted areas indicate that the peak pool elevation exceeds the flood pool elevation.

Exceedence curves for New Bullards Bar follow the same patterns as the curves for Shasta and Oroville dams. When temperatures are increased, curves shift to the left, with water storage volumes decreasing as temperatures increase. When precipitation intensities are increased, water storage volumes also increase and exceedence curves shift to the right.

## Chapter VI. Discussion

Though each of the three basins has unique hydrologic characteristics, broad trends are illustrated in our results and are consistent with previous studies. These characteristics include the impact of increasing temperature on mid- and low-elevation basins, the different responses of warm and cold storms to temperature increases, and the poor performance of static flood control rule curves. Each of these results indicates how existing flood control operations will be challenged given any of the studied climate change scenarios.

For mid to low elevation basins, the hydrologic regime is sensitive to small shifts in temperature. Both warm and cold storms react to small temperature increases. For all three study basins, the smallest temperature increase (0.8°F) alters cold storms' rain to snow ratio, causing more of the storm to fall as rain and less as snow. Even events during which their observed temperatures are below the freezing point are affected, indicating that elevations in the Sacramento basin are low enough to respond to any temperature shift. The coldest storms are not cold enough to escape being affected by temperature increases. The basin-wide response to increasing temperatures is larger rainfall runoff volumes. This forces dams to accommodate larger inflow volumes over shorter periods. The increased fraction of rain in precipitation also accelerates the rate at which the basin achieves its infiltration saturation; because the basin saturates earlier, ensuing storm events generate more surface runoff due to the ground's reduced infiltration capacity.

Warm storms are affected indirectly by increasing temperatures. Warm storms do not change precipitation composition due to temperature increases because temperatures are already above the freezing point; no physical change of state occurs. However, the basin is affected by temperature increases. Evaporation and transpiration rates increase, creating dryer basin conditions. Drier basin conditions allow for larger volumes of water to percolate into the soil tanks (NOAA 2002). The increased infiltration capacity results in less surface runoff. This is illustrated by two of the warmest storms, December 1964 and January 1997, which generated less runoff in the warmest temperatures scenarios. Increased basin wetness combined with smaller, antecedent cold events also affect warm storms similarly to cold storms: the warm temperatures cause earlier, cold events to precipitate more rain than snow causing the basin to reach saturation sooner. Even though the composition of warm storms is unaffected due to the small fraction of snow in the observed event, runoff volumes still increase due to the reduced infiltration capacity from the wetness caused by the earlier storm event. These larger runoff volumes again force dams to handle larger flood volumes.

Increased temperatures also can affect storm runoff more strongly than changes in precipitation intensities. Some of the sampled study storms simulated an overall decrease of the observed precipitation record by 6.6 percent. However, in some instances, discharge volumes from these storms still increased. In these cases, basin wetness plays a key role that affects runoff volumes. While the storms themselves are not changed, the basin is affected by antecedent conditions. Earlier, colder events are affected by the small temperature increase. They yield more rainfall runoff as temperatures increase, causing the basin to contain more ground moisture. Greater ground moisture decreases the basin's infiltration capacity, with less absorption of later rainfall for each subsequent event. When future storms arrive, the basin can absorb less of its rainfall runoff, causing discharge volumes to increase for a storm that is not affected by changes in precipitation intensities. These effects are magnified as temperatures continue to increase until all storms become "warm" storms.

Increasing temperatures also overcome the effects of decreased precipitation intensities. Decreased precipitation scenarios may decrease storm intensities, but do not always decrease flow volumes.  Primarily during cold storms, temperatures change the storms precipitation composition, increased the fraction of rain and decreasing the fraction of snow. The increasing rainfall runoff is sometimes enough to overcome the decrease in precipitation intensity, yielding more overall discharge than the observed event. Basin wetness also plays a role in increasing runoff volumes despite decreases in precipitation intensity. The January 1969 event illustrates how antecedent flood events affect the runoff volumes of future events. Earlier events saturate the basin, preventing water from infiltrating and forcing it to runoff as surface flow. Therefore, even though less water may fall in a storm due to decreased precipitation intensities, discharge volumes will still increase if the water that had infiltrated is now forced to become surface runoff.

The flood control rule curves also supported previous hypotheses about the utility of static curves given a changed climate. The flood control curve for New Bullards Bar, which incorporates no basin state parameter and does not take advantage of the basin's rainflood characteristics, performed poorly under most climate change scenarios. Reservoir pool elevations exceeded the flood pool zone during 19 of the 144 sampled and overtopped the dam during eight sampled flood events. This is the only study basin that indicates a need for more flood control space in the reservoir than already exists. For each storm, including those that filled the reservoir to the surchange pool and overtopped the dam, the maximum flood space was available at the beginning of each event. Nevertheless, maximum release limits prevented the reservoir from releasing water quickly enough to avoid overtopping. Release volumes are often restricted due to common control points with Oroville dam that prevent more water being released from New Bullards Bar until its pool reaches critical zones.

Both Shasta and Oroville dams demonstrate how adding flexibility to flood control curves can improve both flood protection and water supply operations. Shasta's alternative refill schedule allowed for both good flood protection and good refill volumes at the end of the flood season. Oroville's curve provided both good flood protection and refill volumes during flood years; using the alternative curves that do not draw down the flood pool to provide maximum flood control space may provide superior refill capabilities during dry years as well.

## Chapter VII. Future Studies and Conclusions

### *Future Studies*

While this study provides a preliminary evaluation of how flood control curves for projects in the Sacramento basin respond to climate change, future studies can provide a more refined look at the question. Primarily, the method by which climate change is applied to the study areas can be improved as can the model used to analyze each dam's response to inflows.

This study increased all temperatures by a fixed amount. However, temperature increases are likely to vary on both diurnal and seasonal cycles; the largest increases occur from January to March (Duffy, P.B. Personal communication, 2008). Knowles et al. (2006) found that declines in snow versus rain occurred the most in January in the Northern Sierra Nevada and Pacific Northwest, indicating that intra-annual patterns of warming are worth examining as they occur during peak precipitation periods in the Sacramento basin. Also, minimum temperatures increase more than maximum temperatures in the diurnal cycle (Walther et al. 2002). Refining this study by refining the temperature increase pattern could yield significant results.

Also, improving ResSim to apply dynamic rule curves to reservoirs will improve the ability to test the performance of existing curves. While alternative curves can be applied using scripting, the inclusion of dynamic curves into upcoming versions of ResSim would be advantageous (Klipsch, J.D. Personal communication, 2008).

*Conclusions*

Both the hydrologic regime and flood control operation in the Sacramento basin are affected by increasing temperatures. Among the effects are:

1. *Hydrologic regimes in the Sacramento basin will respond to even the smallest changes projected in the range of possible climate change scenarios for the year 2025.* Most importantly, small increases in temperature affect the precipitation composition of storms, causing more rainfall runoff in previously cold storms.
2. *Increased precipitation intensities lead to an increase in the volume of rainfall runoff; however, decreased precipitation intensities do not always decrease volumes of rainfall runoff.* Temperature effects are sometimes strong enough to overcome the effects of reduced precipitation intensities, resulting in increased runoff volumes. In all cases, the result of these increased runoff volumes is increased flood risk.
3. *Static rule curves, such as the curve for New Bullards Bar Dam, perform poorly for a range of climate scenarios.* At times, reservoir pool levels rise above the dam's crest to overtop the structure. Changes that may improve the performance of New Bullards Bar's flood control operations include reviewing the drawdown rates of the flood pool, incorporating a state parameter to allow more flexible release decisions or incorporating forecast information into release decisions to allow larger releases earlier in the flood event.
4. *Dynamic rule curves, such as the curves designed for Oroville and Shasta dams, provide more flexible drawdown and refill requirements, resulting in better flood protection and refill performance.* However, the specific benefits of using dynamic curves remain to be sufficiently quantified.

**References**

Aguado, E., D. Cayan, L. Riddle, M. Roos. 1992. Climatic Fluctuations and the Timing of West Coast Streamflow. *American Meteorological Society* **5:**1468-1483.

Barnett, T.P., D. W. Pierce, H.G. Hidalgo, C. Bonfils, B.D. Santer, T. Das, G. Bala, A.W. Wood, T. Nozawa, A.A. Mirin, D.R. Cayan, M.D. Dettinger. 2008. Human-Induced Changes in the Hydrology of the Western United States. *Science* **319:** 1080-1082.

Bonfils, C.J., P.B. Duffy, B.D. Santer, D.B. Lobell, T.M. Wigley. 2006. Understanding observed and simulated historical temperature trends in California. Conference paper: *American Geophysical Union Fall Meeting*

Carpenter, T.M. and Georgakakos, K.P. 2001. Assessment of Folsom lake response to historical and potential future climate scenarios: 1. Forecasting. *Journal of Hydrology* **249:** 148-175

Carpenter, T.M., K.P. Georgakakos, N.E. Graham, A.P Georgakakos, H. Yao. 2003. Incorporating Hydroclimatic Variability in Reservoir Management at Folsom Lake, California. Paper #7.10. AMS 83 Annual meeting, Long Beach, CA 9-13 February 2003.

Cayan, D.R. and Riddle L.G. 1993. The Influence of Precipitation and Temperature on Seasonal Streamflow in California. *Water Resources Research* **29:**1127-1140

Collins, R. and Whitin, B. 2004. Variability in snow affecting reservoir operation. Workshop presentation: *USACE Climate Impacts Workshop*. United States Army Corps of Engineers. Sacramento

Countryman, J. Personal communication. 9/10/2007

Countryman, J. Personal communication. 8/21/2008

Delworth TL et al. 2005 GFDL's CM2 global coupled climate models part 1: formulation and simulation characteristics. *J Climate* **19**:643–674

Diansky NA and Volodin EM. 2002. Simulation of present-day climate with a coupled atmosphere–ocean general circulation model. *Izv Atmos Ocean Phys* (Engl Transl) **38**(6):732–747

Droz, M. and Wunderle, S. 2002. Snow line analysis in the Alps based on NOAA-AVHRR data spatial and temporal patterns for winter and springtime in 1990, 1996 and 1999. Conference paper: *EARSeL-LISSIG-Workshop Observing our Cryosphere from Space*

Duffy, P.B. Personal communication. 02/01/2008

Faber, B.A. Personal communication. 09/14/2007

Faber, B.A. Personal communication. 07/16/2008

Georgakakos, K.P., N.E. Graham, T.M. Carpenter, A.P. Georgakakos, and H. Yao. Integrating climate-hydrology forecasts and multi-objective reservoir management for northern California. *Eos* **86**: 122-127

Gordon C., C. Cooper, C.A. Senior, H.T. Banks, J.M. Gregory, T.C. Johns, J.F.B. Mitchell, R.A.Wood RA. 2000. The simulation of SST, sea ice extents and ocean heat transports in a version of the Hadley Centre coupled model without flux adjustments. *Clim Dyn* **16**:147–168

Gordon H.B., L.D. Rotstayn, J.L. McGregor, M.R. Dix, E.A. Kowalczyk, S.P. O'Farrell, L.J. Waterman, A.C. Hirst, S.G. Wilson, M.A. Collier, I.G. Watterson, T.I. Elliott. 2002 The CSIRO Mk3 climate system model, CSIRO Atmospheric Research Technical Paper No.60, CSIRO. Division of Atmospheric Research, Victoria, Australia, p 130

Hamlet, A.F. and D.P. Lettenmaier. 2007. Effects of 20$^{th}$ century warming and climate variability on flood risk in the western U.S. *Water Resources Research* **43**

Howat, I.M. and Tulaczyk, S. 2005. Climate sensitivity of spring snowpack in the Sierra Nevada. *Journal of Geophysical Research-Earth Surface* **110**

IPSL. 2005. The new IPSL climate system model: IPSL-CM4. Institut Pierre Simon Laplace des Sciences de l'Environnement Global, Paris, France, p 73

Jungclaus J.H., M. Botzet, H. Haak, N. Keenlyside, J-J. Luo, M. Latif, J. Marotzke, U. Mikolajewicz, E. Roeckner. 2006. Ocean circulation and tropical variability in the AOGCM ECHAM5/MPI-OM. *J Climate* **19**:3952–3972

K-1 model developers (2004) K-1 coupled model (MIROC) description, K-1 technical report, 1. In: Hasumi H, Emori S (eds) Center for Climate System Research, University of Tokyo, p 34

Karl, T.R., S.J.Hassol, C.D. Miller and W.L. Murray (Eds), 2006: Temperature trends in the lower atmosphere: Steps for understanding and reconciling differences. A Report by the Climate Change Science Program and Subcommittee on Global Change Research, Washington D.C., 180 pp. Available at http://www.climatescience.gov/Library/sap/sap1-1/finalreport/default.htm

Kim, J, N. Miller, A. Guetter, and K. Georgakakos. 1998. River flow response to precipitation and snow budget in California during the 1994/95 winter. *J. of Climate* **11**: 2376-2386.

Klispch, J.D. Personal communication. 06/08/2008

Knowles, N. and Cayan D.R. 2004. Elevational dependence of projected hydrologic changes in the San Francisco estuary and watershed. *Climate Change* **62:** 319-336

Knowles, N., M.D. Dettinger, D.R. Cayan. 2006. Trends in Snowfall versus Rainfall in the Western United States. *Journal of Climate* **19:** 4545-4559.

Lee, S.Y, A.F. Hamlet, C.J. Fitzgerald, S.J. Burges, D.P. Lettenmaier. 2006. Optimized Flood Control in the Columbia River Basin for a Global Warming Scenario. *Operating Reservoirs in Changing Conditions. Proceedings of the ASCE Operations Management Conference.* August 14-16.

Maurer, E.P. 2007. Uncertainty in hydrologic impacts of climate change in the Sierra Nevada, California, under two emissions scenarios. *Climate Change* **82**: 309-325.

McCabe, G.J. and Clark, M.P. 2005. Trends and Variability in Snowmelt Runoff in the Western United States. *Journal of Hydrometeorology* **6**: 476-482.

Medellin-Azuara, J., J.J. Harou, M.A. Olivares, K. Madani, J.R. Lund, R.E. Howitt, S.T. Tanaka, M.K. Jenkins, T. Zhu. 2008. Adaptability and adaptations of California's water supply system to dry climate warming. *Climate Change* **87**: S75-S90

Miller, N. L. 2003. California Climate Change, Hydrologic Response and Flood Forecasting. Conference paper: *International Expert Meeting on Urban Flood Management.*

Miller, N, Bashford, K, and Strem, E. 2003. Potential impacts of climate change on California hydrology. *J. of the American Water Resources Association (JAWRA)* **39**(4): 771-784.

Milly, P.C.D., J. Betancourt, M. Falkenmark, R.M. Hirsch, Z. W. Kundzewicz, D.P. Lettenmaier, R.J. Stouffer. 2008. Stationarity is dead: whither water management? *Science* **319:** 573-574.

Mote, P.W. 2003. Trends in snow water equivalent in the Pacific Northwest and the climatic causes. *Geophysical Research Letters* **30**: 3-1 – 3-4

Mote, P.W., A.F. Hamlet, M. P. Clark, and D.P. Lettenmaier. 2005. Declining Mountain Snowpack in Western North America. *American Meteorological Society*: 39-49.

Mount, J. 1995 California Rivers and Streams: The Conflict Between Fluvial Process and Land Use. *University of California Press*

Nakicenovic, N.et al. 2000. Special report on emissions scenarios. Cambridge University Press, Cambridge, U.K.

National Oceanic and Atmospheric Administration. 2002. National Weather Service River Forecast System User's Manual: Part 2.

Peterson, D.H., R.E. Smith, M.D. Dettinger, D.R. Cayan, L. Riddle. 1999. An Organized Signal in Snowmelt Runoff Over the West. Specialty conference on consequences of climate variability and change to water resources of the United States. American Water Resources Association.

Peterson, D., R. Smith, S. Hager, D. Cayan and M. Dettinger. 2003. Air temperature and snowmelt discharge characteristics, Merced River at Happy Isles, Yosemite National Park, central Sierra Nevada. *Proceedings of the Twentieth Annual Pacific Climate Workshop*, p. 53-64.

Regonda, S.K., B. Rajagopalan. 2005. Seasonal Cycle Shifts in Hydroclimatology over the Western United States. *Journal of Climate* **18**: 372-384

Russell G.L., J.R. Miller, D. Rind. 1995. A coupled atmosphere–ocean model for transient climate change studies. *Atmos–Ocean* **33**:683–730

Russell G.L., J.R. Miller, D. Rind, R.A. Ruedy, G.A. Schmidt, S. Sheth. 2000. Comparison of model and observed regional temperature changes during the past 40 years. *J Geophys Res* **105**:14891–14898

Salas-Mélia D., F. Chauvin, M. Déqué, H. Douville, J.F. Gueremy, P. Marquet, S. Planton, J.F. Royer, S. Tyteca. 2005. Description and validation of the CNRM-CM3 global coupled model. *Clim Dyn* (in review)

Saunders, S., C. Montgomery, T. Easley. 2008. Hotter and Drier: The West's Changed Climate. *The Rocky Mountain Climate Organization.*

Smith, R. L. and Smith, T. M. 2006. *Elements of Ecology*. 6th edition.

Townsley, E.S. Personal communication. 05/11/2007

United States Army Corps of Engineers. 2005. Oroville Dam and Lake, Feather River, California: Water Control Manual.

United States Army Corps of Engineers. 2004. New Bullards Bar Dam and Reservoir, North Yuba River, California: Water Control Manual.

United States Army Corps of Engineers. 1977. Shasta Dam and Lake: Report on Reservoir Regulations for Flood Control.

United States Army Corps of Engineers. 1959. Master Manual of Reservoir Regulation: Sacramento River Basin, California.

United States National Oceanic and Atmospheric Administration. 2008. National Weather Service River Forecast System: Total River and Hydrologic Forecasting System.

Walther, G.R., E. Post, P. Convey, A. Menzel, C. Parmesan, T. J. C. Beebee, J.M. Fromentin, O. Hoegh-Guldberg, F. Bairlein. 2002. Ecological responses to recent climate change. *Nature* **416**: 389-395

Washington W.M., J.W. Weatherly, G.A. Meehl, A.J. Semtner, T.W. Bettge, A.P. Craig, W.G. Strand, J. Arblaster, V.B. Wayland, R. James, Y. Zhang. 2000. Parallel climate model (PCM) control and transient simulations. *Clim Dyn* **16**:755–774

Wood, A.W., E.P. Maurer, A. Kumar, D.P. Lettenmaier. 2002. Long range experimental hydrologic forecasting for the eastern U.S. *J Geophys Res.* **107**: 4429

Yao, H. and Georgakakos, A. 2001. Assessment of Folsom lake response to historical and potential future climate scenarios. *Journal of Hydrology* **249**: 176-196

Yukimoto S, A. Noda, A. Kitoh, M. Sugi, Y. Kitamura, M. Hosaka, K. Shibata, S. Maeda, T. Uchiyama. 2001. The new Meteorological Research Institute coupled GCM (MRI-CGCM2) – model climate and variability. *Pap Meteorol Geophys* **51**:47–88

Zhu, T., J.R. Lund, M.W. Jenkins, G.F. Marques, and R.S. Ritzema. 2007. Climate Change, Urbanization, and Optimal Long-term Floodplain Protection. *Water Resources Research* **43**

# Appendix A: Climate change scenario effects on New Bullards Bar inflows

Ensemble charts of sampled flood events for New Bullards Bar basin and their accompanied volume changes.

| | **New Bullards Bar @ Downieville** | | |
|---|---|---|---|
| | Precipitation during past 30 days (inches) | past WY | basin conditions |
| Jan-63 | 6.3 | Below Normal | Dry |
| Dec-64 | 12.07 | Dry | Wet |
| Jan-69 | 14.5 | Below Normal | Wet |
| Jan-80 | missing | Below Normal | N/A |
| Dec-82 | 11.09 | Dry | Wet |
| Mar-83 | 12.47 | Wet | Wet |
| Feb-86 | 9.8 | Dry | Dry |
| Mar-95 | 2.16 | Critical | Dry |
| Jan-97 | 35.25 | Wet | Wet |

**Table 14. Basin wetness conditions above New Bullards Bar dam preceding the sampled flood events**

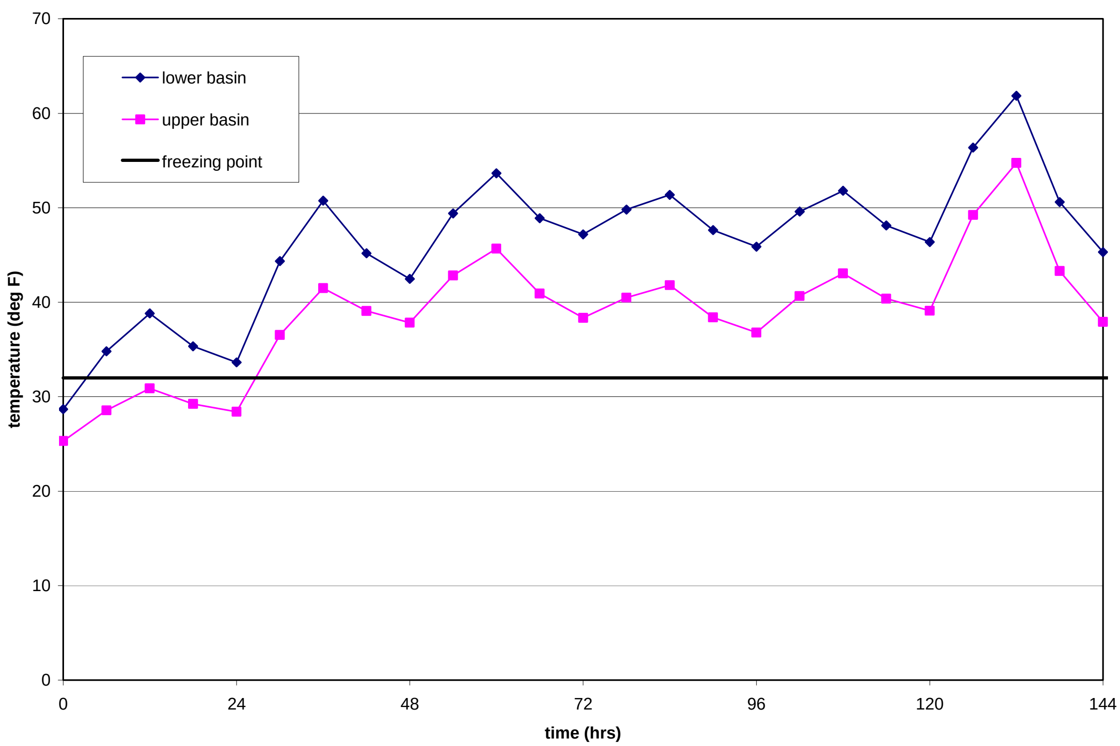


**Figure 29. Temperature trends for the January 1963 rain event.** Temperatures are above freezing for the whole storm event, implying that the event resulted in little snowpack and mainly consisted of rainfall

runoff. As such, increasing temperatures are not expected to result in a significant discharge volume increase.

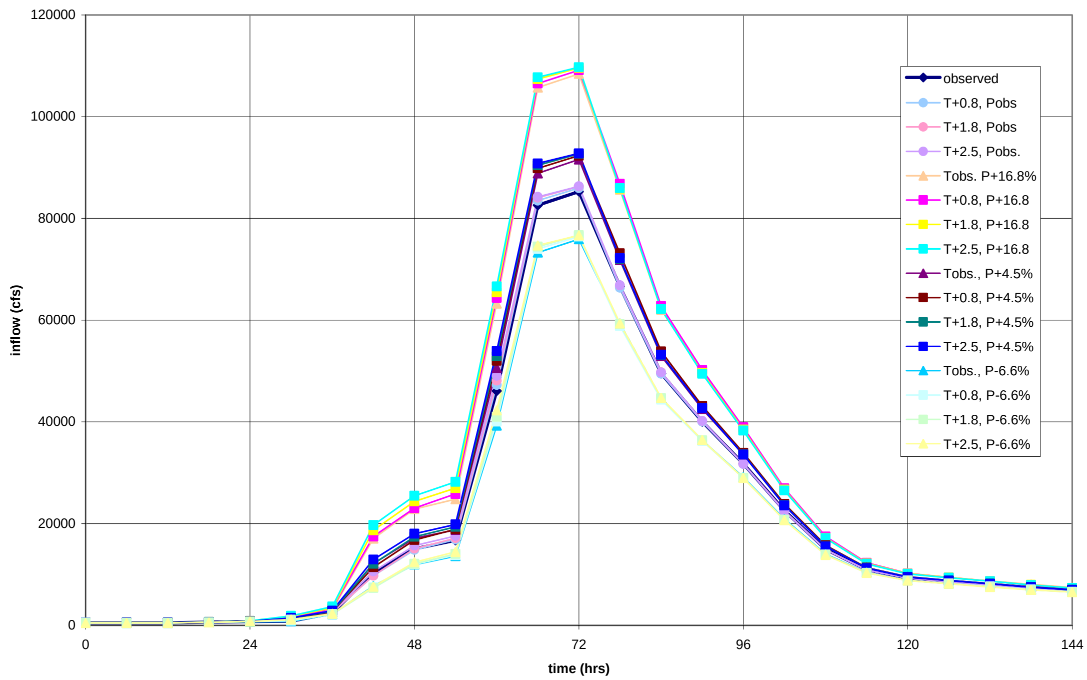


**Figure 30. Climate change inflows for the January 1963 event in the New Bullards Bar basin.** The 1963 event is a predominantly rain event. Temperature increases do not cause a significant change in discharge volumes. Large shifts in discharge volumes are caused by precipitation shifts.

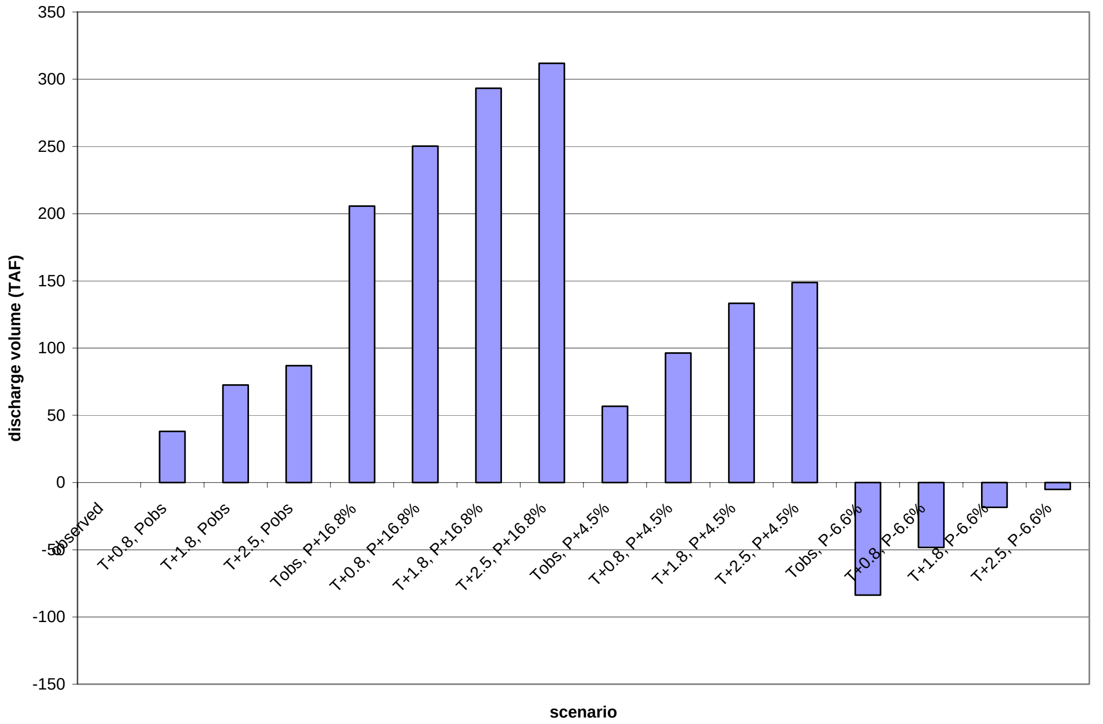


**Figure 31. Change in runoff volumes for the January 1963 rain event.** Although the event was warm, temperature increases still cause increases in overall discharge volume. Because temperatures are above freezing during the observed event (meaning the storm is mostly rain), increased temperatures are unlikely to have a large impact on the rain-snow ratio. One possible reason for increased runoff volumes is an increase in snowmelt from the existing snowpack.

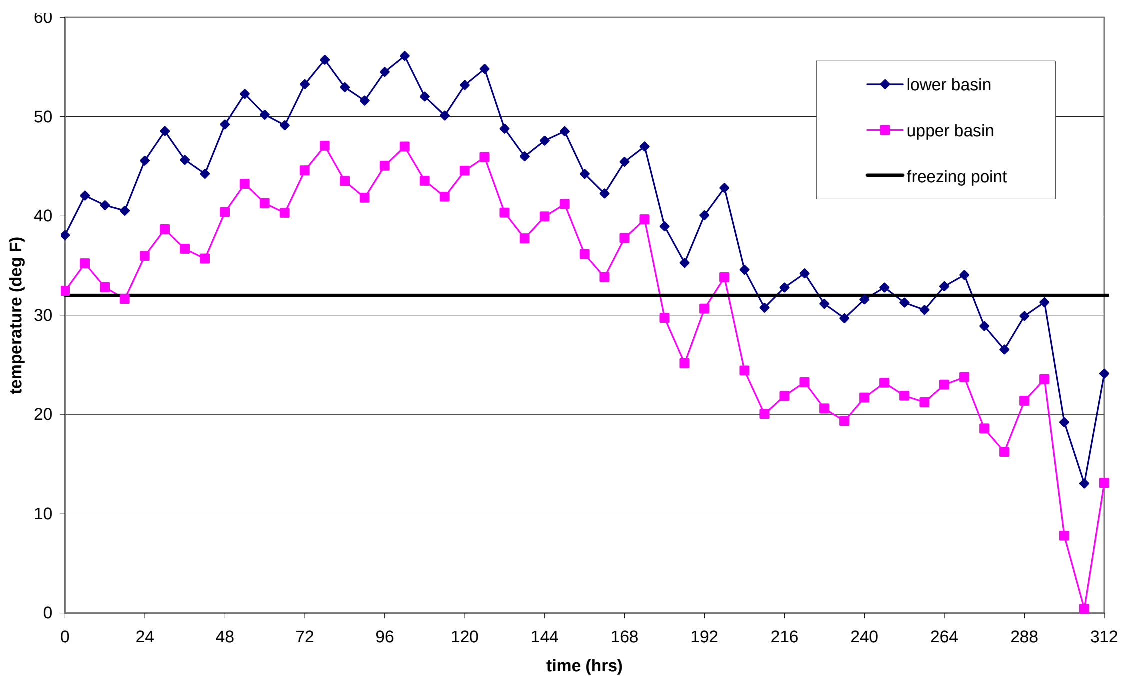


**Figure 32. Temperature trends for the December 1964 rain event.** Though this event is considered a rain event due to the above-freezing temperatures during the event peak (hours 72-96), cold temperatures occur during the post-peak event (hours 160-192). This post peak event is affected as temperatures increase, resulting in a higher rain to snow ratio.

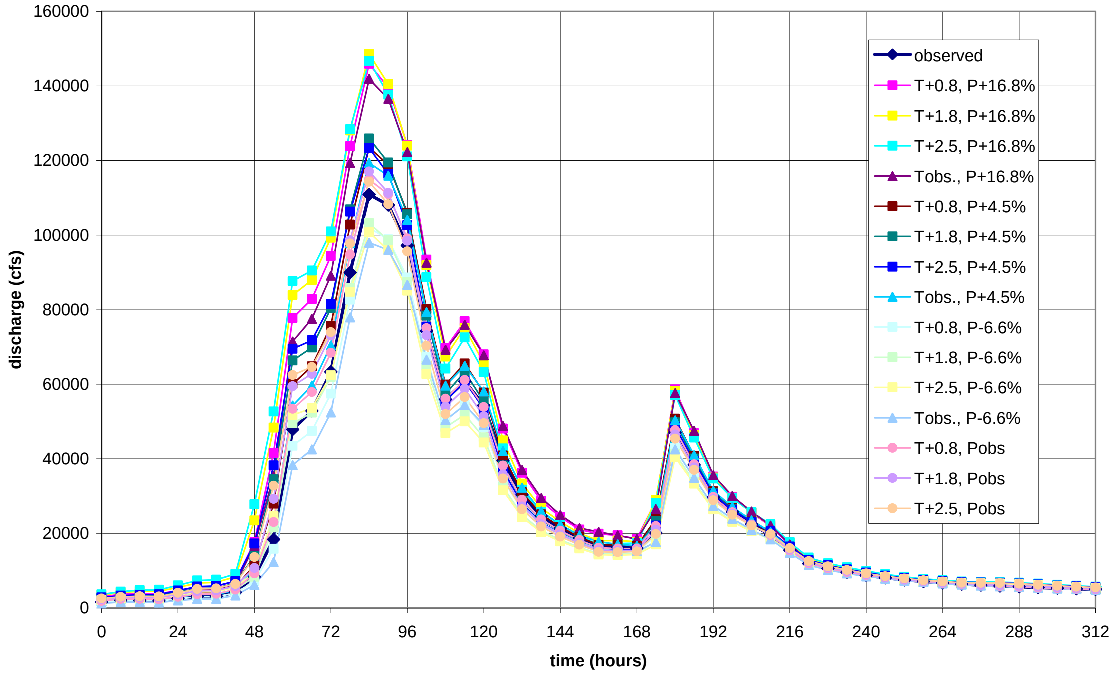


**Figure 33. Climate change inflows for the January 1965 rain event in the New Bullards Bar basin.** The main event peaks during a period of above-freezing temperatures. Therefore, increasing temperatures do not significantly increase the amount of rainfall runoff. The second, smaller peak occurs during a period of below-freezing temperatures. Increasing the temperature regime affects the discharge volume, which increases proportionally to temperature changes.

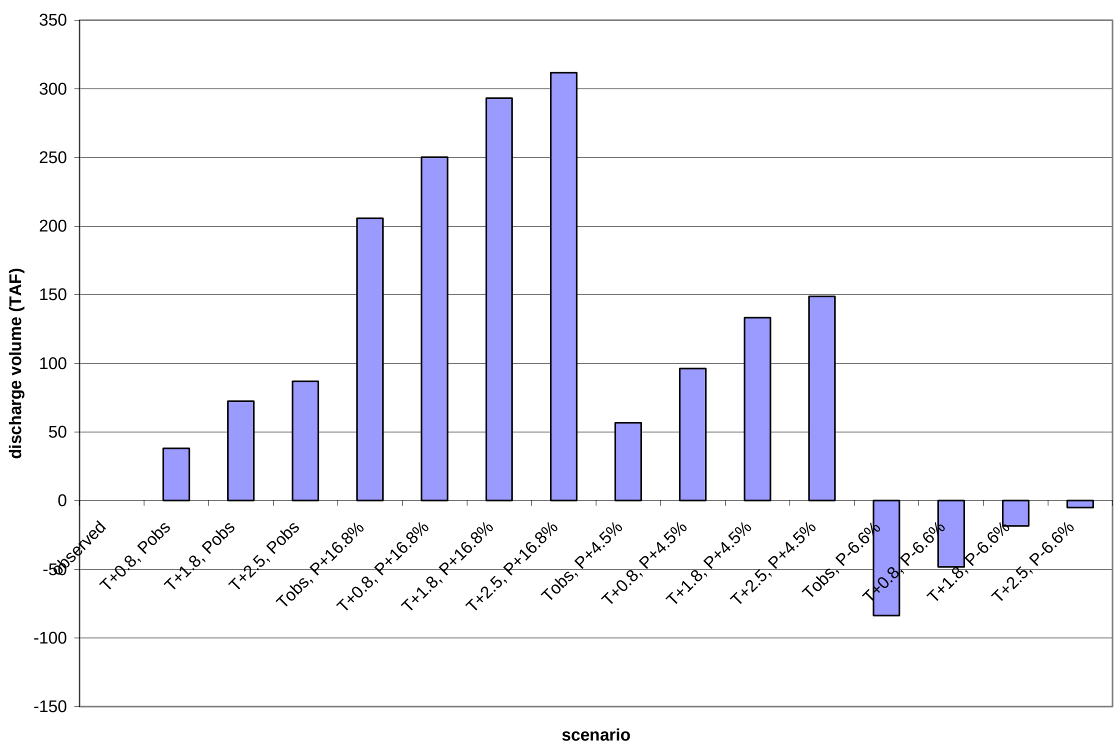


**Figure 34. Changes in discharge volume from the observed December 1964 rain event.** Though the event was mainly warm, a smaller, cold event occurred soon after the flood event. Increased flow volumes are likely due to temperature effects on the colder, second event.

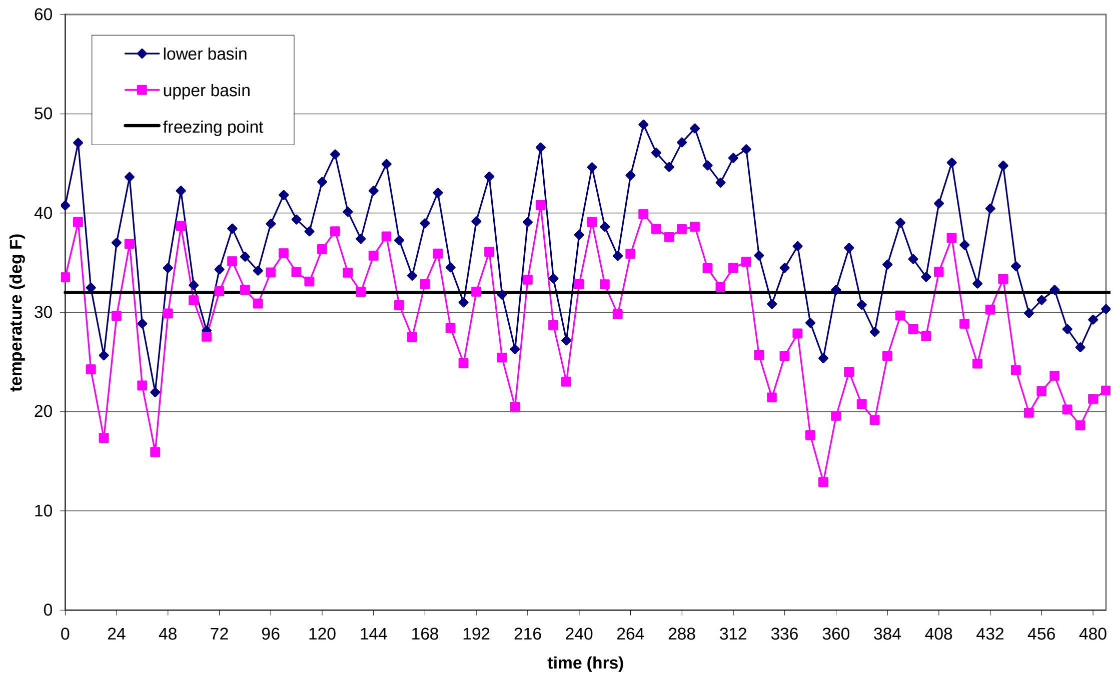


**Figure 35. Temperature trends for the January 1969 snow event.** During this event, temperatures oscillated around the freezing point, causing the storm to consist of a mix of rain and snow. Because storm temperatures are near freezing, the storm is sensitive to small temperature increases.

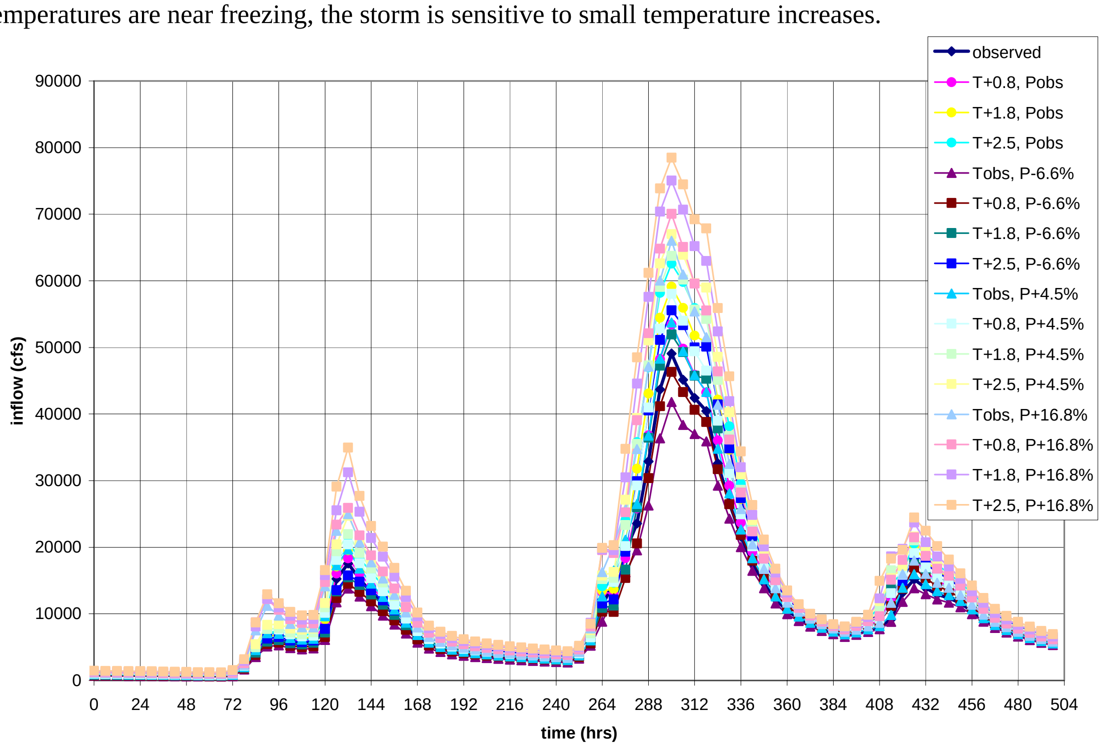


**Figure 36. Climate change inflows for the January 1969 snow event.** Temperatures hovered around the freezing point in this event, resulting in a mix of rain and snow. Increasing temperatures caused significant changes in discharges.

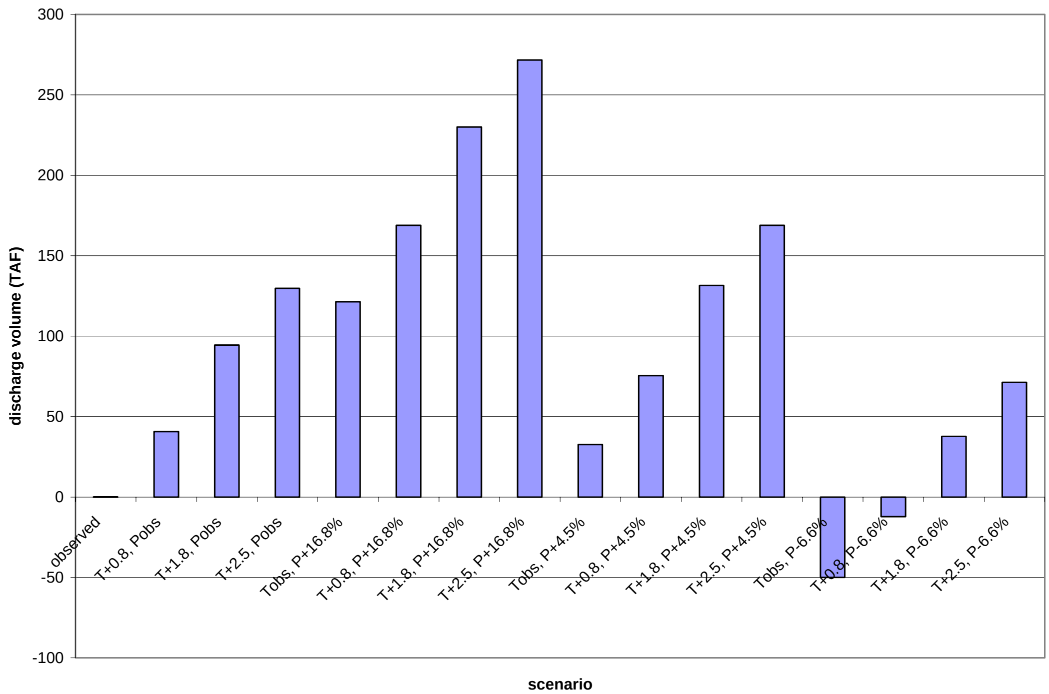


**Figure 37. Changes in discharge volume from the January 1969 observed event.** Increasing temperatures have a significant effect on discharge volumes. Also, this event illustrates the first example of flow volumes that surpass the observed volumes despite simulating an overall decrease in precipitation intensity. One reason of this increase is due to increased rain to snow ratios due to increased temperatures. Also, the main flood event occurred after a smaller, earlier event. The increased rainfall during the earlier event caused the basin to saturate more quickly, resulting in less infiltration capacity during the main flood event. The earlier saturation caused rainfall runoff to increase, resulting in larger inflow volumes despite decreased precipitation intensity.

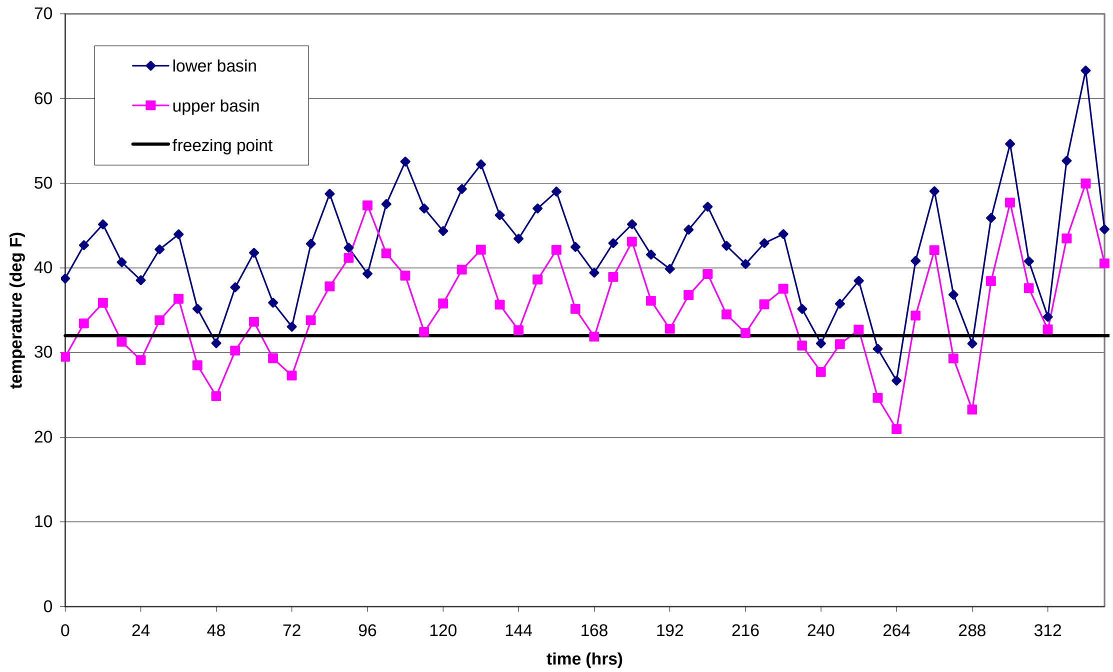


**Figure 38. Temperature trends during the January 1980 snow event.** Temperatures occur at and above freezing, with few periods occurring below the freezing point. Because temperatures occur near the freezing point, this storm is sensitive to small temperature increases.

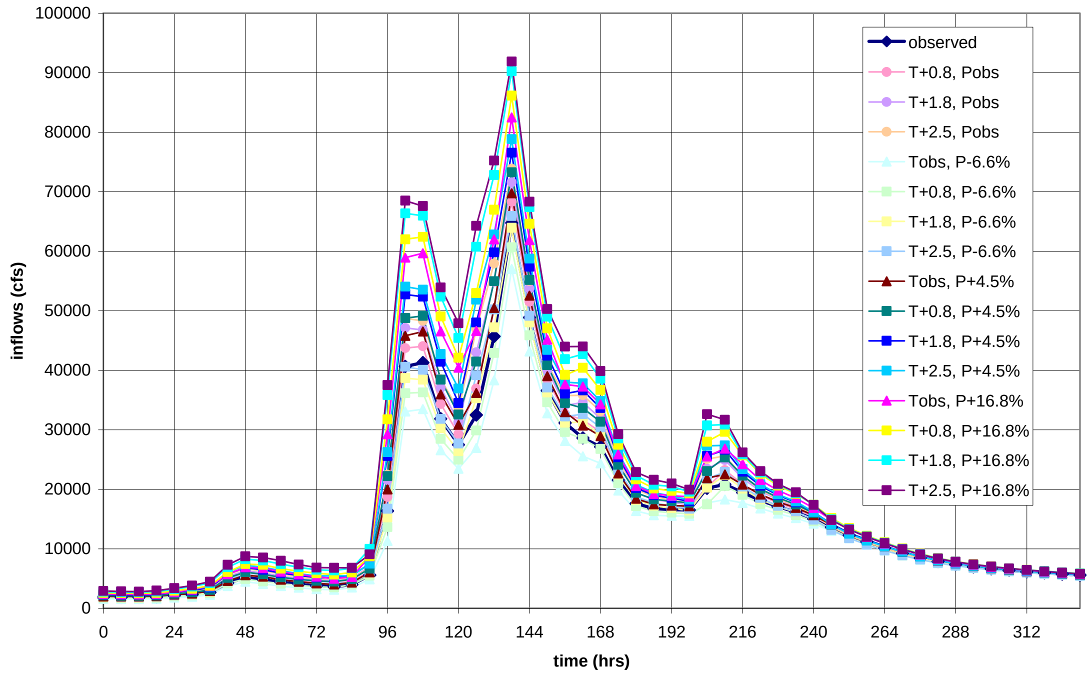


**Figure 39. Climate change inflows for the January 1980 snow event.** As temperatures during the observed event are near the freezing point, small temperature increases result in a significant change of inflows.

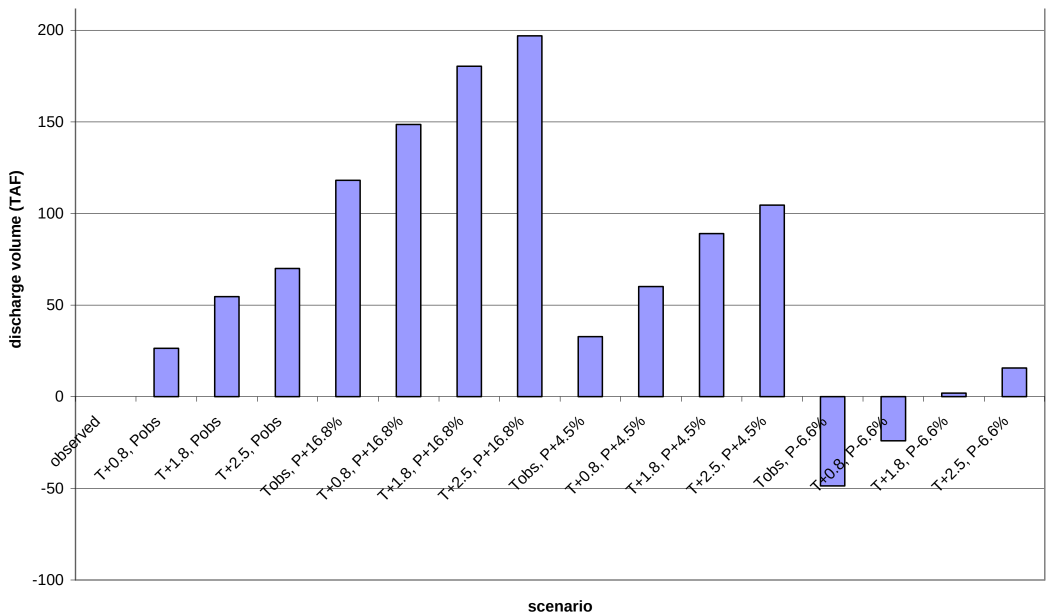


**Figure 40. Changes in runoff volumes from the observed January 1980 snow event.** Increasing temperatures have a significant effect on discharge volumes. Also, this event illustrates the first example of flow volumes that surpass the observed volumes despite simulating an overall decrease in precipitation intensity. One reason of this increase is due to increased rain to snow ratios due to increased temperatures. Also, as in the January 1969 event, the main flood event occurred after a smaller, earlier event. The main peak was then succeeded by another smaller event. The increased rainfall during the earlier event caused the basin to saturate more quickly, resulting in less infiltration capacity during the main flood event. The earlier saturation caused rainfall runoff to increase, resulting in larger inflow volumes despite decreased precipitation intensity.

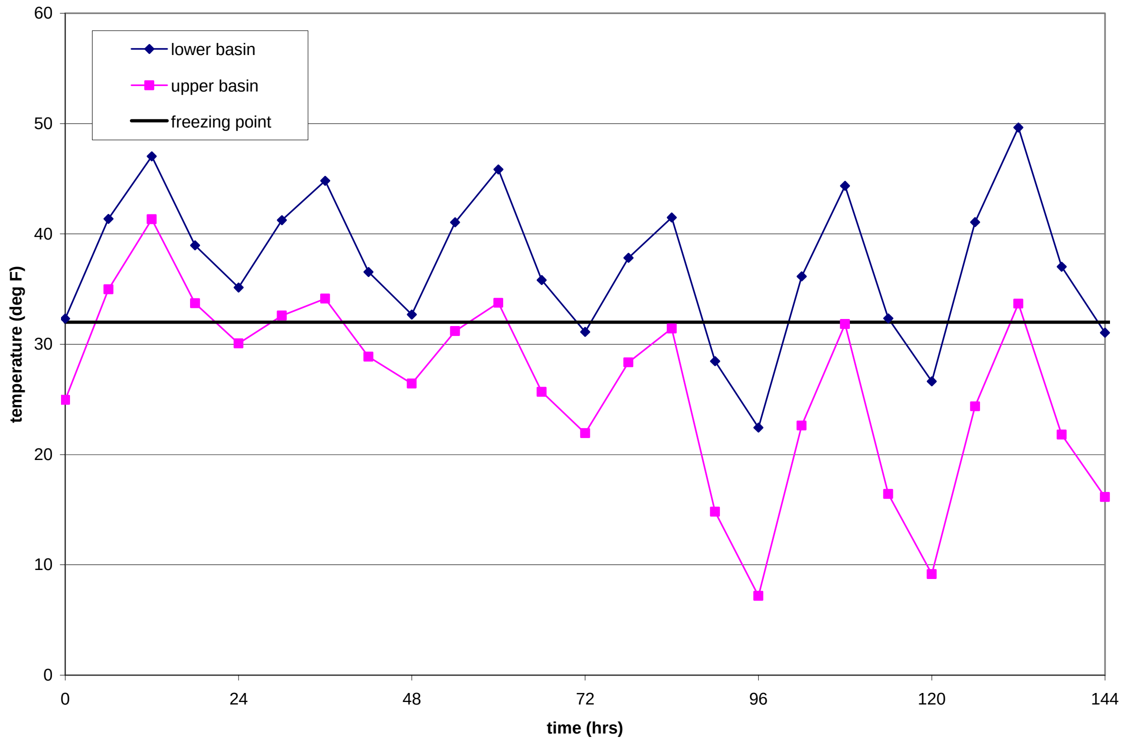


**Figure 41. Temperature trends for the December 1982 snow event.** Again, temperatures hover around the freezing point. Small temperature increases affect the storm event by increasing the rain to snow ratio, resulting in more rainfall runoff and less potential long-term snowpack storage.

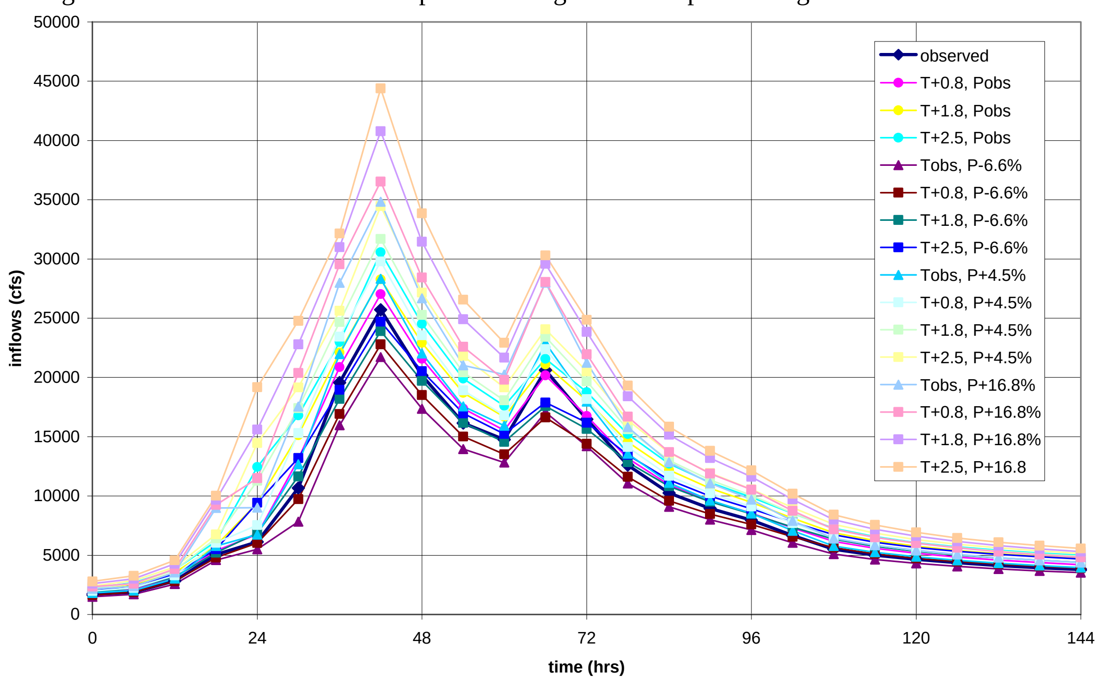


**Figure 42. Climate change inflows for the December 1982 snow event.** Because temperatures are near the freezing point during the observed event, small temperature increases result in significant inflow changes.

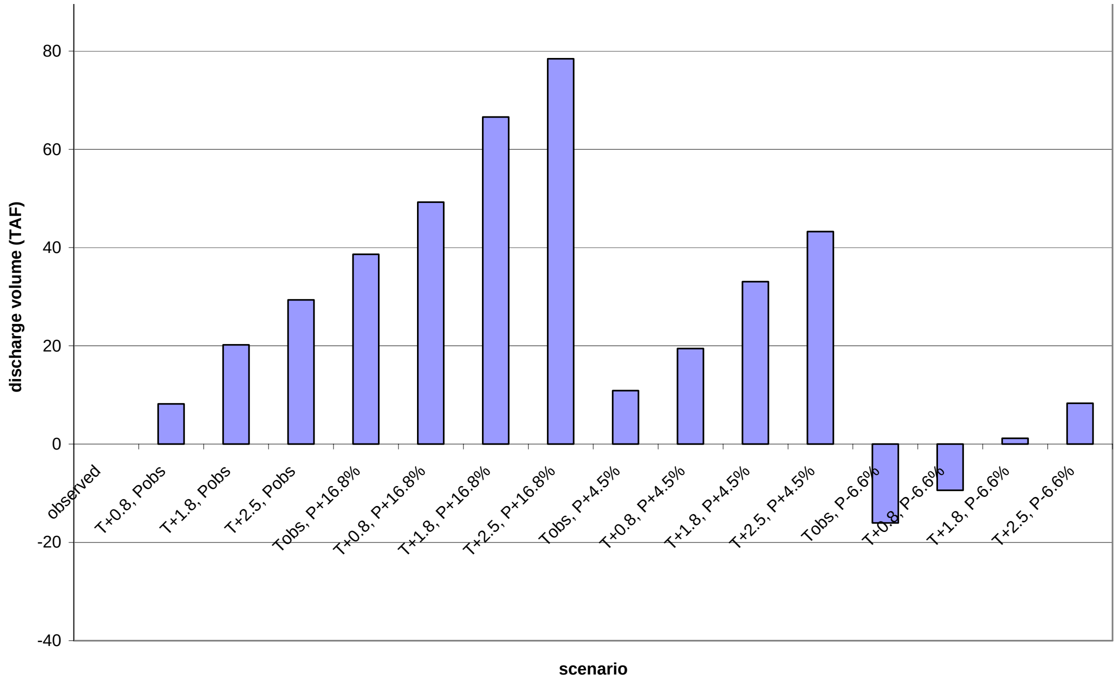


**Figure 43. Changes in runoff volume from the observed December 1982 snow event.** Again, this event illustrates the trend of discharge volumes that are greater than the observed event despite simulating decreased precipitation intensities. Though this event does not contain an antecedent wave to the main flood event, a succeeding event contributes to the overall discharge volume. Basin infiltration capacities change disproportionally to temperatures. As temperatures increase, cold events convert more snow to rain, increasing the basin wetness more quickly. The basin infiltration capacity is then reached more quickly, resulting in larger volumes of rainfall runoff.

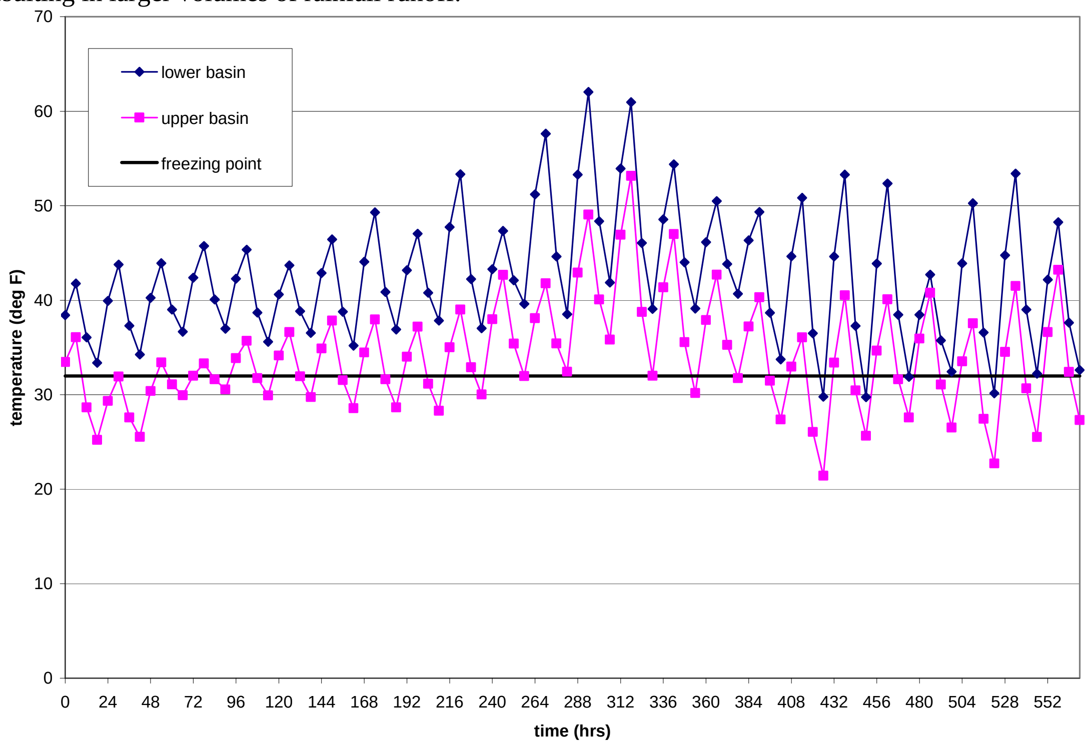


**Figure 44. Temperature trends during the March 1983 snow event.** Temperatures hover around the freezing point, causing this event to be sensitive to small temperature increases.

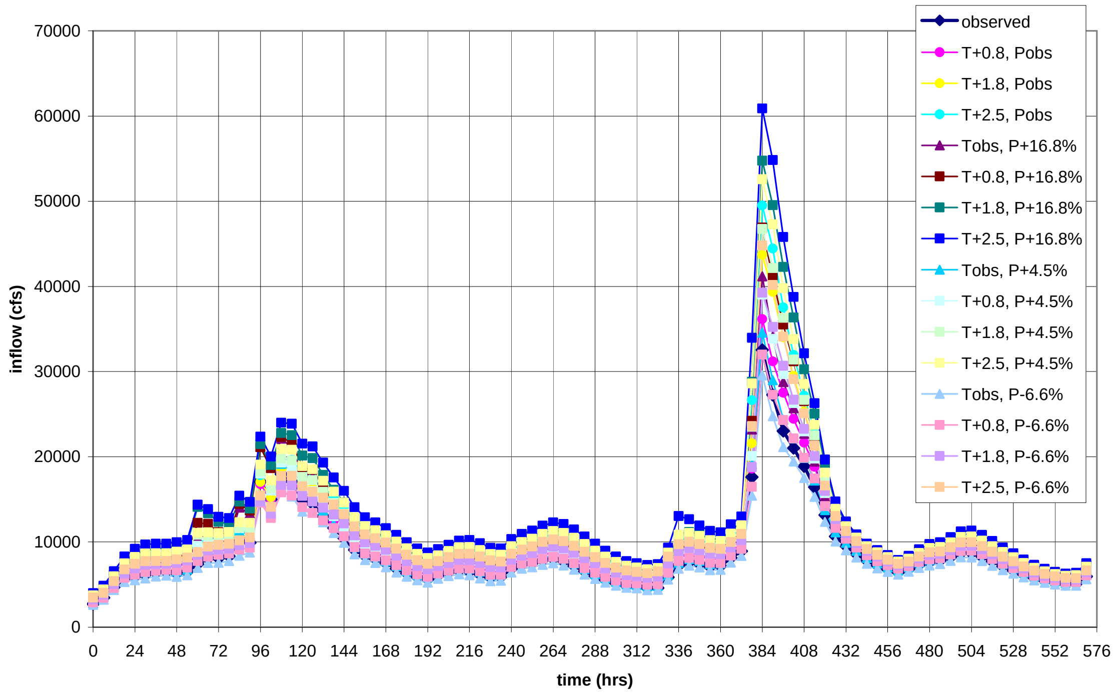


**Figure 45. Climate change inflows for the March 1983 snow event.** The observed event has a low rain to snow ratio. However, because temperatures are near the freezing point, small temperature increases have a significant effect on precipitation composition. Fractions of rain in the precipitation composition increase as temperatures rise above freezing while fractions of snow decline. This results in increasing volumes of rainfall runoff as the basin reaches its infiltration capacity more quickly. The antecedent event also increases the basin wetness leading to the main flood event.

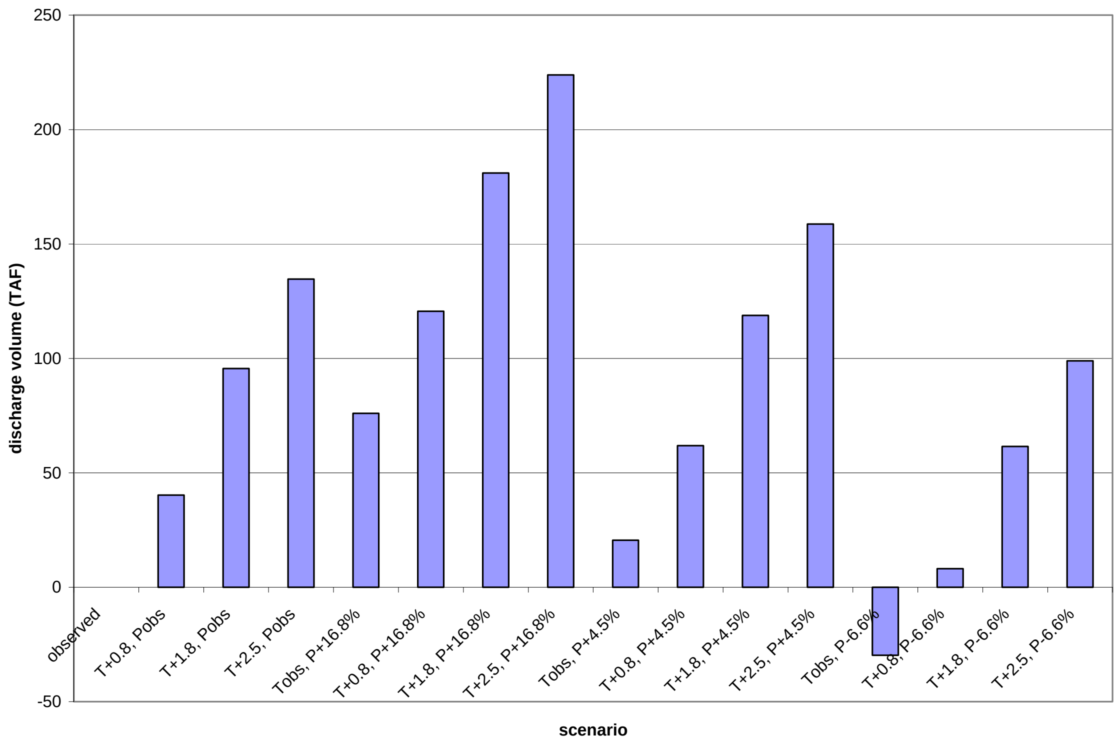


**Figure 46. Changes in discharge volume from the observed March 1983 event.** Similarly to the other cold events during which temperatures are near the freezing point, small temperature increases result in large inflow volume increases. For the first time, the smallest temperature increase (T+0.8$^o$F) causes inflow volumes to surpass the observed discharge volume despite simulating decreased precipitation intensity. Also, as the flood event occurs later in the year, it is more likely that antecedent basin conditions are wet and contain a ripening snowpack.

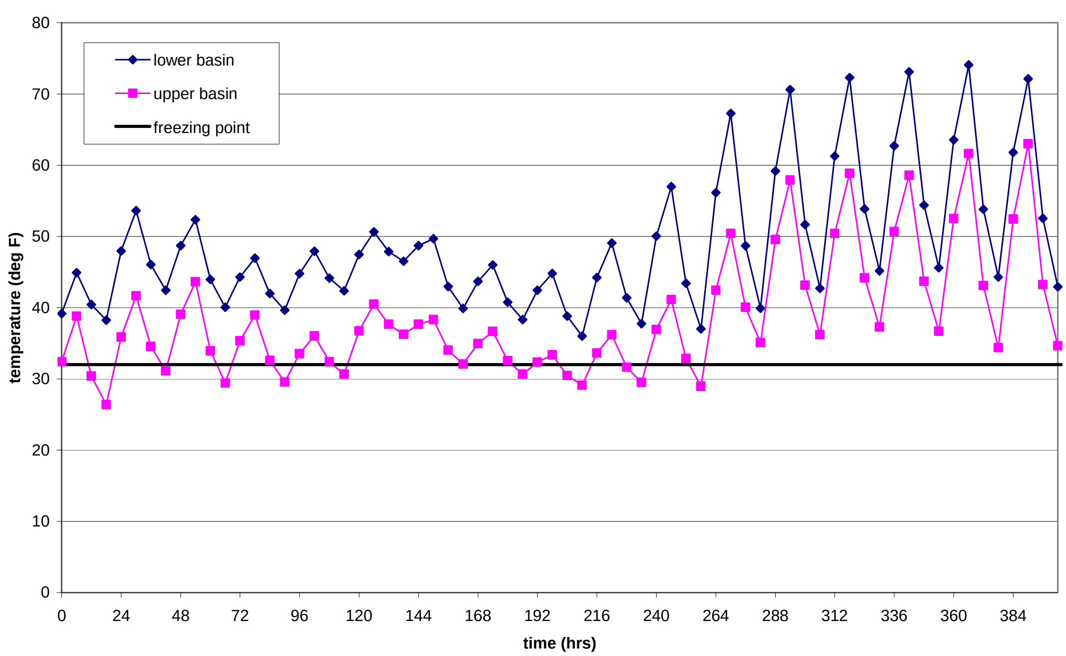


**Figure 47. Temperature trends during the February 1986 event.** Though temperatures are mostly above freezing, temperatures during the wave succeeding the main flood peak are at or below freezing. This implies that while most of this event is characterized as a rain event, inflows may be sensitive to increasing temperatures as they are affected during the post-main peak runoff.

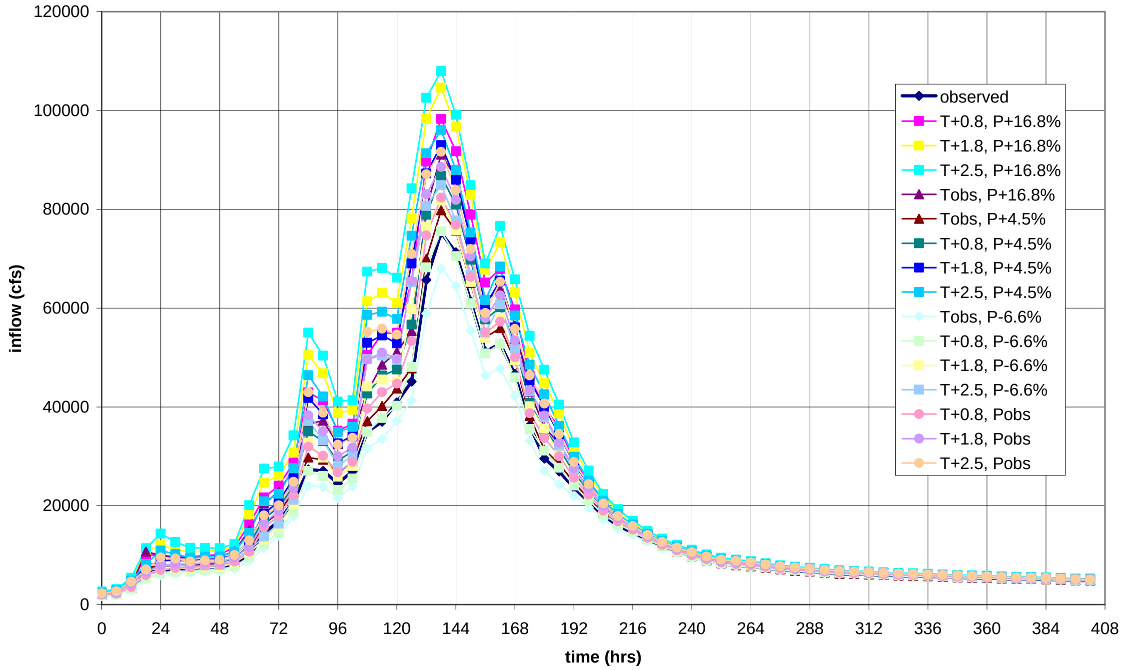


**Figure 48. Climate change inflows for the February 1986 event.** While this event is considered a rain event, temperatures hover around the freezing point just before and after the main flood peak. Therefore, while the main event may not be sensitive to temperature shifts, both preceding and succeeding events are affected.

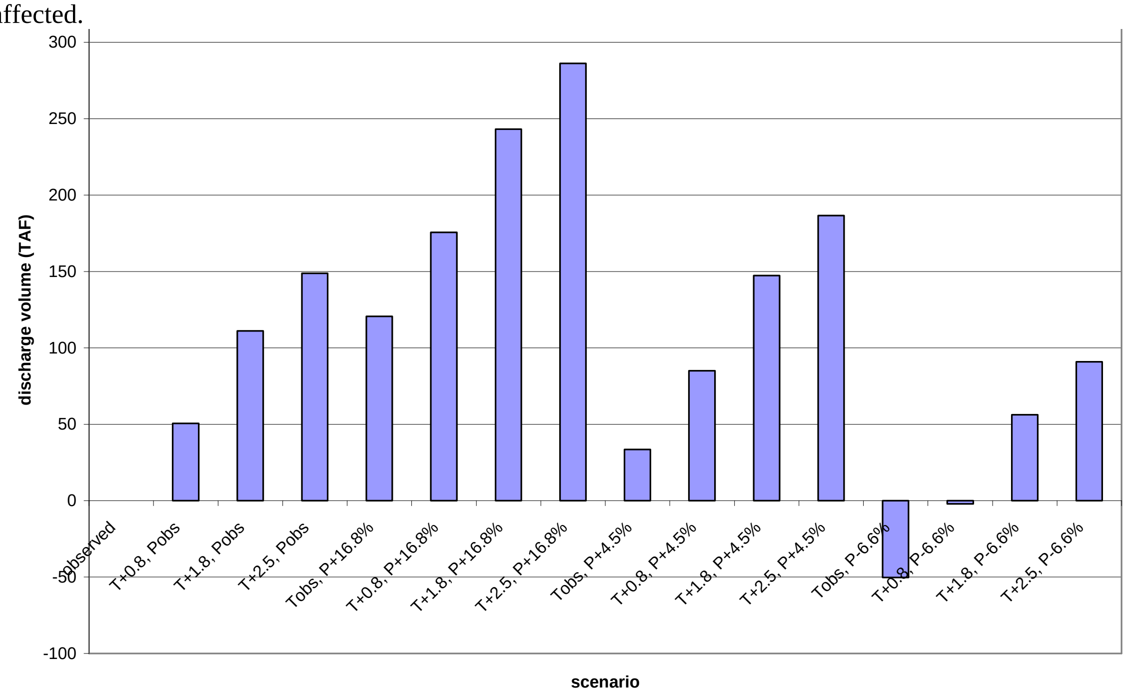


**Figure 49. Changes in runoff volume from the observed February 1986 event.** Though this event is considered a rain event, its inflow volumes are sensitive to temperature increases. Because the main flood peak occurs during a period when temperatures are above freezing, it is less sensitive to temperature increases. However, the antecedent and succeeding peaks occur during periods when temperatures are at or below freezing, causing them to be more sensitive to temperature increases. As the overall discharge volumes take all three events into account, the results reflect the runoff's sensitivity to temperature. Also, as this event occurs several months into the flood season, the basin is more likely to have wetter conditions and a larger snowpack.

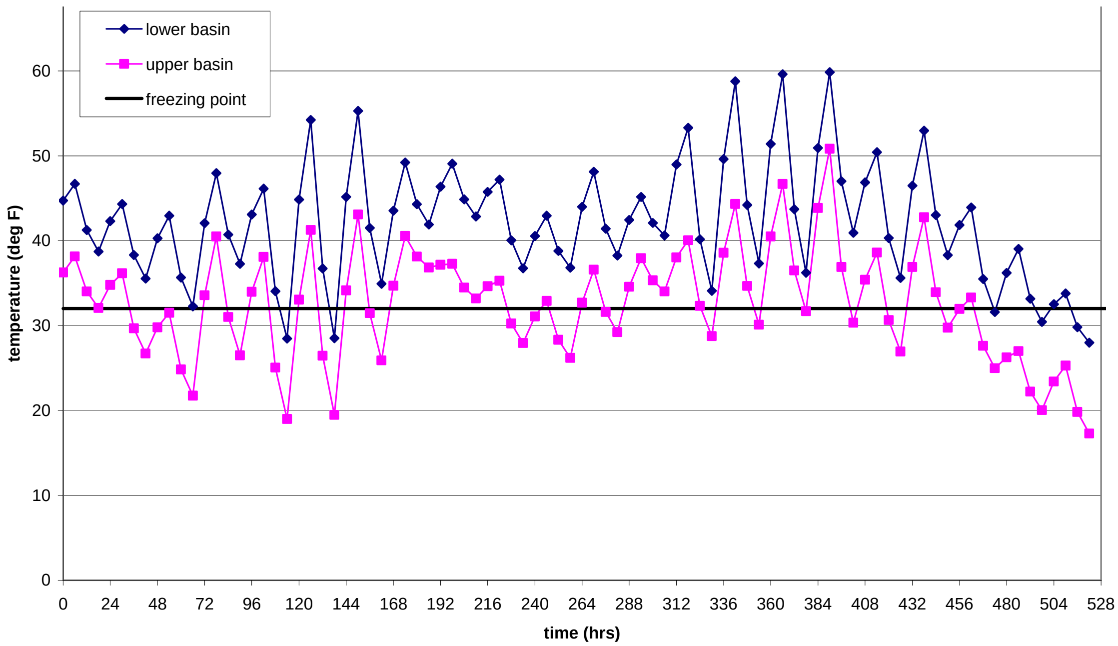


**Figure 50. Temperature trends during the March 1995 snow event.** Temperatures during this cold event range from over 8°F above to over 10°F below the freezing point, indicating that small shifts in temperatures may not affect this event as much as other during which the temperatures vary less around the freezing point.

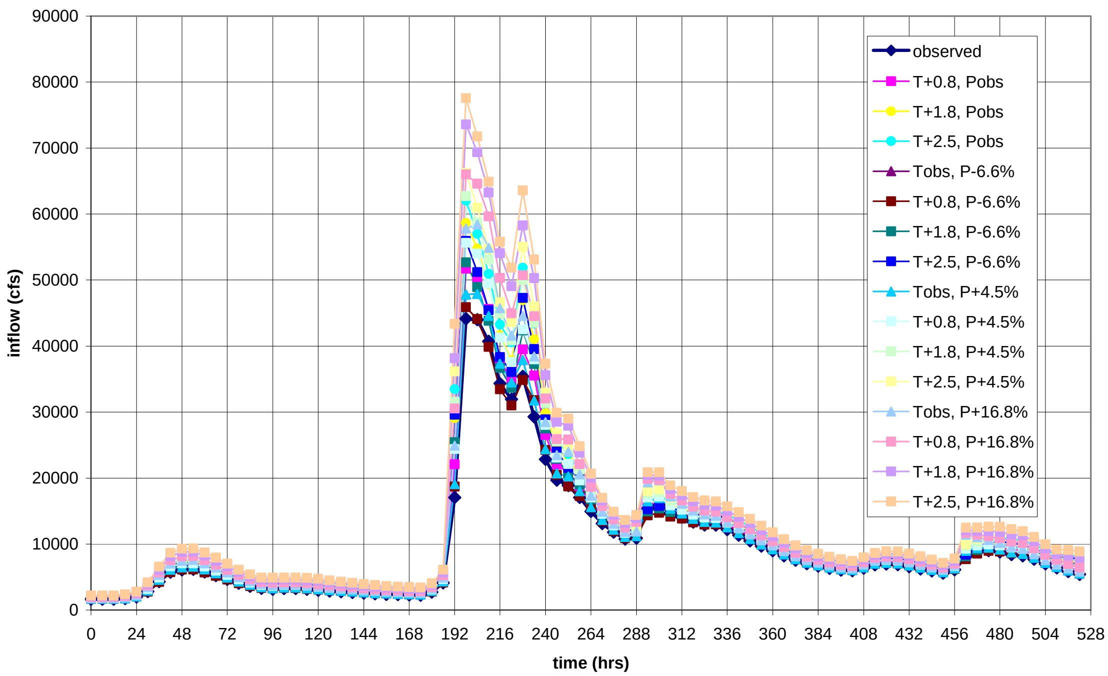


**Figure 51. Climate change inflows for the March 1995 event.** Inflows are sensitive to temperature increases. However, as this event occurs towards the end of the flood season, likely it is also affected by antecedent basin conditions and the response of the existing snowpack to increasing temperatures.

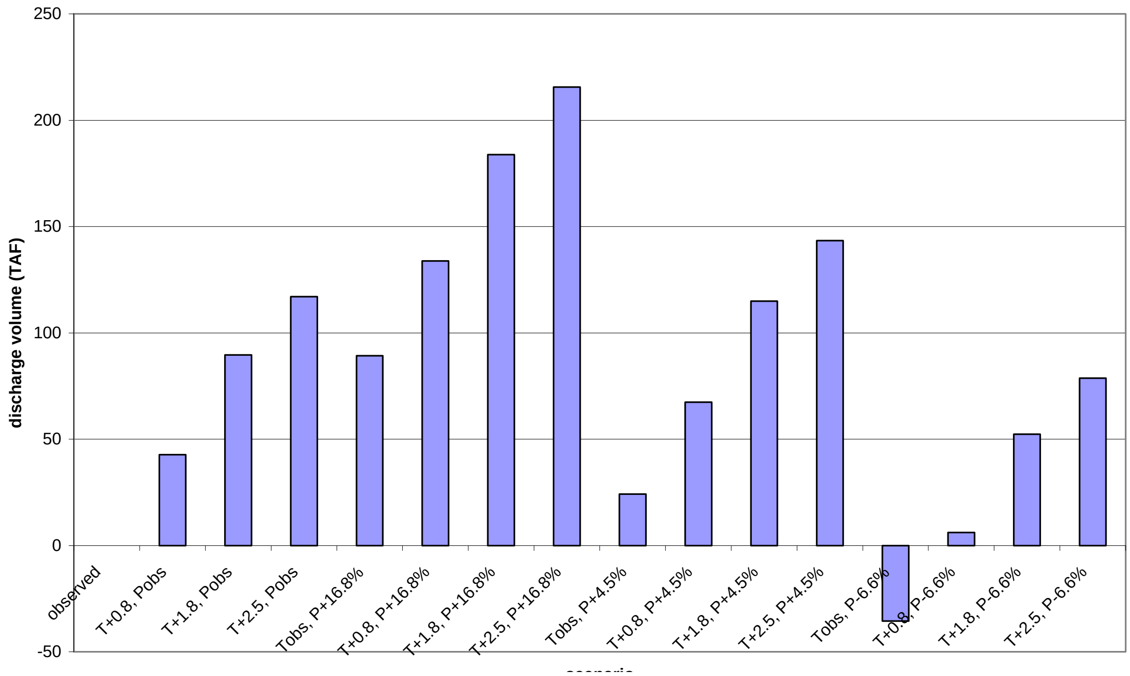


**Figure 52. Changes in runoff volume from the observed March 1995 event.** Runoff volumes surpass observed volumes under any temperature increase scenario. As event temperatures are similar to other events that responded less strongly to increasing temperatures, conditions other than the increasing rain to snow ratio may affect the runoff response. The only other sampled event in which all temperature change scenarios cause inflow volumes to exceed observed volumes is the March 1983 event. As both of these events occur toward the end of the flood season, likely they are also affected by antecedent basin wetness conditions and the effects of increasing temperatures on existing snowpacks. The effects of increasing temperatures seem to magnify as events occur later in the flood season.

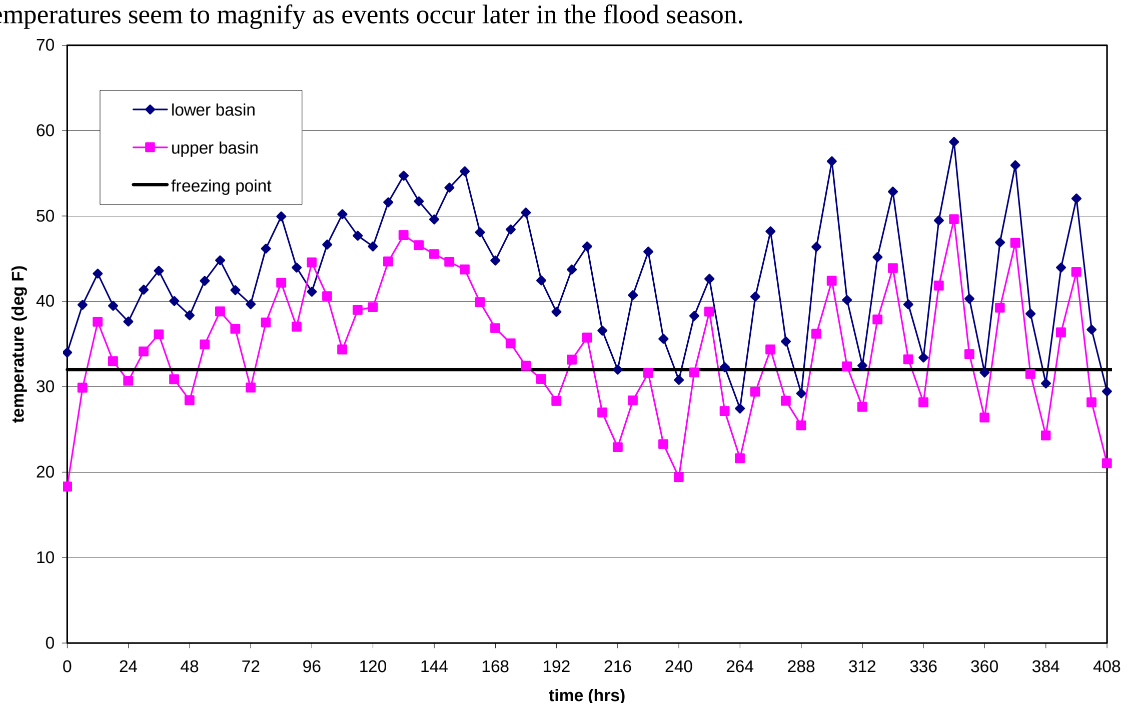


**Figure 53. Temperature trends during the January 1997 rain event.** Temperatures before and during the event peak are well above the freezing point in both the upper and lower basin. Increasing temperatures are not expected to significantly increase runoff volumes.

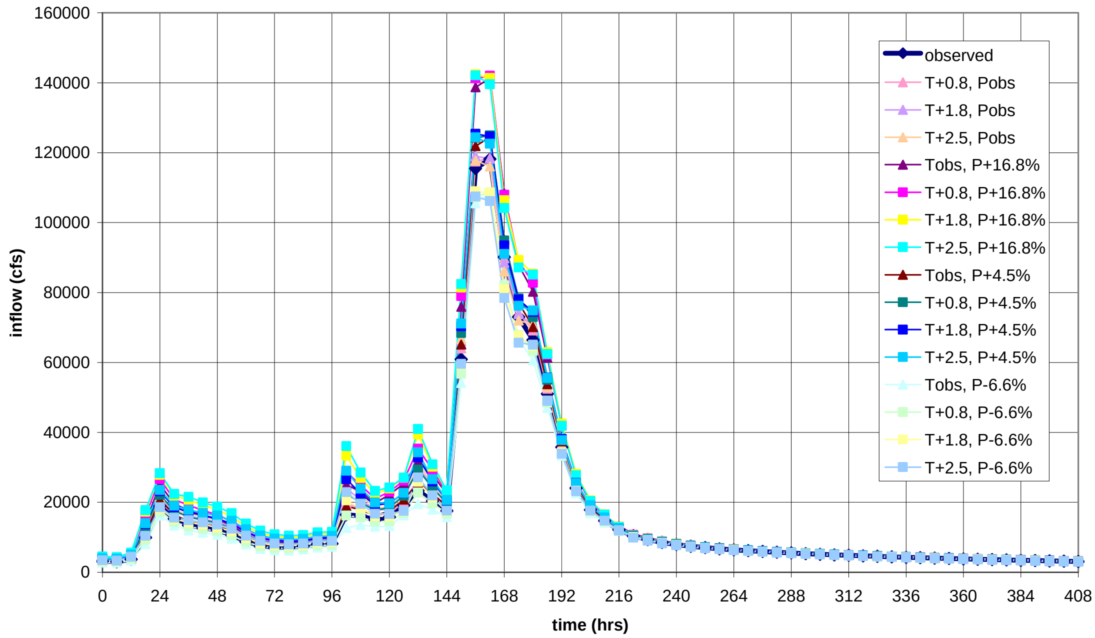


**Figure 54. Climate change inflows for the January 1997 rain event.** Temperature does not have a significant effect on inflow volumes; rather, results from climate scenarios cluster around precipitation shifts.

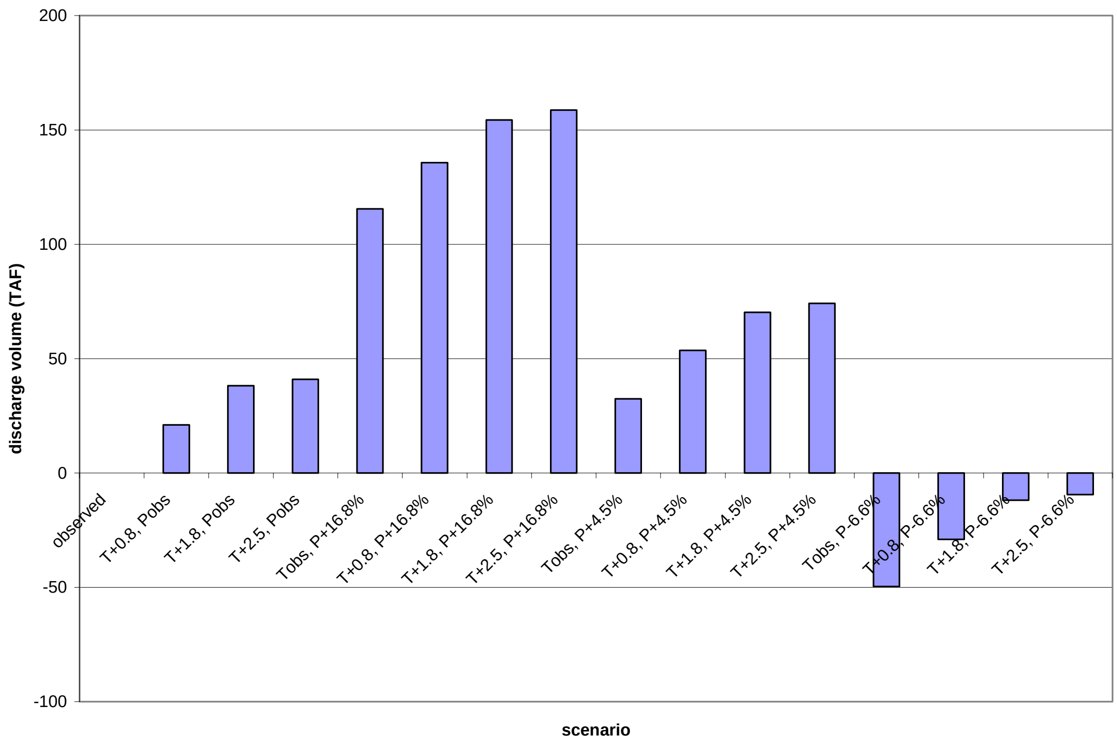


**Figure 55. Changes in runoff volume for the January 1997 rain event.** Increasing temperatures have a slight effect on runoff volumes; however, the event is more sensitive to changes in precipitation intensities. Changes due to temperature changes are likely caused by increasing basin wetness due to antecedent event peaks. Therefore, while isolated events are not sensitive by increased temperatures, other factors that affect runoff patterns such as basin wetness, infiltration capacity and existing snowpack conditions, may still cause significant shifts in runoff volumes because of their own sensitivity to increasing temperatures.

# Appendix B: Climate change scenario effects on Oroville inflows

Ensemble charts of sampled flood events for Oroville basin and their accompanied volume changes.

| | **Oroville @ Sierraville** Precipitation during past 30 days (inches) | past WY | basin conditions |
|---|---|---|---|
| Jan-63 | 2.35 | Below Normal | Dry |
| Dec-64 | 3.99 | Dry | Below normal |
| Jan-69 | 5.59 | Below Normal | Wet |
| Jan-80 | missing | Below Normal | N/A |
| Dec-82 | 6.13 | Dry | Wet |
| Mar-83 | 6.15 | Wet | Wet |
| Feb-86 | 2.98 | Dry | Dry |
| Mar-95 | 0.89 | Critical | Dry |
| Jan-97 | 16.53 | Wet | Wet |

**Table 15. Basin wetness conditions above Oroville Dam preceding the sampled flood events**

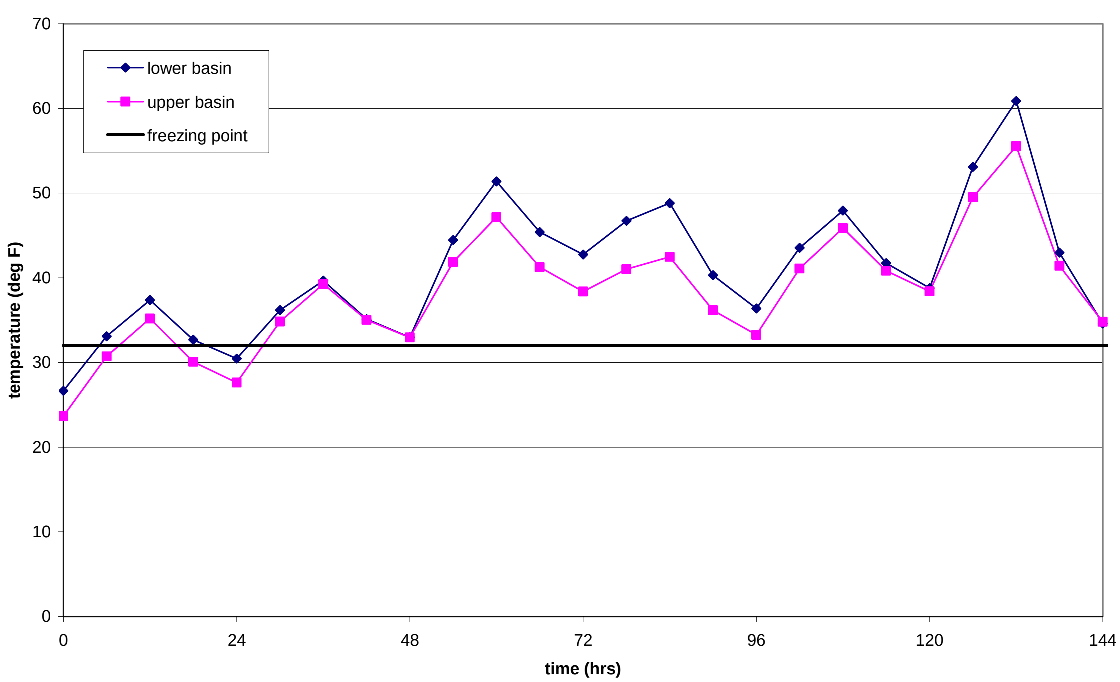


**Figure 56. Temperature trends during the January 1963 rain event.** Temperatures are above the freezing point during the event, implying that little change will occur in the rain-snow ratio when temperatures increase.

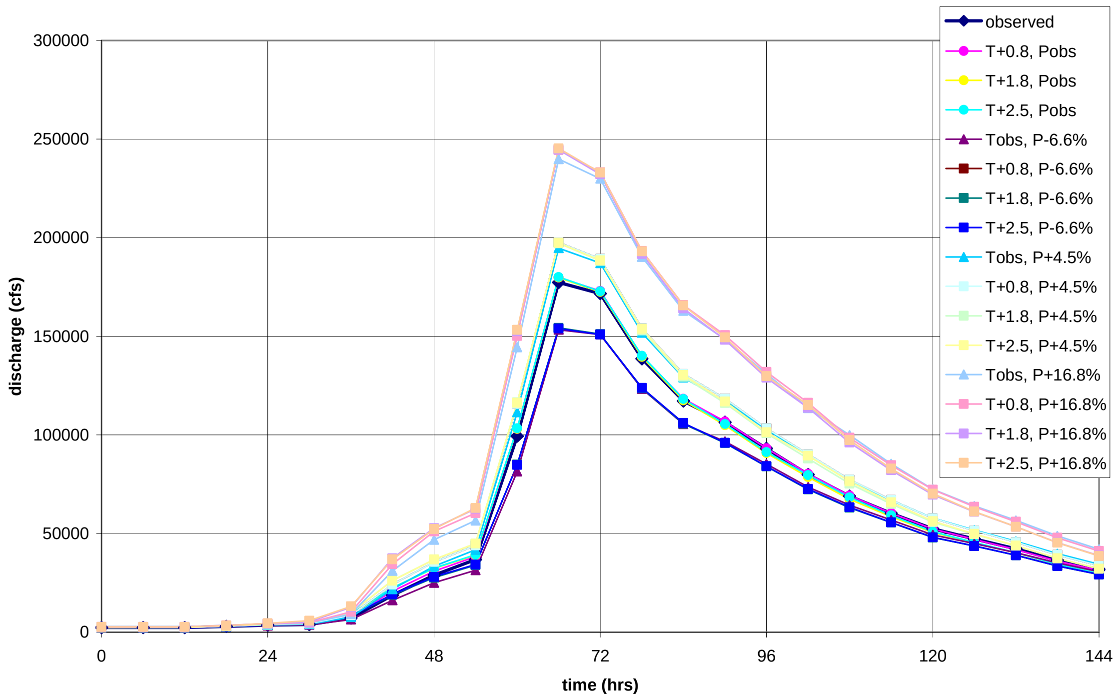


**Figure 57. Climate change inflows for the January 1963 rain event.** Inflows do not change significantly with temperature shifts. Large inflow shifts are due to precipitation changes.

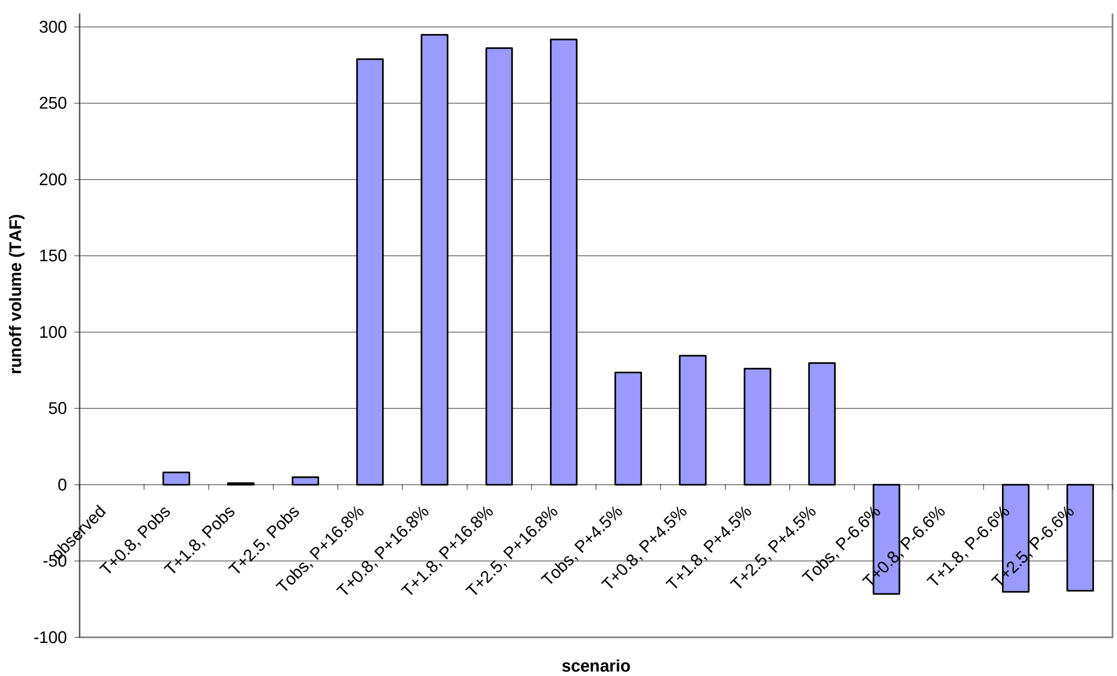


**Figure 58. Changes in runoff volumes from the observed January 1963 event.** Small temperature increases do not affect inflow volumes significantly. Basin wetness conditions preceding the storm event are dry, indicating that the basin can absorb rainfall.

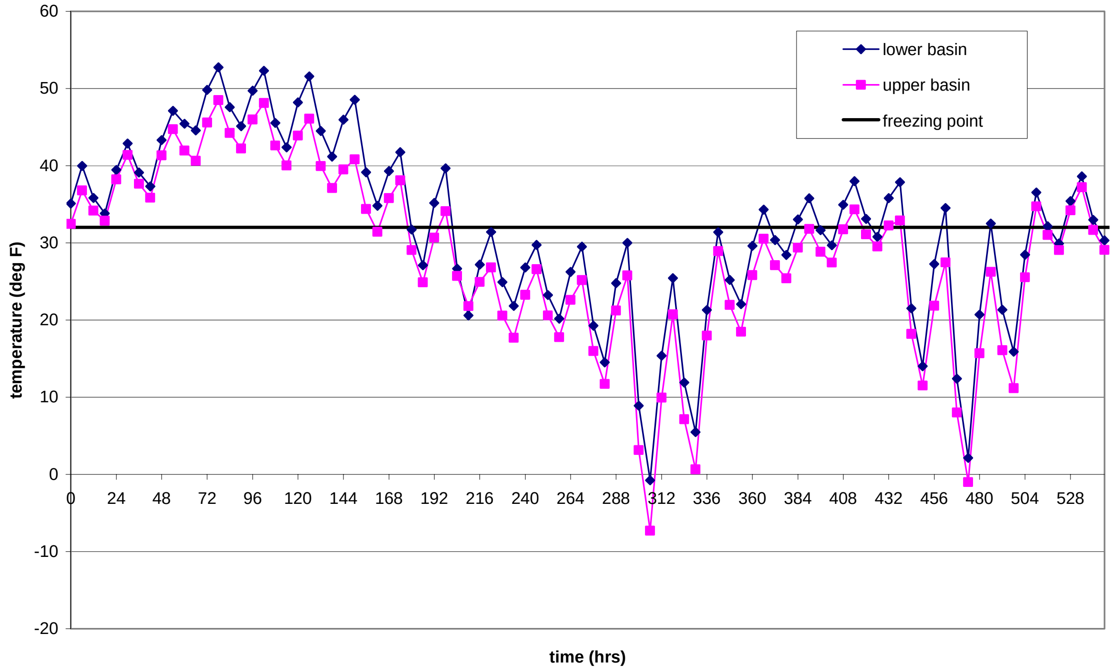


**Figure 59. Temperature trends during the December 1964 rain event.** Temperatures during the main storm peak (hours 48-168) are significantly above freezing, implying that small temperature increases will not affect the rain-snow ratio. However, temperatures decrease below freezing during two small events that occur after the main peak (hours 168-216 and 382-502). Temperature increases will have a greater affect on those two smaller events.

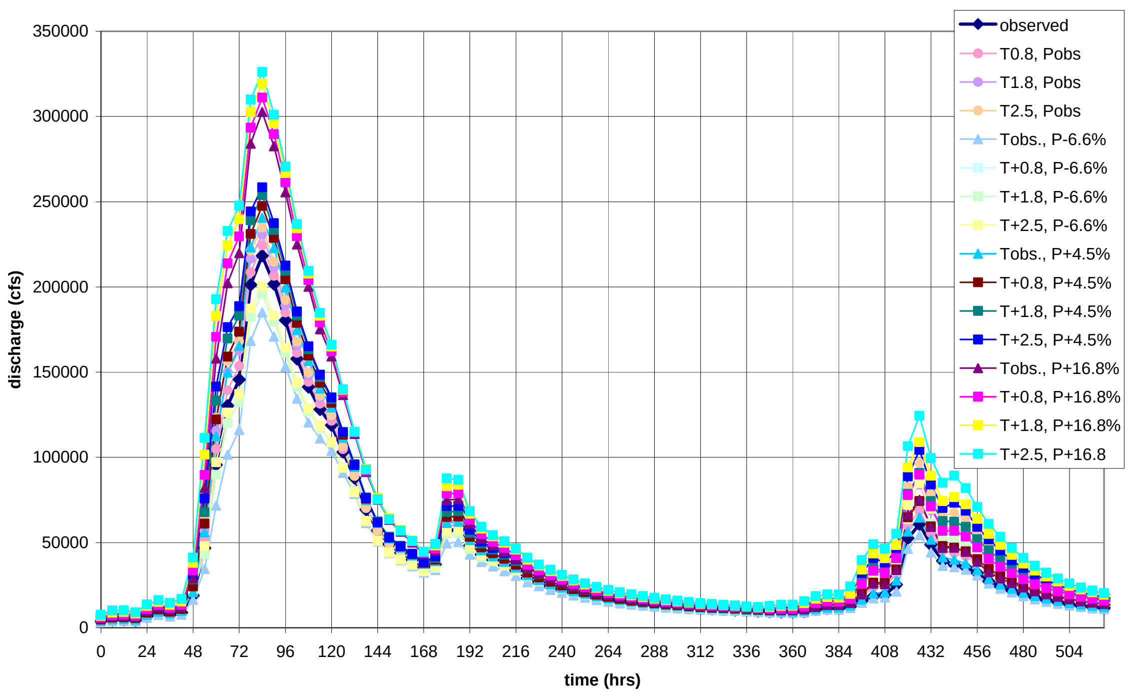


**Figure 60. Climate change inflows for the December 1964 rain event.** Inflows are not highly variable during the main storm event (hours 38-168), however, they become more variable during the two smaller events that occur after the main peak. Temperatures during these smaller events are around freezing. Small temperature increases increase the fraction of precipitation falling as rain, generating increased runoff.

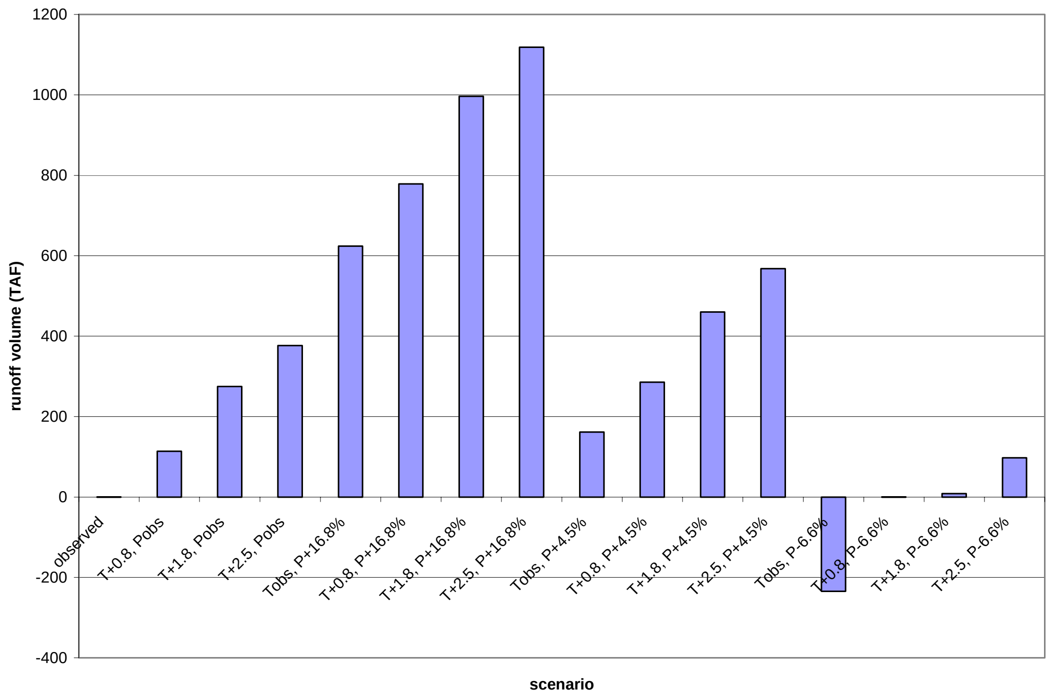


**Figure 61. Changes in runoff volume from the observed December 1964 event.** Temperature increases generate higher inflow volumes. Though the main storm event is warm, smaller storm events that follow have observed temperatures at and below the freezing point. Temperature increases increase the fraction of precipitation falling as rain, generating more surface inflows. The initial heavy storm event saturates the basin, forcing more surface runoff and reducing the basin's infiltration capacity for smaller events. Basin wetness conditions preceding the December 1964 event are below normal, indicating that the small increases of runoff despite decreases of precipitation intensity are probably due to shifting precipitation composition of the small event that follows the main flood wave.

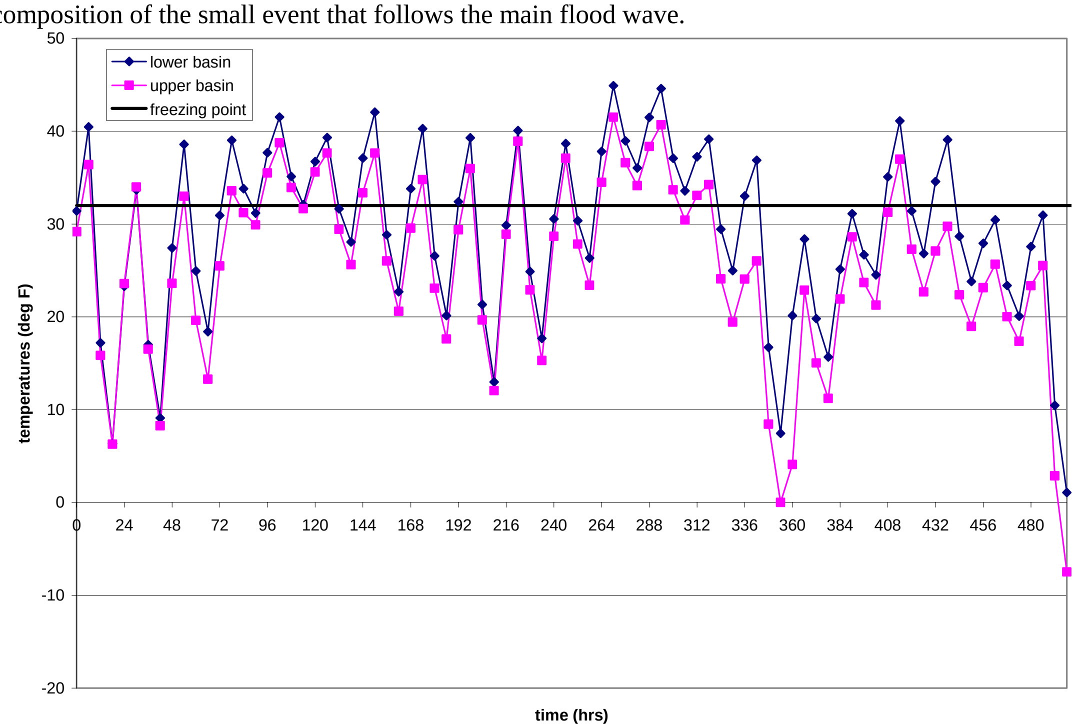


**Figure 62. Temperature trends during the January 1969 snow event.** Temperatures occur near the freezing point, causing the event to be sensitive to small temperature increases.

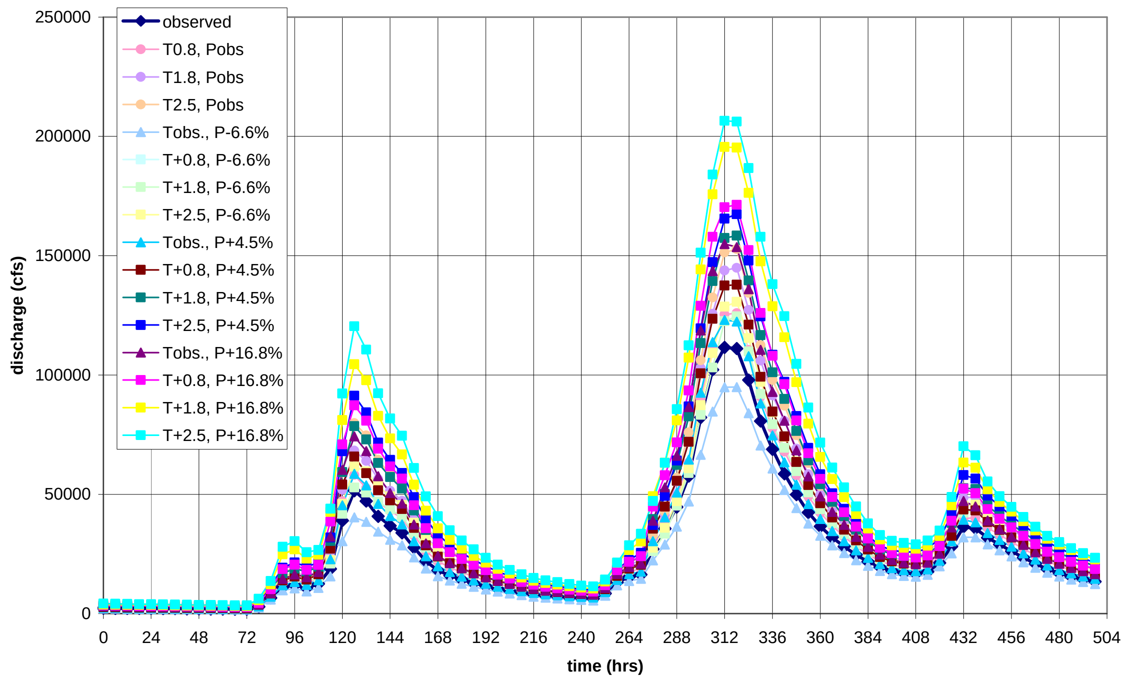


**Figure 63. Climate change inflows for the January 1969 snow event.** Inflows are sensitive to small temperature increases. As the temperature trends for the observed event oscillate around the freezing point, this storm exemplifies the type most sensitive to small temperature increases. As temperatures are driven above freezing, precipitation that would have fallen as snow now falls as rain, significantly affecting inflow volumes. The increased rainfall runoff also causes the basin to saturate more quickly, forcing future rainfall to runoff on the surface rather than infiltrating.

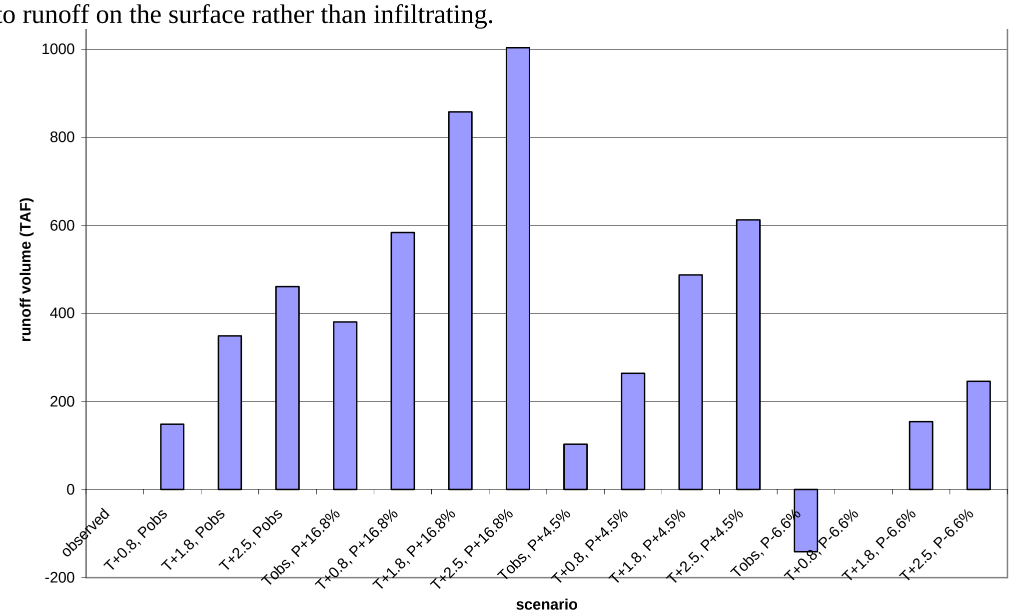


**Figure 64. Changes in runoff volumes from the observed January 1969 snow event.** Small temperature increases significantly affect runoff volumes as the fraction of rainfall increases with temperature. Overall runoff volumes in scenarios that simulate a decrease in precipitation intensity surpass the observed record. Two reason may explain this: increased temperatures generate enough extra rainfall to overcome the effects of decreased precipitation intensities. Also, as two smaller events occur before and after the main storm event, the basin becomes saturated quickly and forces rainfall to become surface runoff rather than infiltrate. Basin conditions preceding the January 1969 event are wet, supporting the observation that the basin's infiltration capacity is low, forcing more surface runoff.

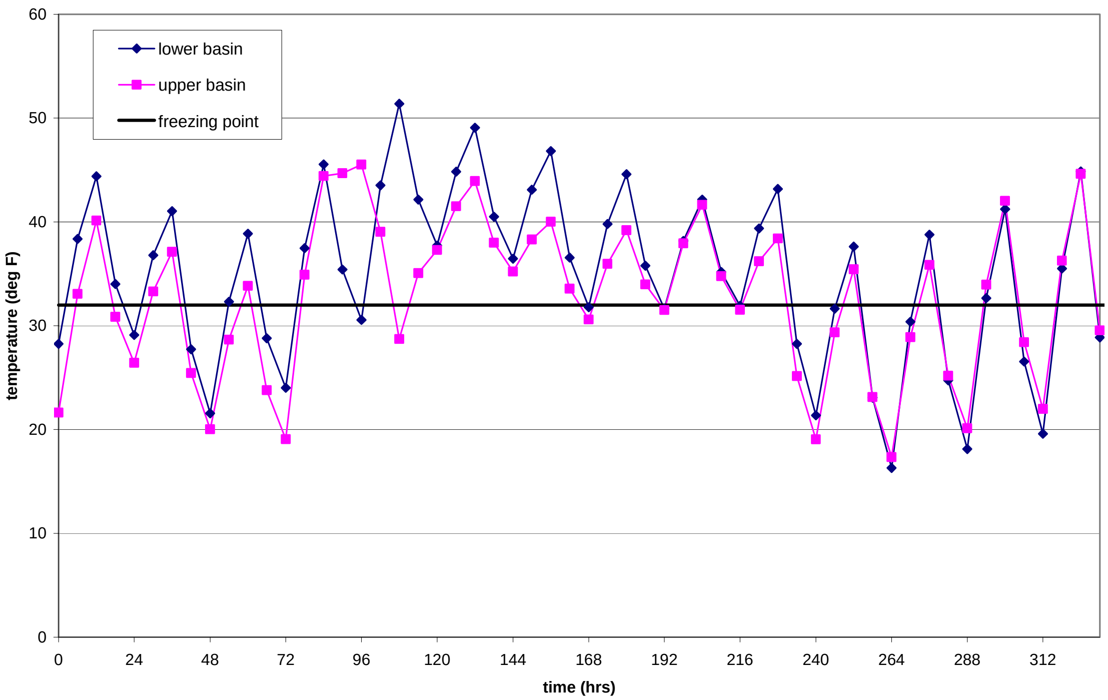


**Figure 65. Temperature trends during the January 1980 snow event.** Temperatures vary around the freezing point except during the main event (hours 96-216), when they increase above freezing. As the temperatures during the event are above freezing, the storm may react less to temperature changes as the regime is already mostly warm.

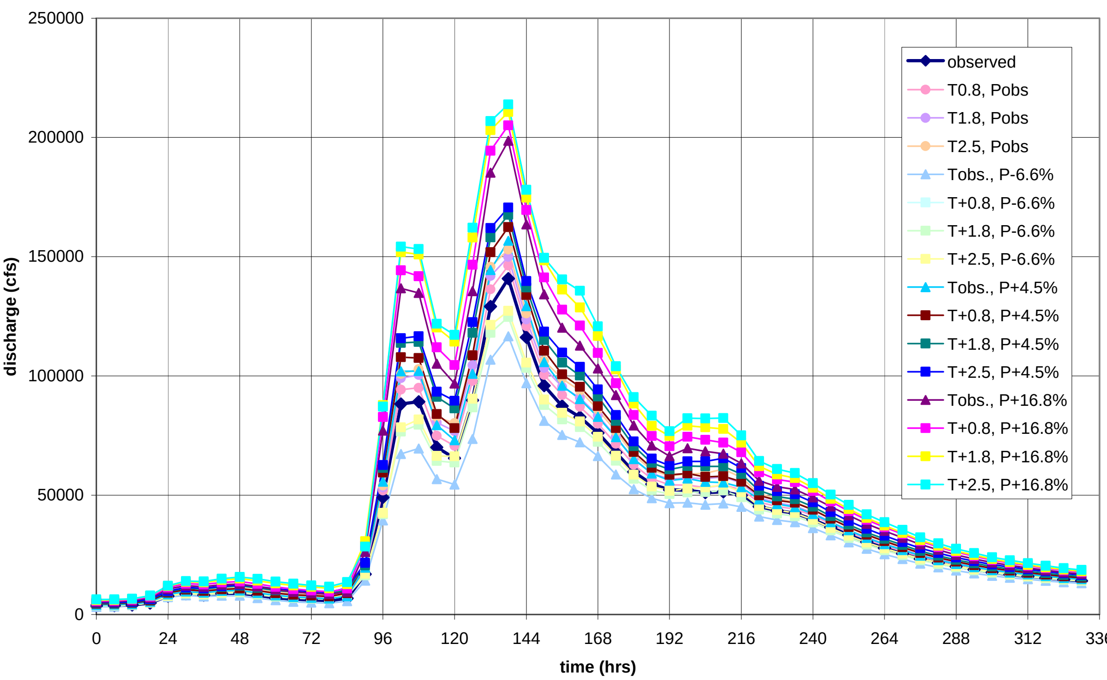


**Figure 66. Climate change inflows for the January 1980 snow event.** Some variability can be seen due to temperature changes, however, most of the shift is apparent when precipitation intensities are altered. Nevertheless, this event is more sensitive to temperature changes than previous rain events such as the January 1963 rain event. Thus some response to increasing temperatures is expected.

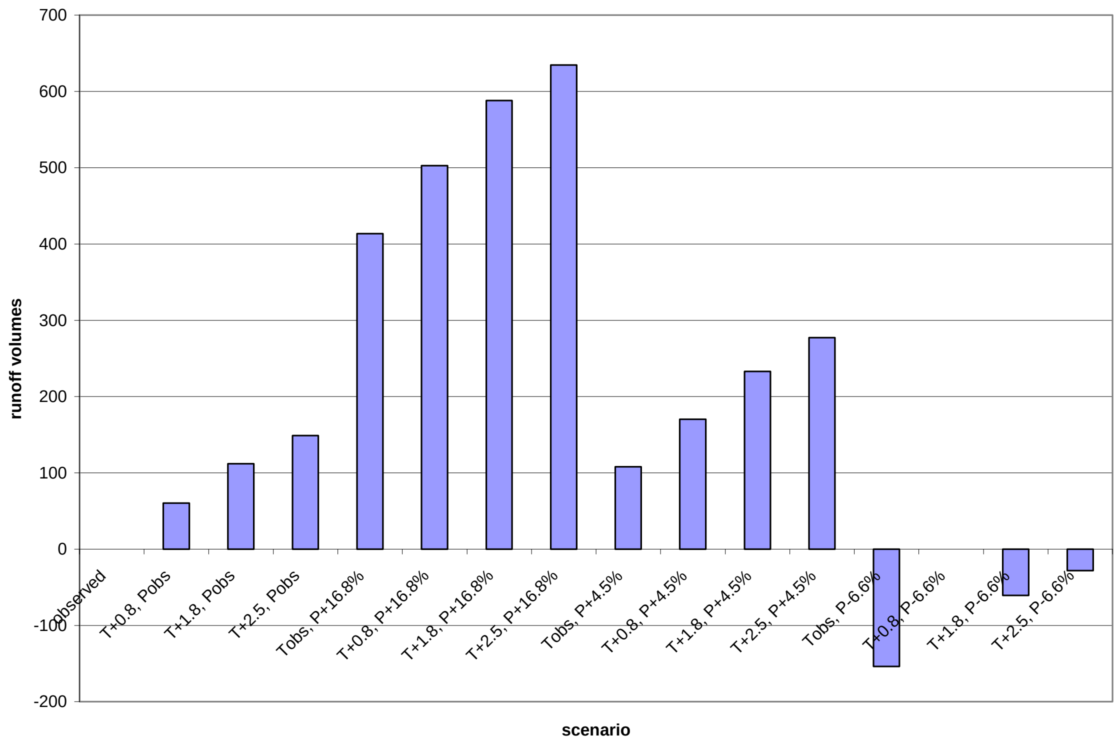


**Figure 67. Changes in runoff volumes from the observed February 1980 snow event.** Increasing temperatures have a small effect on runoff volumes, though this effect is not strong enough to overcome the effect of decreasing precipitation intensity. As temperatures are already above freezing during most of the main event, a strong response to increasing temperatures is not expected.

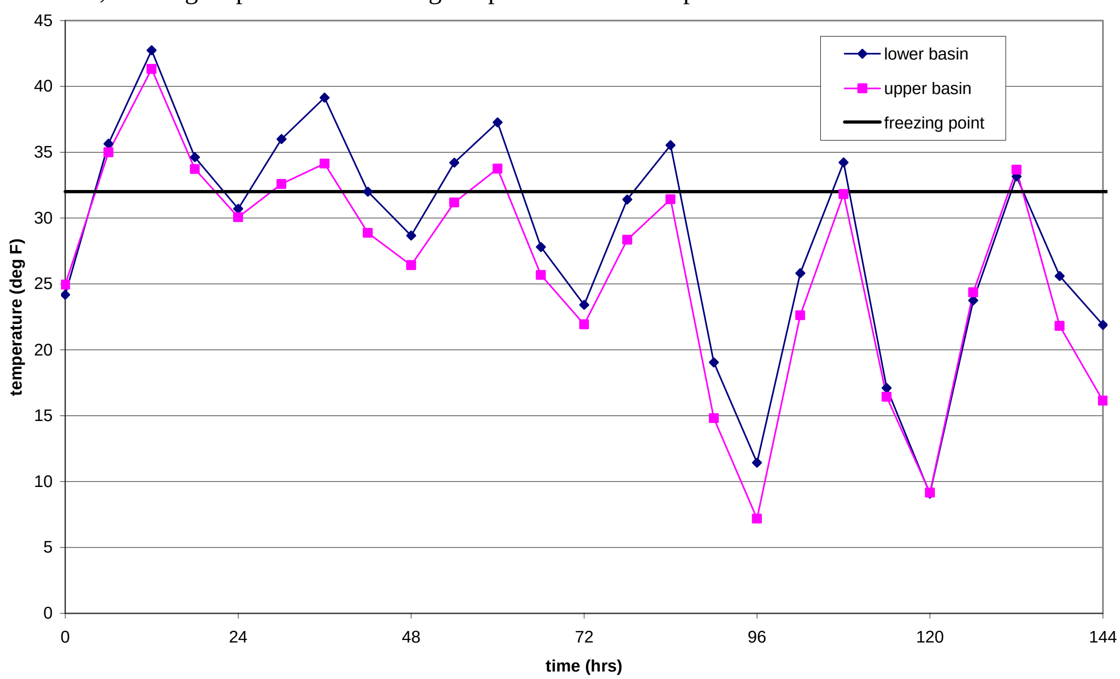


**Figure 68. Temperature trends during the December 1982 event.** Temperatures begin above the freezing point and steadily decrease as the event progresses. Because the temperatures are near the freezing point, increasing temperature regimes affect the hydrologic characteristics of this event.

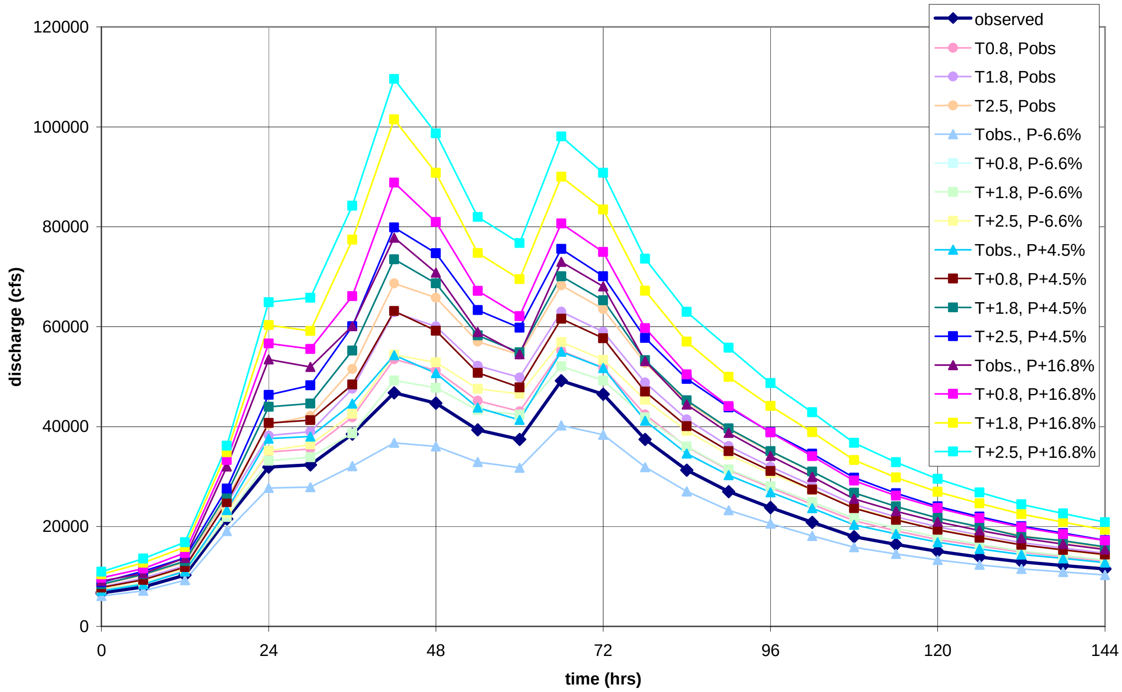


**Figure 69. Climate change inflows for the December 1982 snow event.** Temperature increases have a strong effect on the hydrologic characteristics of this event. Climate scenarios that simulate decreased precipitation intensities and increased temperatures have higher-volume inflows that the observed event.

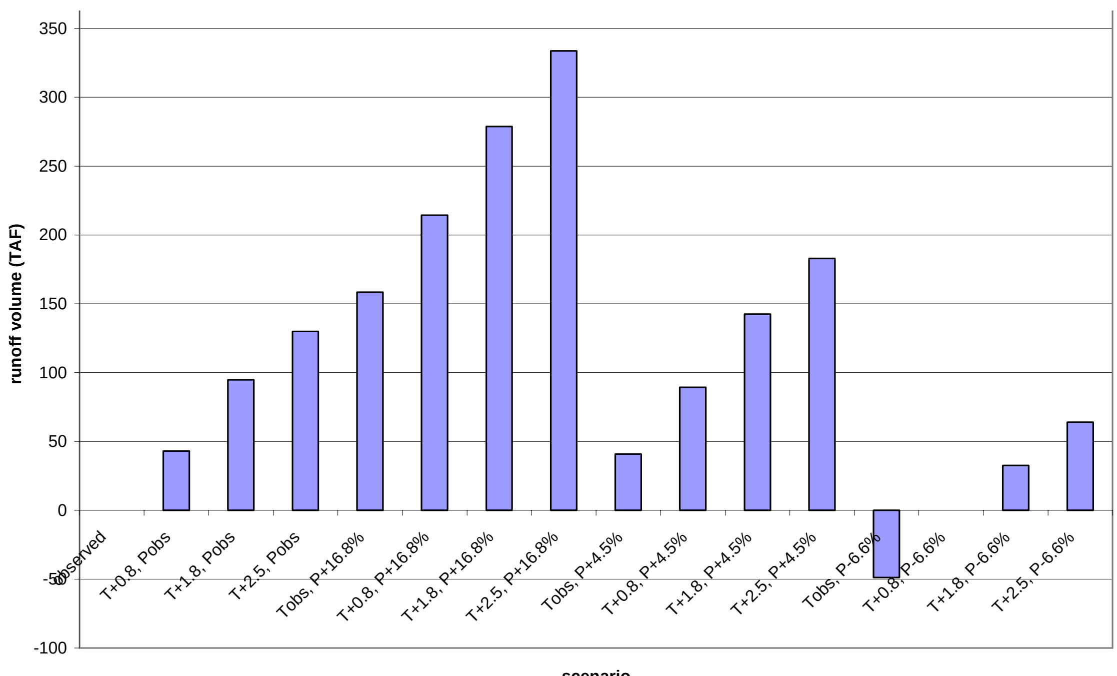


**Figure 70. Changes in runoff volumes from the observed December 1982 event.** Increasing temperatures increase inflow volumes above those in the observed event, indicating that increased temperatures overcome the effects of decreased precipitation intensities. Basin conditions preceding the December 1982 event are wet, supporting the observation that the basin's infiltration capacity is low, forcing larger volumes of surface water to runoff.

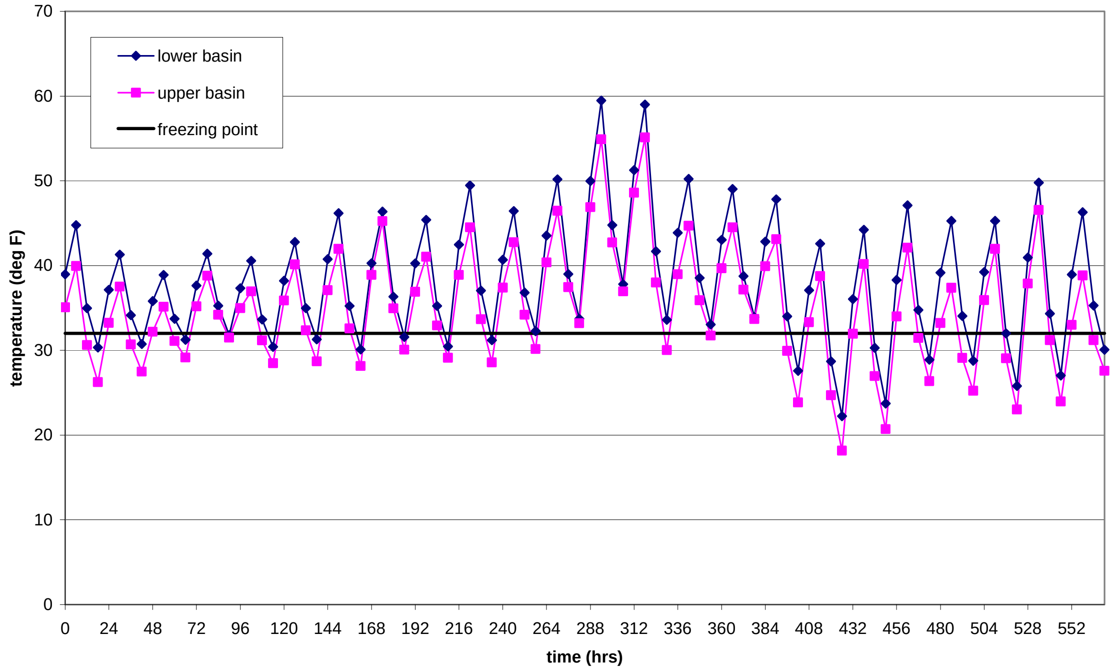


**Figure 71. Temperature trends during the March 1983 snow event.** Temperatures are generally around freezing during each storm event, rising above freezing during the period between the two cold events. This event represents a cold event during which temperatures are close to the freezing point.

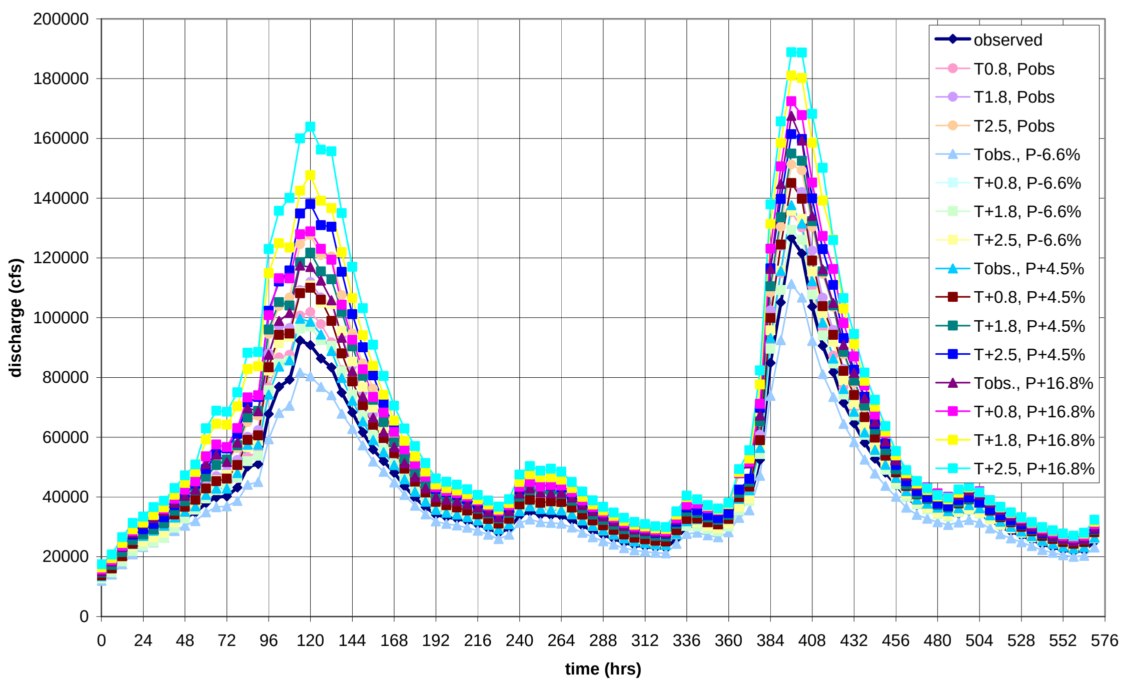


**Figure 72. Climate change inflows for the March 1983 snow event**. Small temperature increases effect the precipitation composition of this event.

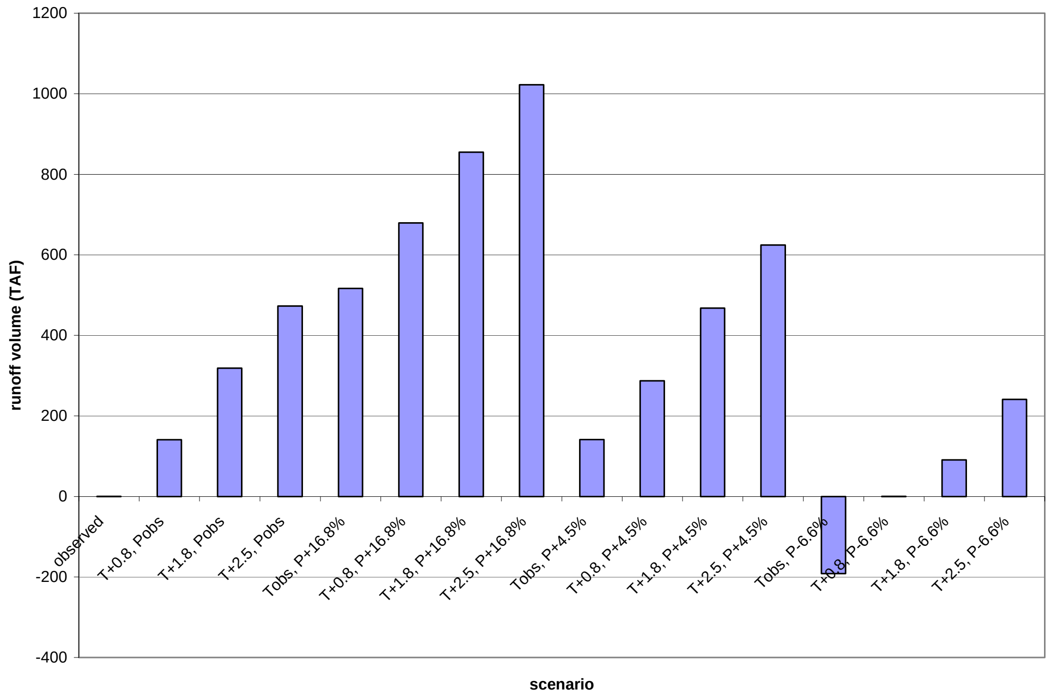


**Figure 73. Inflows are affected both by antecedent basin wetness and existing snowpack levels as well as changes in the event's precipitation composition.** Increasing temperatures cause higher fractions of precipitation to fall as rain than as snow, causing larger volumes of surface runoff. Increased surface runoff accelerates the time to basin saturation, preventing future rainfall from infiltrating and generating more surface runoff. Also, melting rates of previously existing snowpack accelerate with increased temperatures, contributing to basin wetness and surface runoff volumes. Basin conditions preceding the March 1983 event are wet, supporting the observation that the infiltration capacity of the basin is low, forcing larger volumes of surface runoff.

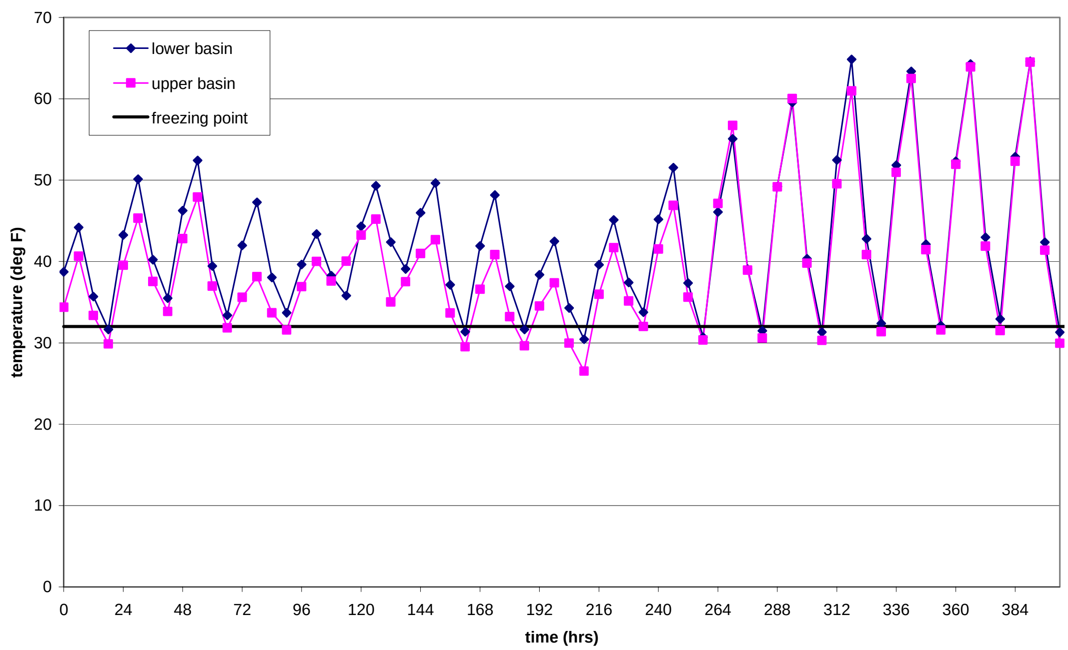


**Figure 74. Temperature trends during the observed February 1986 event.** Temperatures are above freezing for most of this event, indicating that the precipitation composition is mostly rain. Small temperature increases do not have a large effect on the composition of the storm's precipitation.

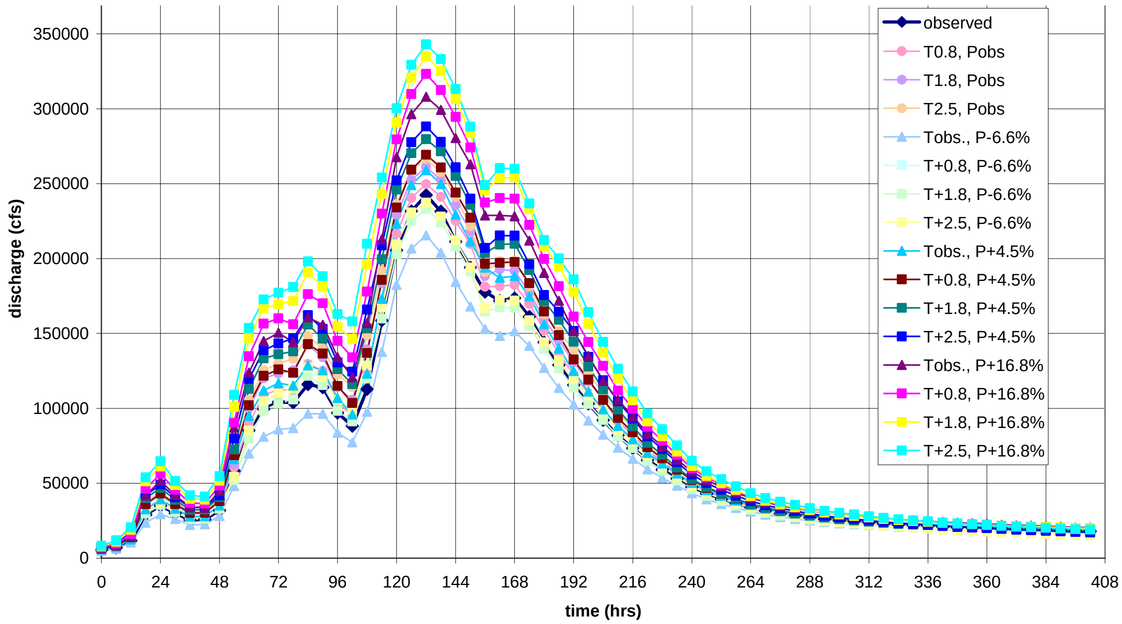


**Figure 75. Climate change inflows for the February 1986 rain event.** Inflows are slightly sensitive to temperature increases. This may be due to either antecedent basin conditions that reduce the infiltration capacity of the basin or to a small increase in the fraction of rain versus snow.

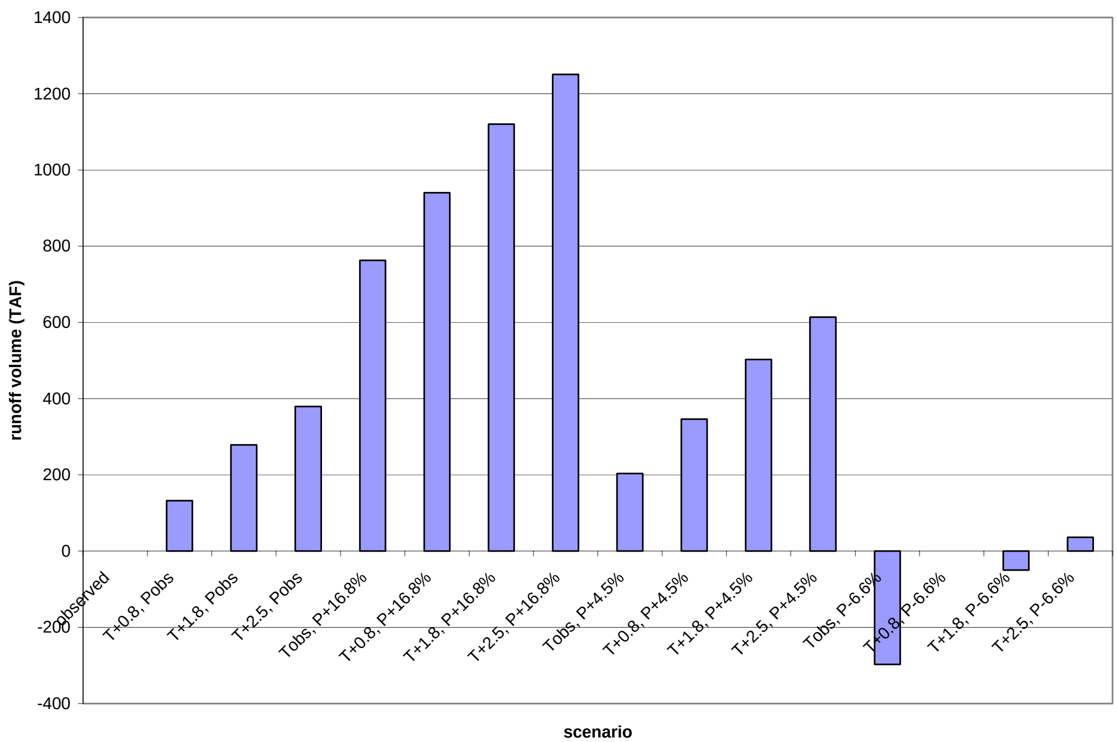


**Figure 76. Changes in runoff volumes from the observed February 1986 event.** Temperature has an effect on overall discharge volumes, causing larger inflows despite decreased precipitation intensities, though only in the climate scenario that also simulates the largest increase in temperatures. Also, antecedent basin conditions are wet, indicating a reduced infiltration capacity, forcing more water to runoff. The higher temperatures also accelerate the snowmelt rate, increasing basin wetness.

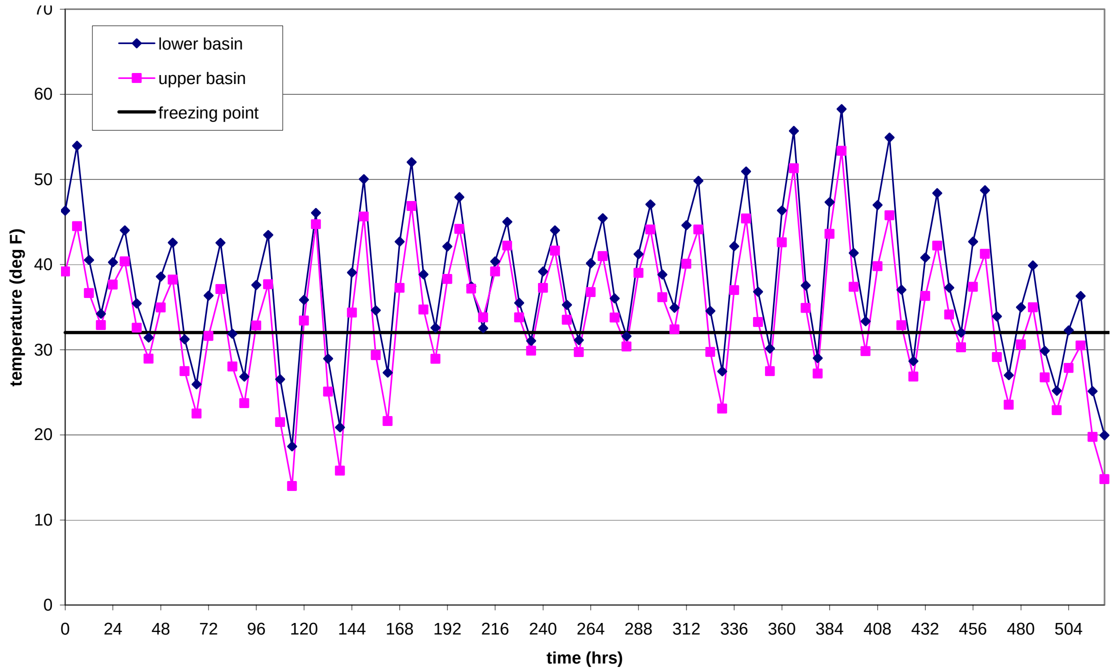


**Figure 77. Temperature trends during the March 1995 snow event.** Temperatures are near the freezing point throughout the storm event, indicating that this event is sensitive to small temperature increases. Increased temperatures increase the rain-snow ratio.

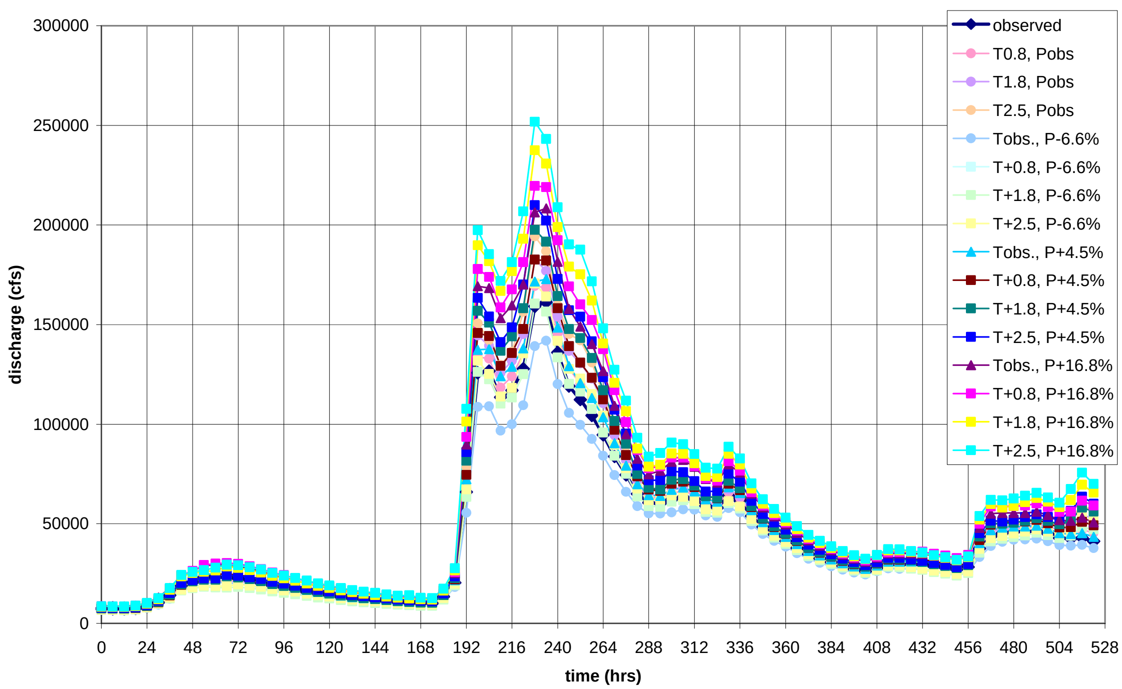


**Figure 78. Climate change inflows for the March 1995 event.** Inflows are sensitive to temperature changes, indicated by the variation in both perturbed temperature and perturbed precipitation climate scenarios. Increasing temperatures cause higher fractions of precipitation to fall as rain than as snow, increasing the volume of rainfall runoff and decreasing the long-term storage in the snowpack.

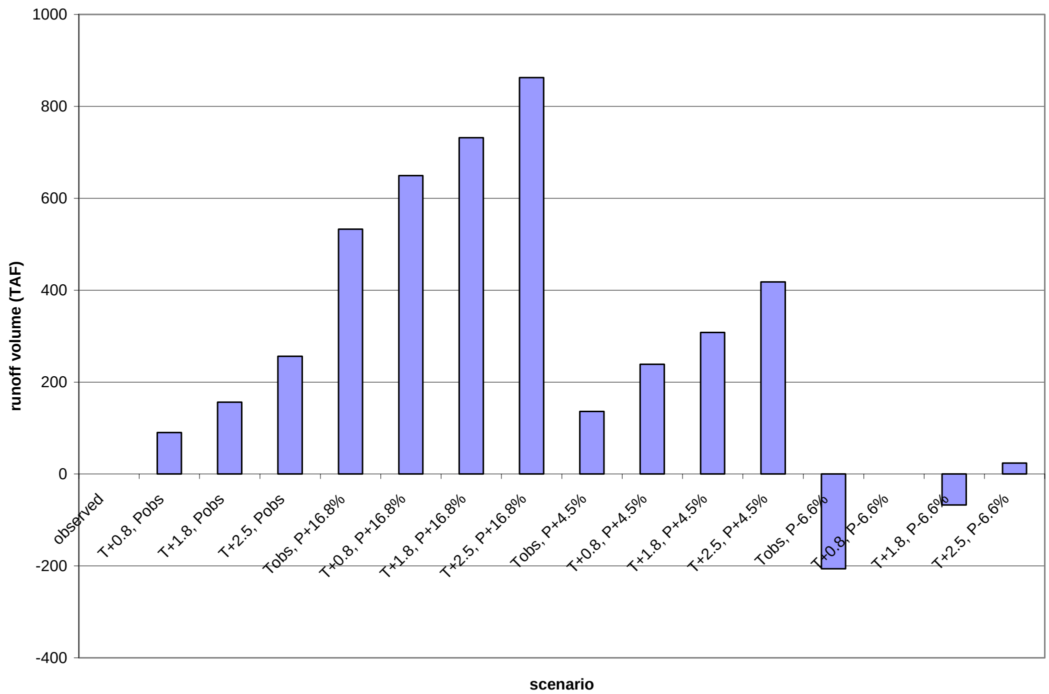


**Figure 79. Changes in runoff volumes from the observed March 1995 snow event.** Inflows respond to both perturbed temperature and precipitation regimes. Temperature has a stronger effect on inflow volumes than precipitation changes. The climate scenarios in which decreased precipitation intensities are simulated do not always result in decreased runoff volumes. In this scenario, antecedent basin wetness does not contribute to increased runoff volumes – the Feather basin is dry. However, preceding snowpack volumes may contribute to the storm's runoff, especially as inflows respond most strongly to the largest temperature increases.

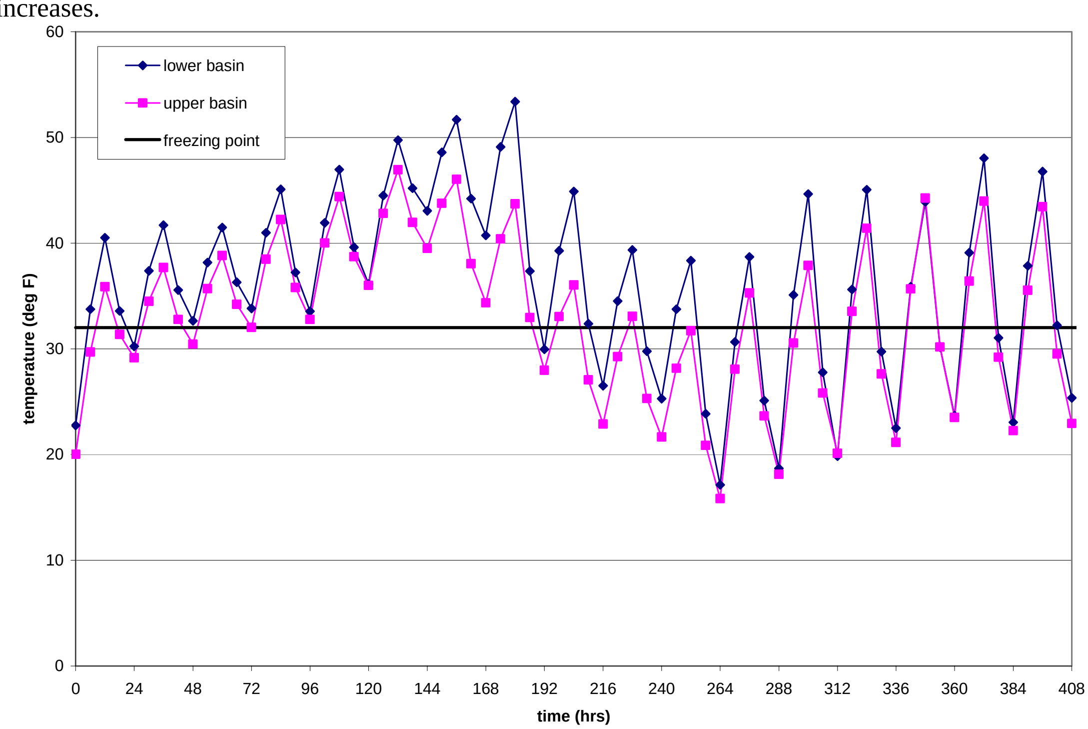


**Figure 80. Temperature trends during the January 1997 event.** Temperatures are well above freezing during the main event (hours 120-192), resulting in a mainly rain storm event. Increasing temperatures do not significantly alter the precipitation composition of the observed event.

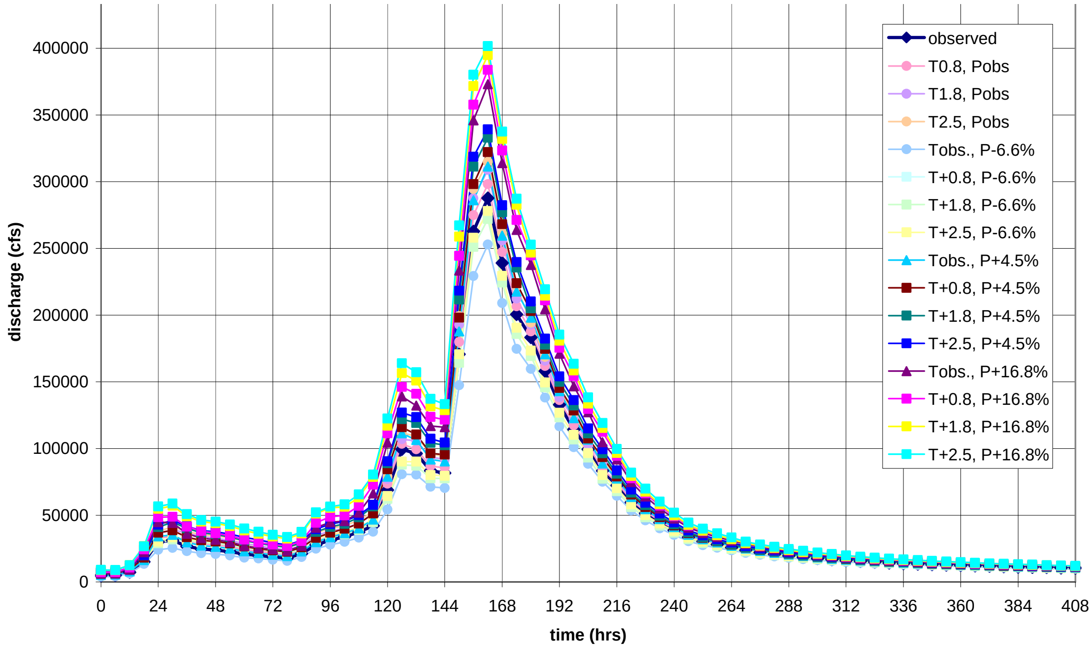


**Figure 81. Climate change inflows for the January 1997 event.** Inflows are slightly sensitive to increasing temperature regimes, though runoff trends tend to group around identical precipitation intensities. Antecedent basin conditions are wet, forcing more surface runoff due to reduced infiltration capacity.

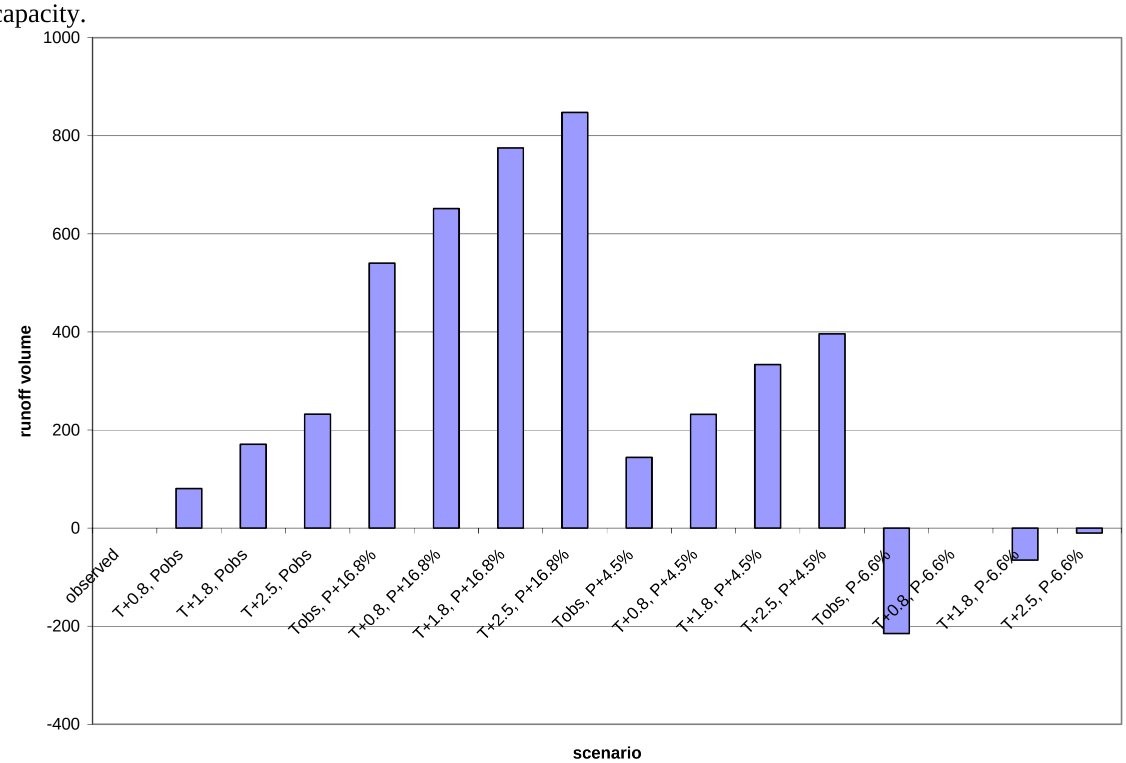


**Figure 82. Changes in runoff volume for the January 1997 rain event.** Temperature affects inflow volumes, though the effects are not strong enough to increase volumes from climate scenarios simulating decreased precipitation intensities above the observed event. Basin conditions preceding the storm event are wet, resulting in more surface runoff as less water infiltrates due to reduced infiltration capacity. Preexisting snowpack also contributes the basin wetness as warmer temperatures accelerate the rate of snowmelt.

# Appendix C: Climate change scenario effects on Shasta inflows

Ensemble charts of sampled flood events for Shasta basin and their accompanied volume changes.

| | Shasta @ Alturas Precipitation during past 30 days (inches) | past WY | basin conditions |
|---|---|---|---|
| Jan-63 | 0.86 | Below Normal | Dry |
| Dec-64 | 1.6 | Dry | Dry |
| Jan-69 | 3.3 | Below Normal | Dry |
| Jan-80 | missing | Below Normal | N/A |
| Dec-82 | 1.55 | Dry | Dry |
| Mar-83 | 0.61 | Wet | Dry |
| Feb-86 | 0.98 | Dry | Dry |
| Mar-95 | 0.53 | Critical | Dry |
| Jan-97 | 3.12 | Wet | Dry |

**Table 16. Basin wetness conditions above Shasta Dam preceding the sampled flood events**

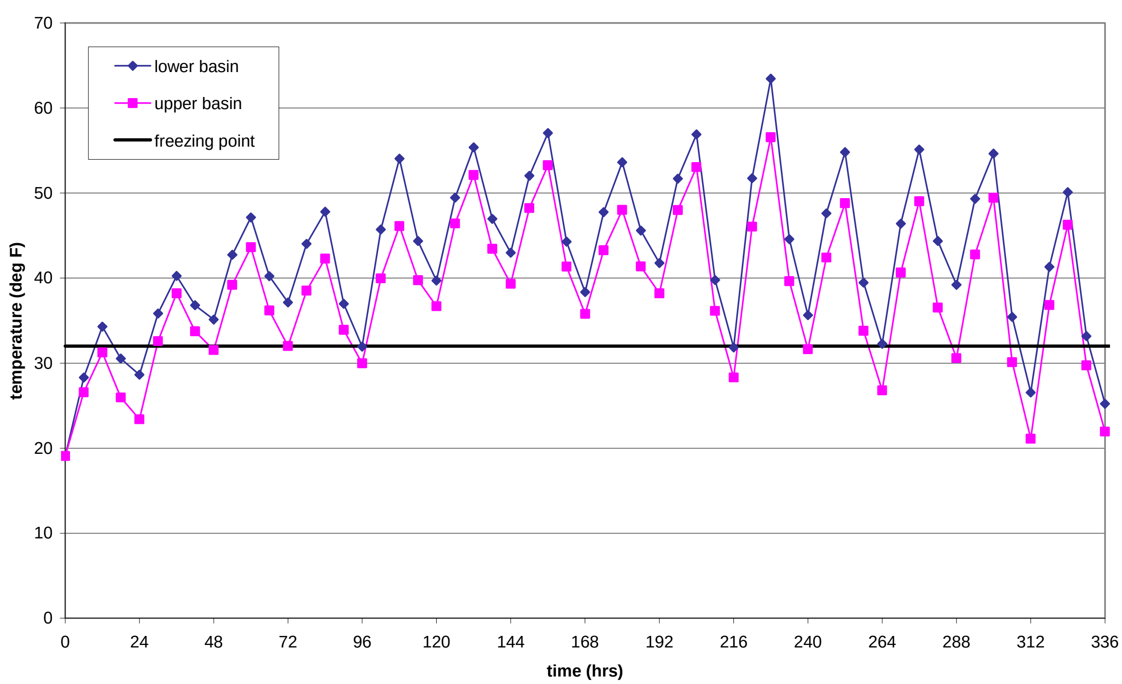


**Figure 83. Temperature trends during the January 1963 event.** Temperatures are above freezing during the storm event (hours 48-192). Small temperature increases do not cause a large shift in rain-snow ratios.

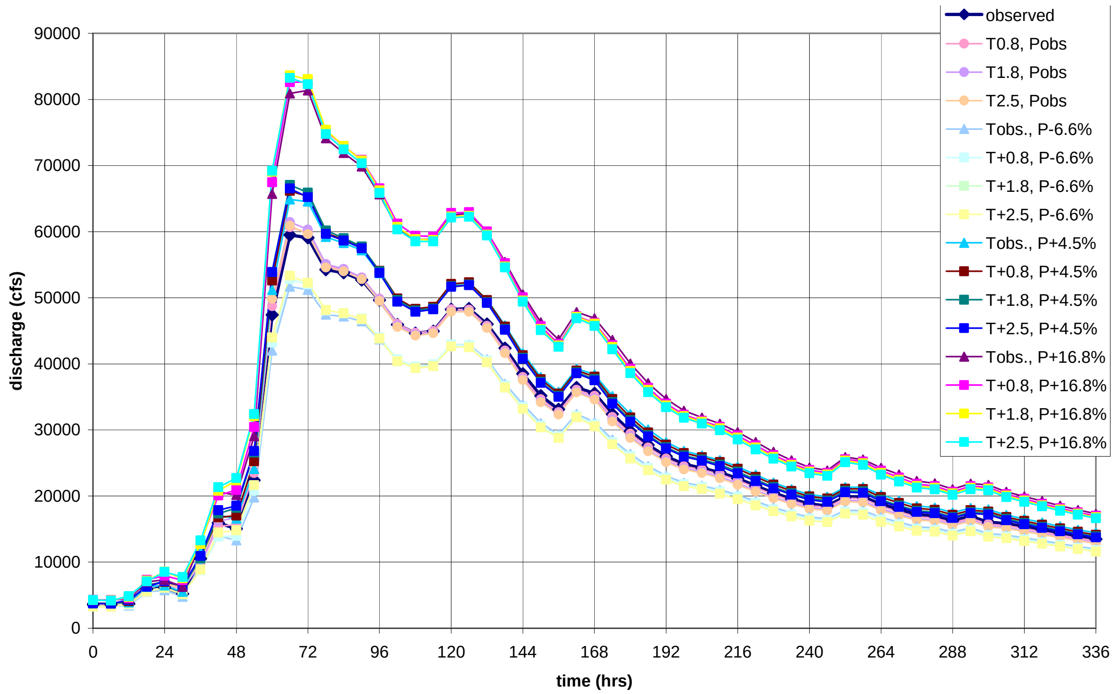


**Figure 84. Climate change inflows for January 1963 rain event.** Inflows are strongly affected by precipitation shifts, forming four distinct groups based on identical precipitation intensities. Increasing temperatures do not have a strong effect on inflow patterns – within climate scenarios that simulate the same precipitation scenarios, temperatures shifts have barely observable effects. As the observed event is comprised of mostly rain and not snow, increasing temperatures have little effect on the rain-snow composition of the storm.

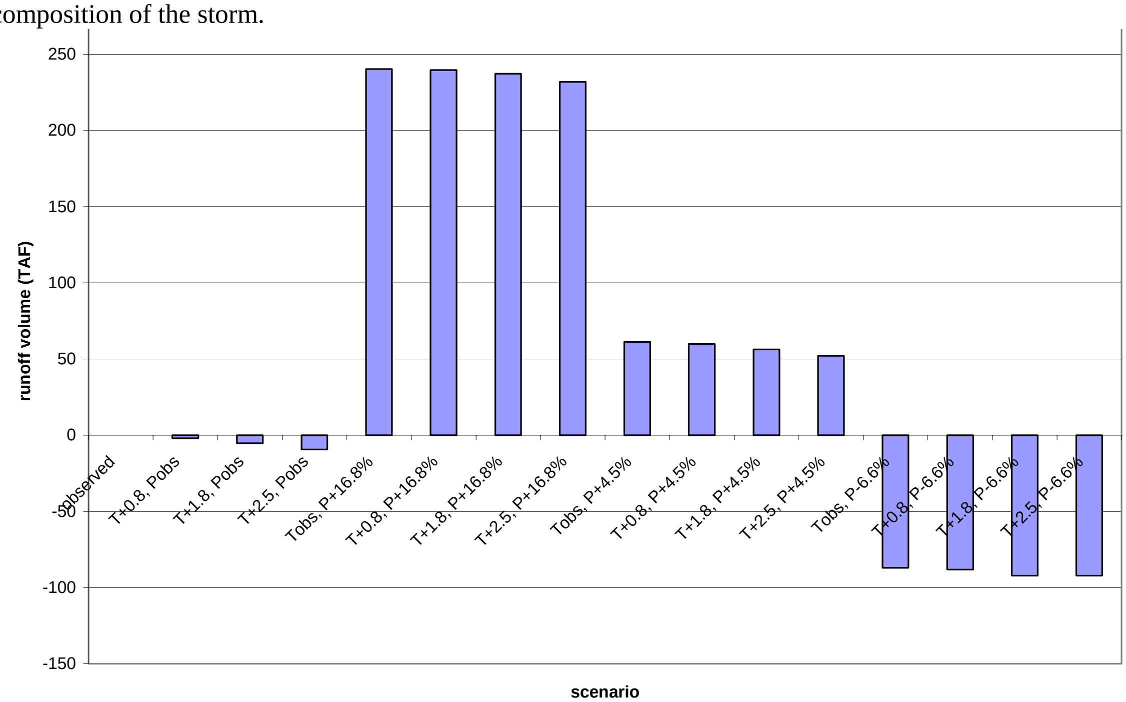


**Figure 85. Changes in runoff volumes from the observed January 1963 event.** Increasing temperatures have little effect on inflow volumes – as most of the observed event contains rain rather than snow, little shifts in precipitation occur despite large temperature increases. Basin conditions are dry and the infiltration capacity of Shasta's basin is high. Therefore, basin saturation has little effect on inflow volumes.

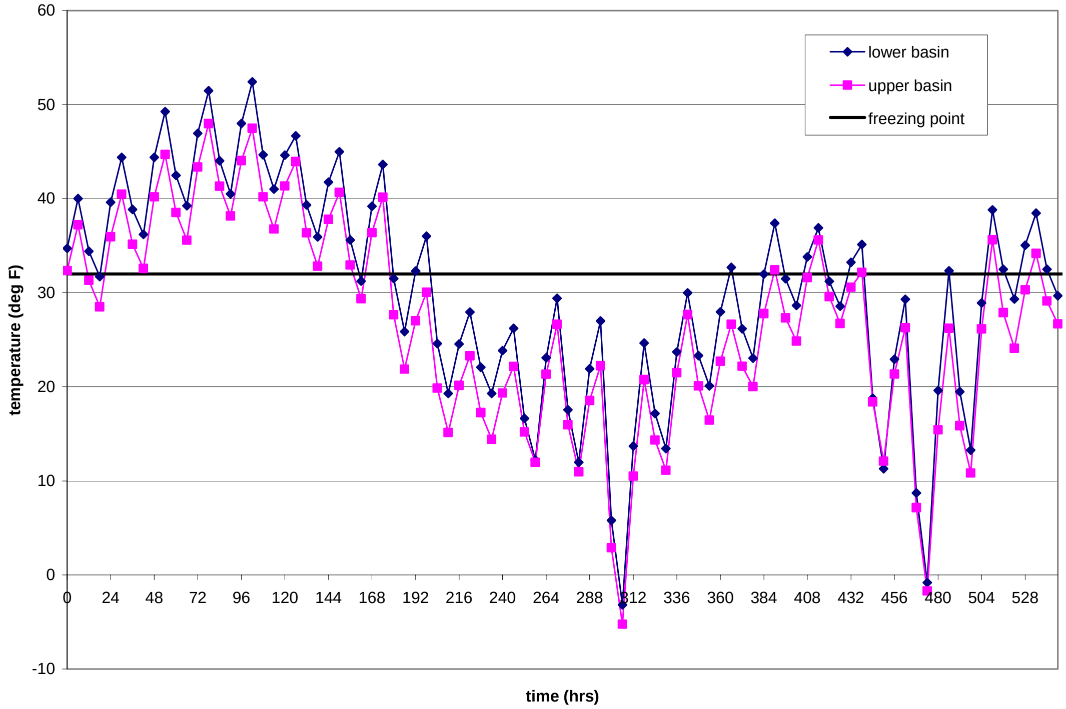


**Figure 86. Temperature trends for the December 1964 event.** Temperatures during the main flood event are above freezing, indicating that the main flood event is not sensitive to small temperature increases. A smaller storm event occurs after the main peak, when the temperatures are at and below the freezing point (hours 408-480). During this event, small temperature increases do affect the rain-snow ratio.

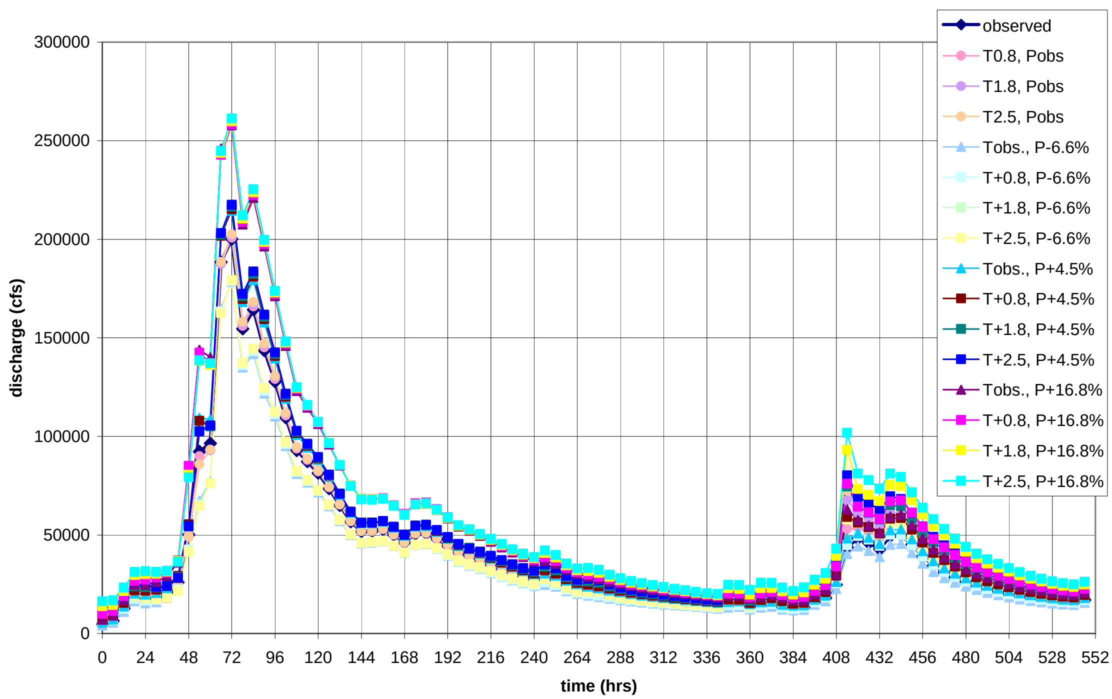


**Figure 87. Climate change inflows for the December 1964 rain event.** Temperature changes have little effect on inflow volumes during the main flood event (hour 48-144). Inflows respond more strongly to precipitation intensity changes as is illustrated by the different inflow groupings during the first flood event. Temperatures have a greater effect on inflows during the smaller storm event, when observed temperatures are at and below the freezing point. Precipitation ratios shift, increasing the fraction of rain.

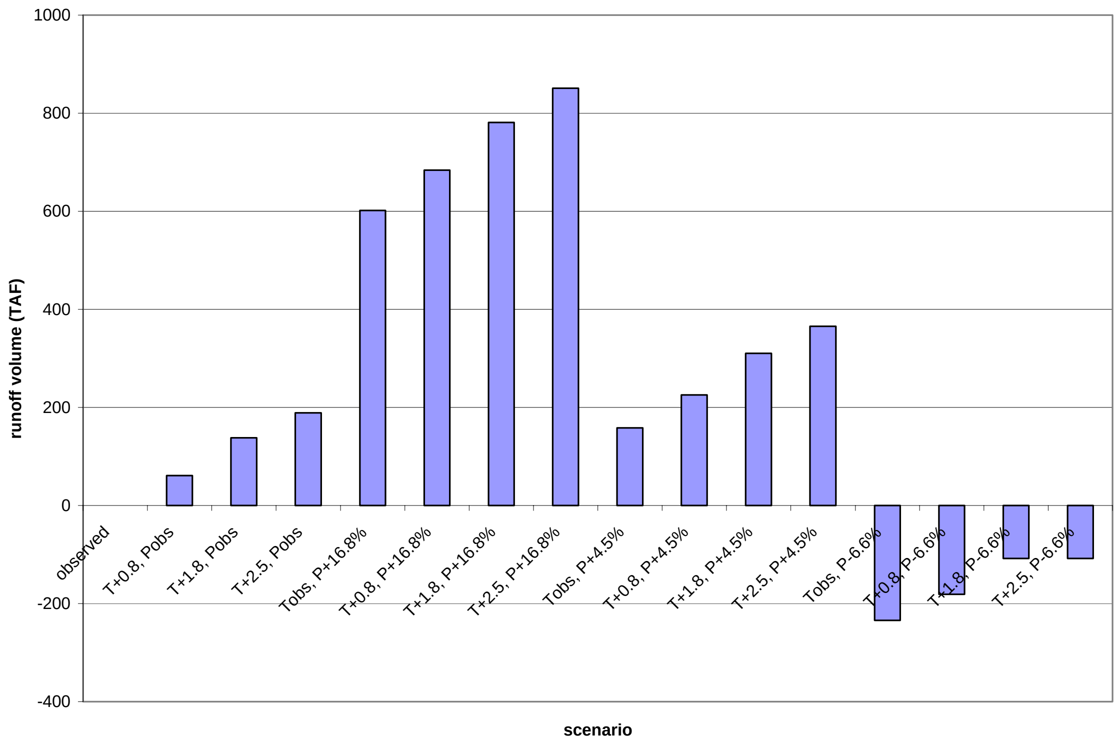


**Figure 88. Changes in runoff volumes from the observed December 1964 event.** Temperature has a small effect on inflow volumes; this is likely due to the impact of temperature on the colder storm event that follows the main storm event, which is mostly unaffected by temperature increases. Basin conditions preceding this event are dry; basin saturation has little effect on surface runoff volumes.

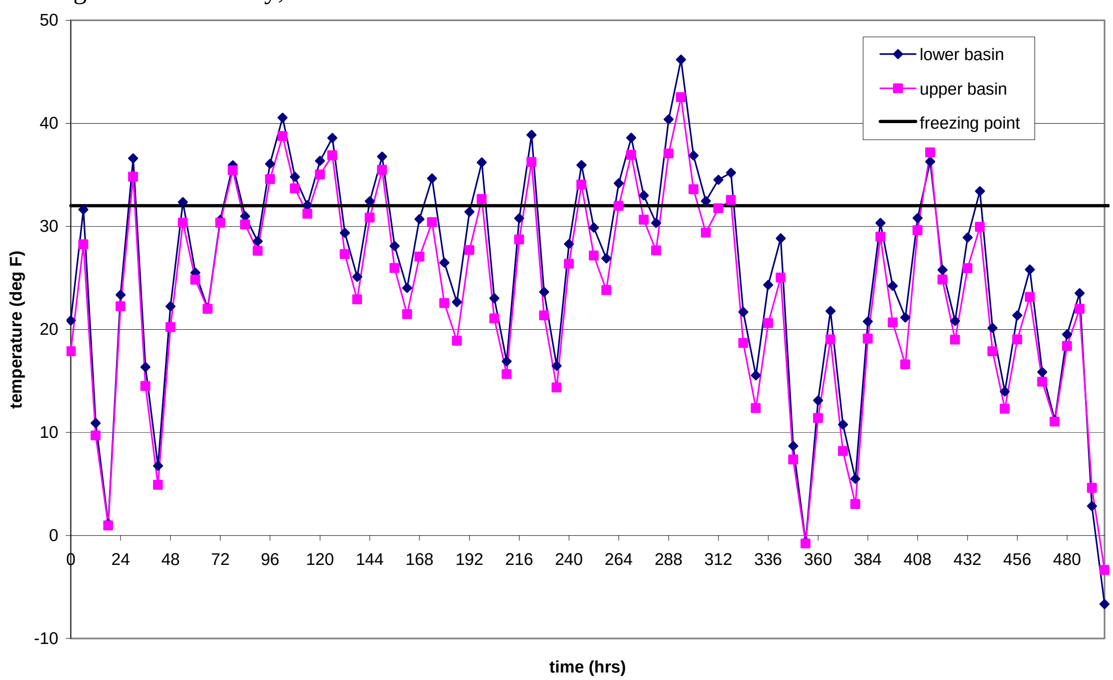


**Figure 89. Temperature trends during the January 1969 event.** Temperature are at and below the freezing point during the main flood event (hours 96-144) and well below the freezing point during the flood event that follows (hours 288-284). Increasing temperatures affect the precipitation composition of these storms, converting snowfall to rainfall and affected short-term runoff patterns.

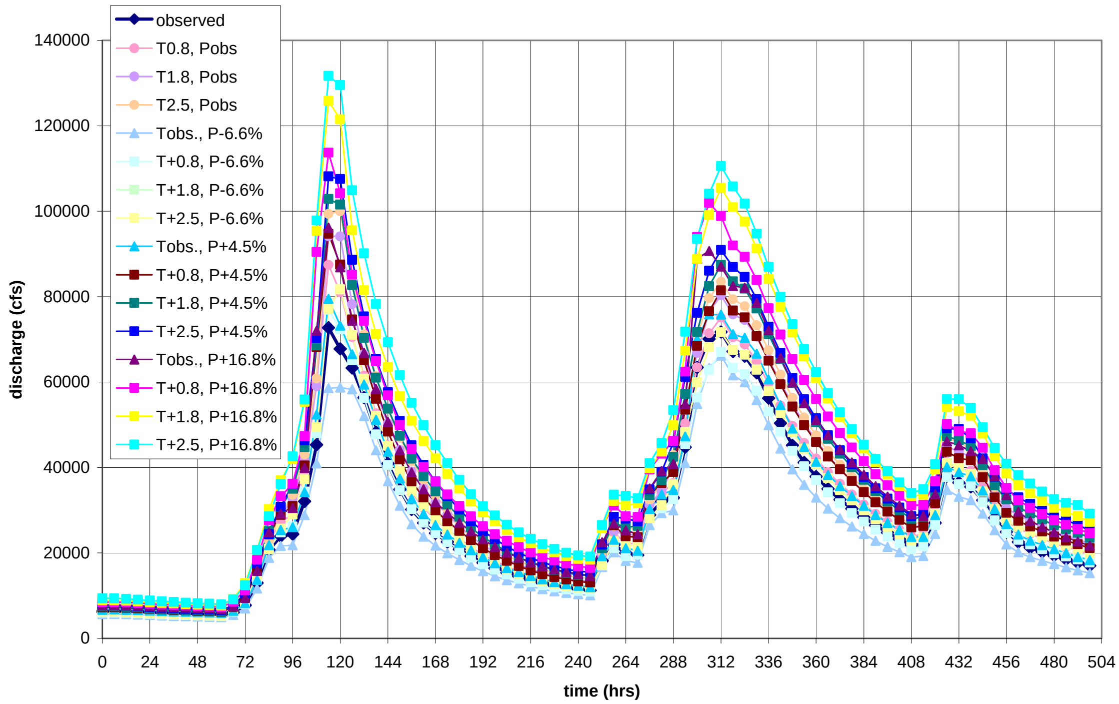


**Figure 90. Climate change inflows for the January 1969 event.** Inflows are sensitive to small temperature increases – this trend is illustrated by the widely varying flows climate scenarios that simulate identical precipitation intensities.

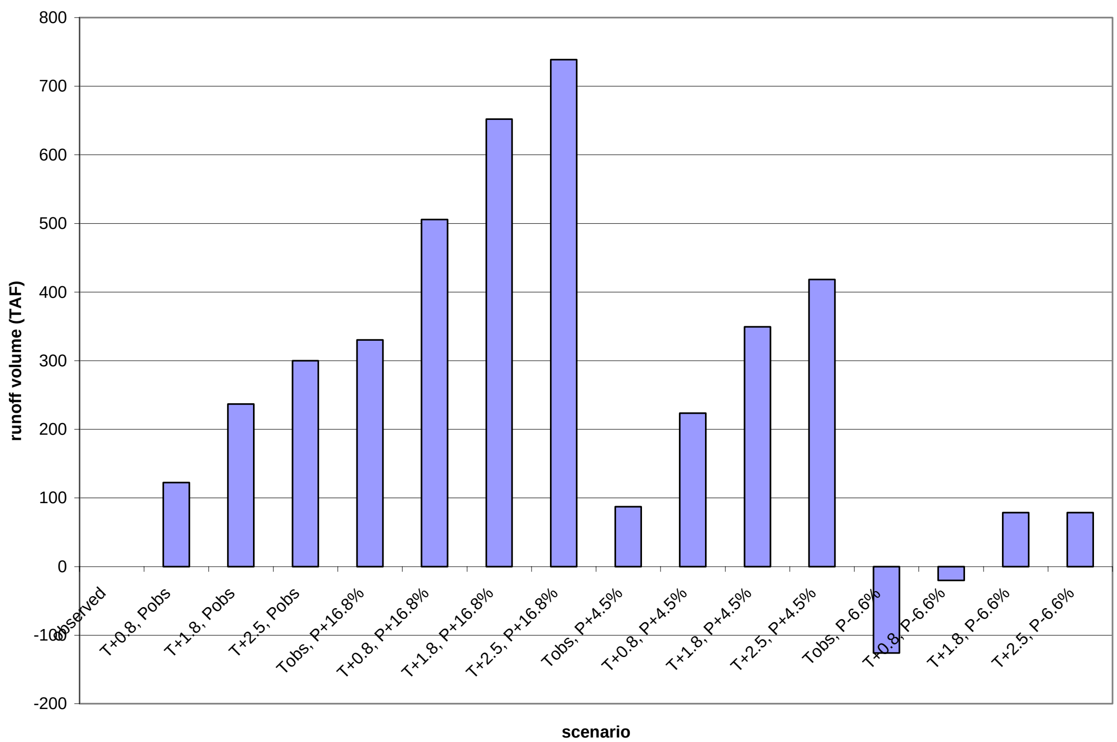


**Figure 91. Changes in runoff volumes from the observed event.** Increasing temperatures have a significant effect on overall discharge volumes. Higher temperatures cause more rainfall runoff as temperature shift away from the freezing point. Though the basin is dry prior to the main flood event, the second storm event is affected by basin saturation caused by the main flood event. With higher ground moisture levels, more runoff is forced along the surface rather than infiltrating.

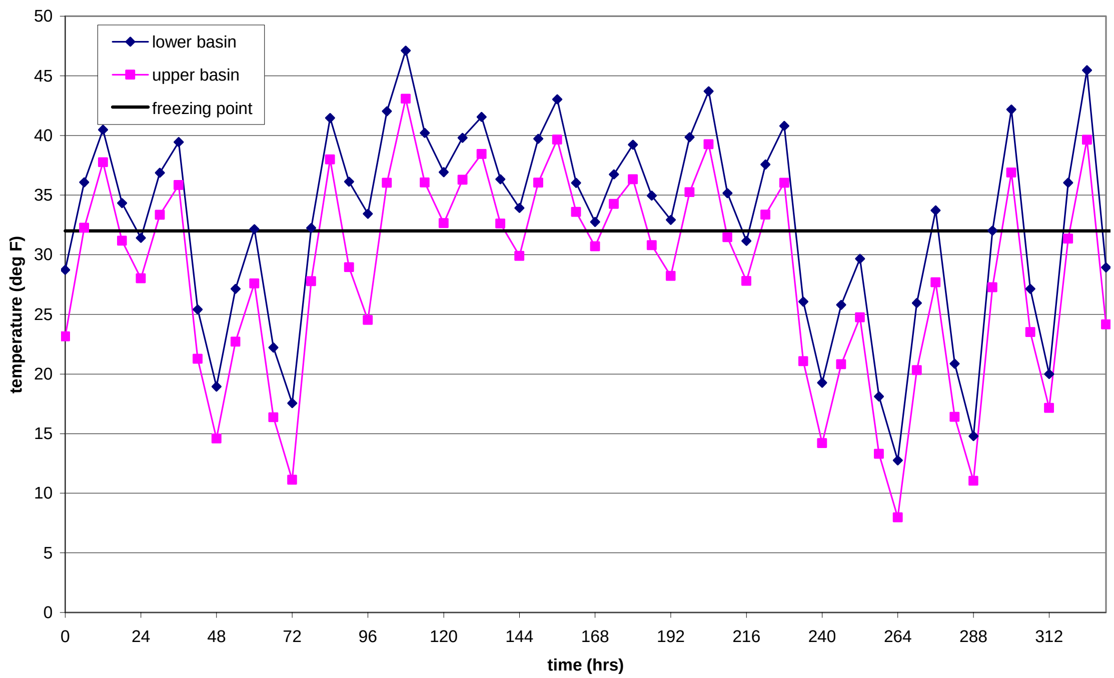


**Figure 92. Temperature trends during the January 1980 snow event.** Temperatures are mostly above the freezing point during the storm event (hours 96-216). Small temperature increases do not significantly affect the precipitation composition of this storm.

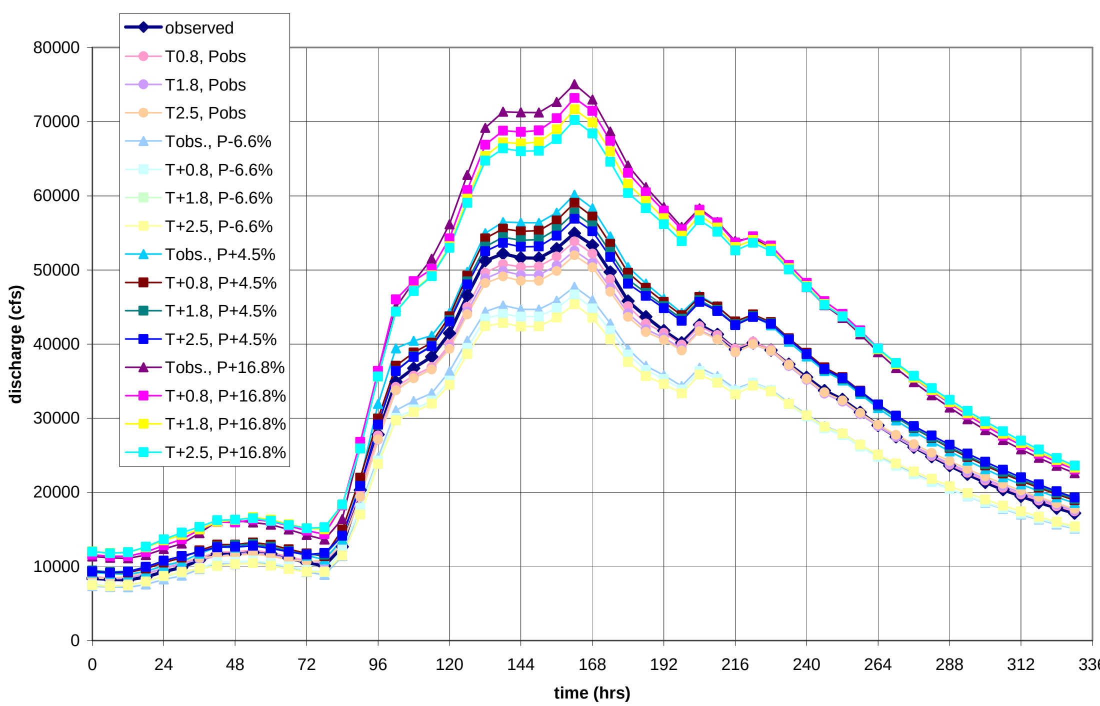


**Figure 93. Climate change inflows for the January 1980 snow event.** Temperatures do not have a strong effect on inflows as is illustrated by the distinct grouping of inflows around climate scenarios that simulate identical precipitation intensities. However, inflows show more variability around temperature shifts than typically observed in rain events where temperatures are well above the freezing point, indicating that some temperature effect is present.

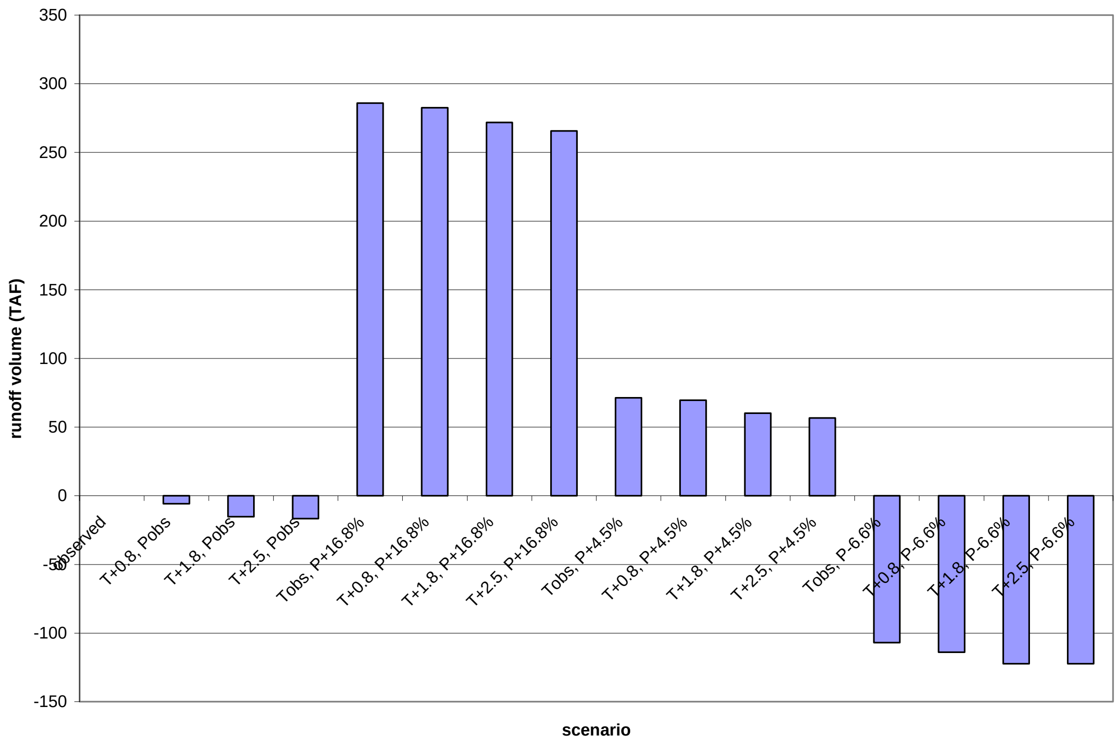


**Figure 94. Changes in runoff volumes from the February 1980 snow event.** One unusual pattern illustrated by these climate scenarios is a decrease in overall runoff volumes given temperature increases. However, temperature does not have as strong an impact on discharge volumes as precipitation intensity changes do.

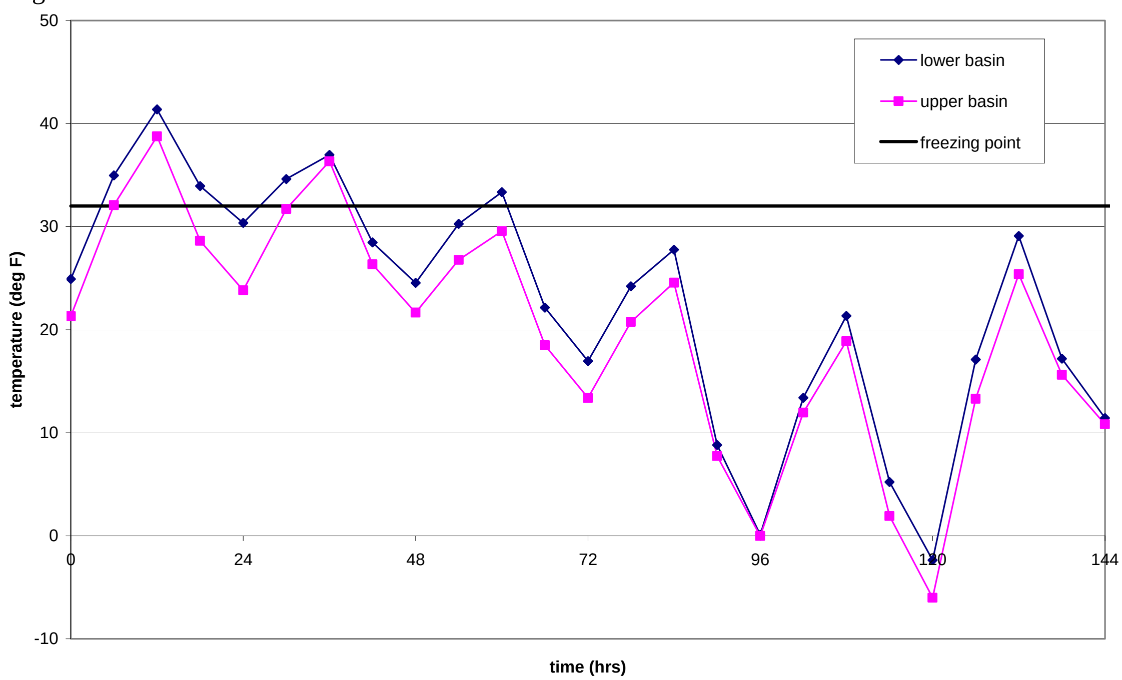


**Figure 95. Temperature trends for the December 1982 snow event.** Temperatures begin near the freezing point and continue to decrease as the event progresses. The flood event shows a greater response to temperature changes near the beginning of the event, when temperatures are near freezing and small temperature increases have a significant effect on the storm's precipitation composition. Toward the end of the event, as temperatures continue to decrease, the storm shows less variability.

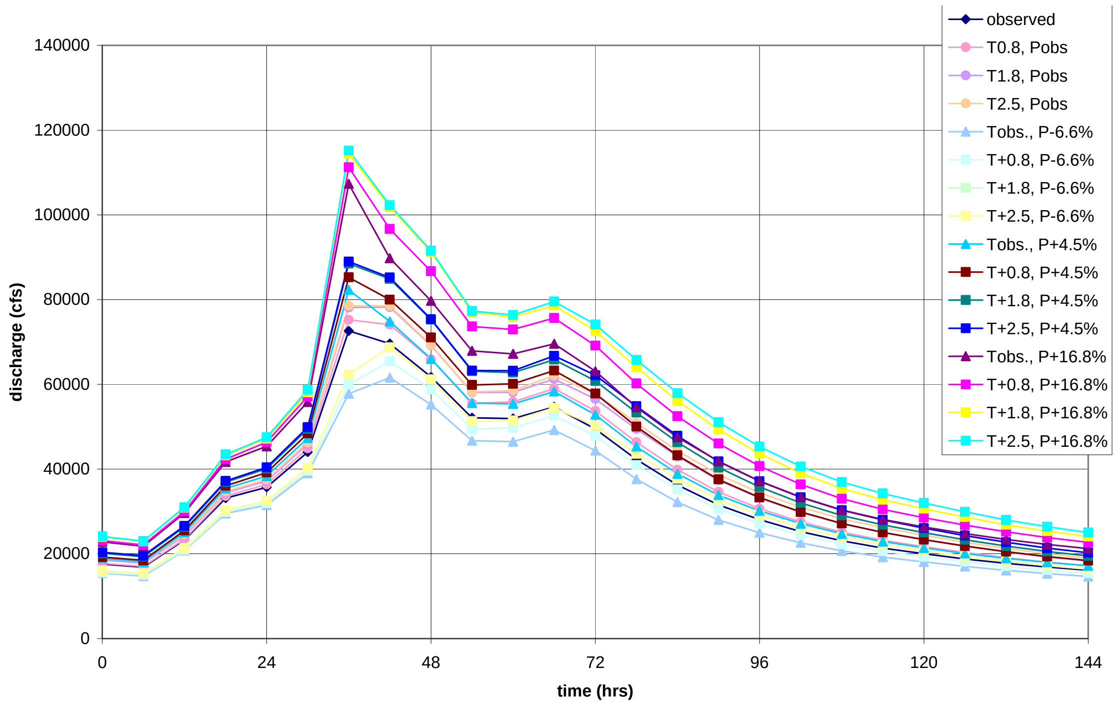


**Figure 96. Climate change inflows for the December 1982 storm event.** Temperature increases have a greater effect at the beginning of the event than at the end. Temperatures continue to decrease throughout the event; small temperature increases no longer force storm temperatures above freezing as the temperatures fall well below freezing.

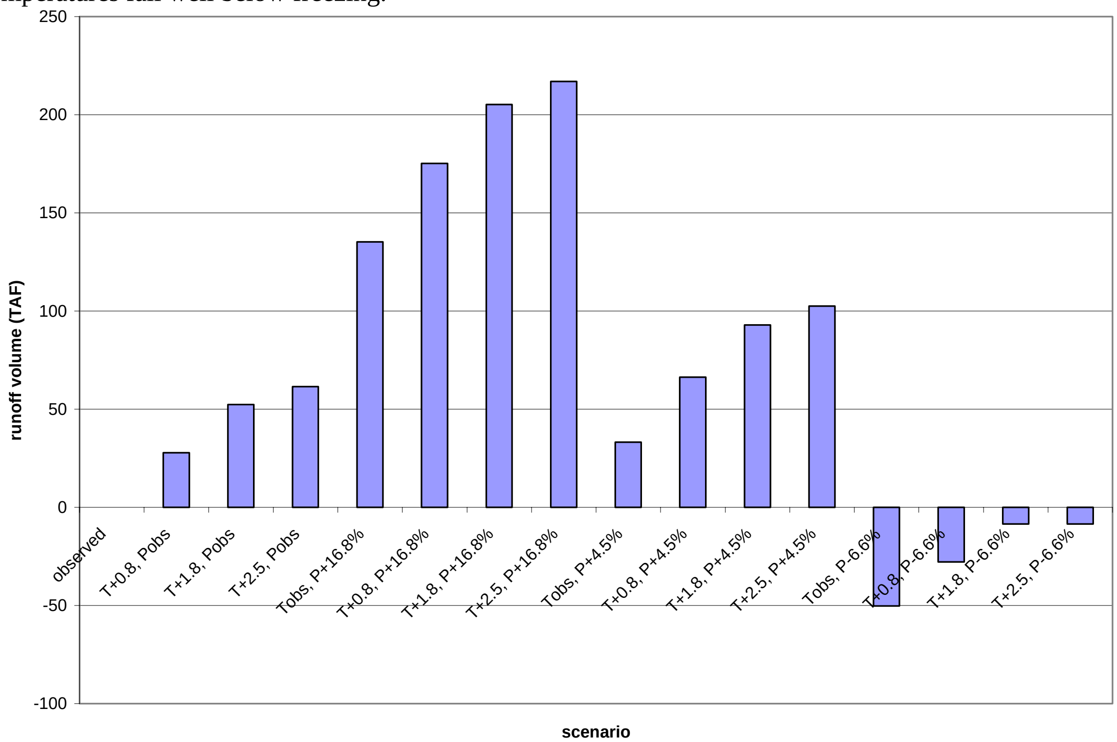


**Figure 97. Changes in runoff volumes from the observed December 1982 snow event.** Temperature increases has some effect on overall inflow volumes, however they are not strong enough to overcome trends due to precipitation intensity decreases. Basin wetness conditions are dry, indicating that basin saturation has little effect on forcing more surface runoff than infiltration.

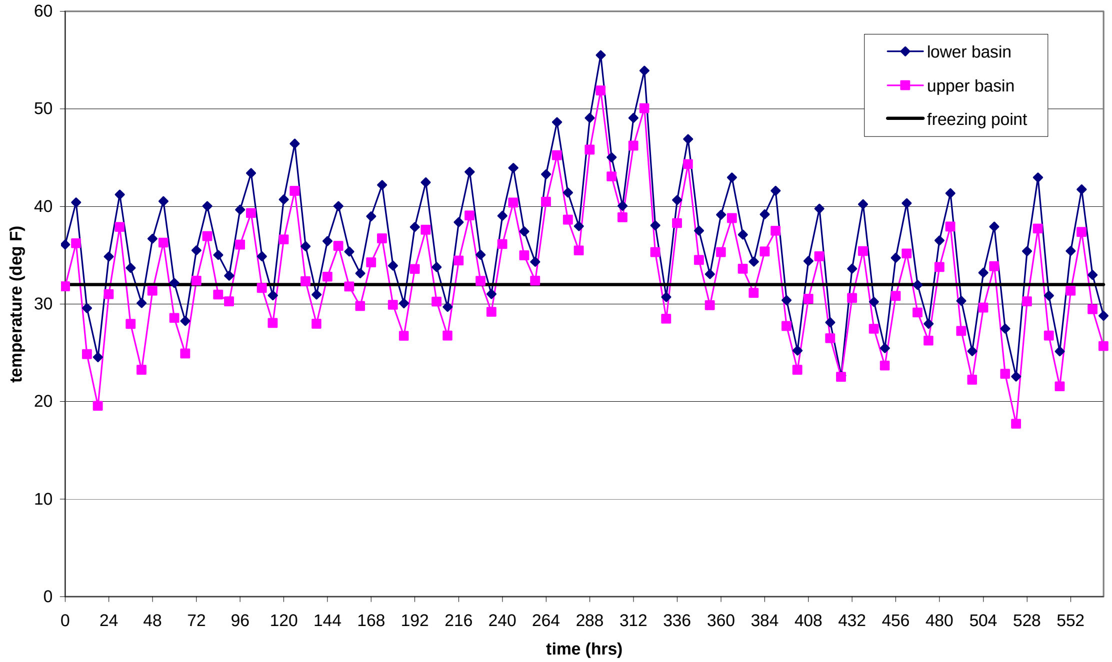


**Figure 29. Temperature trends during the March 1983 snow event.** Temperatures oscillate above and below the freezing point, making this event sensitive to small temperature increases.

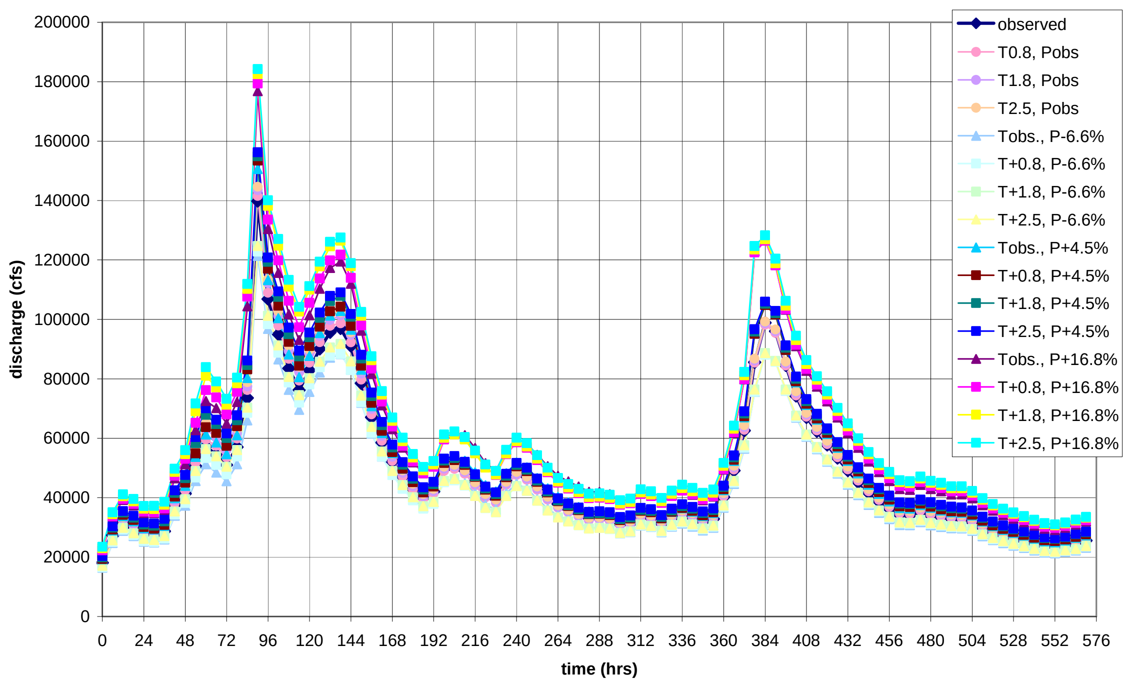


**Figure 99. Climate change inflows for the March 1983 snow event.** Inflows are more sensitive to small temperature changes during the main event (hours 24-192) as small temperature increases force most of the temperature record above the freezing point. A second event, which follows the main flood event, shows less sensitivity to temperature increases. Observed temperatures during the second, smaller event are further below the freezing point and are less likely to rise above the freezing point given small temperature increases.

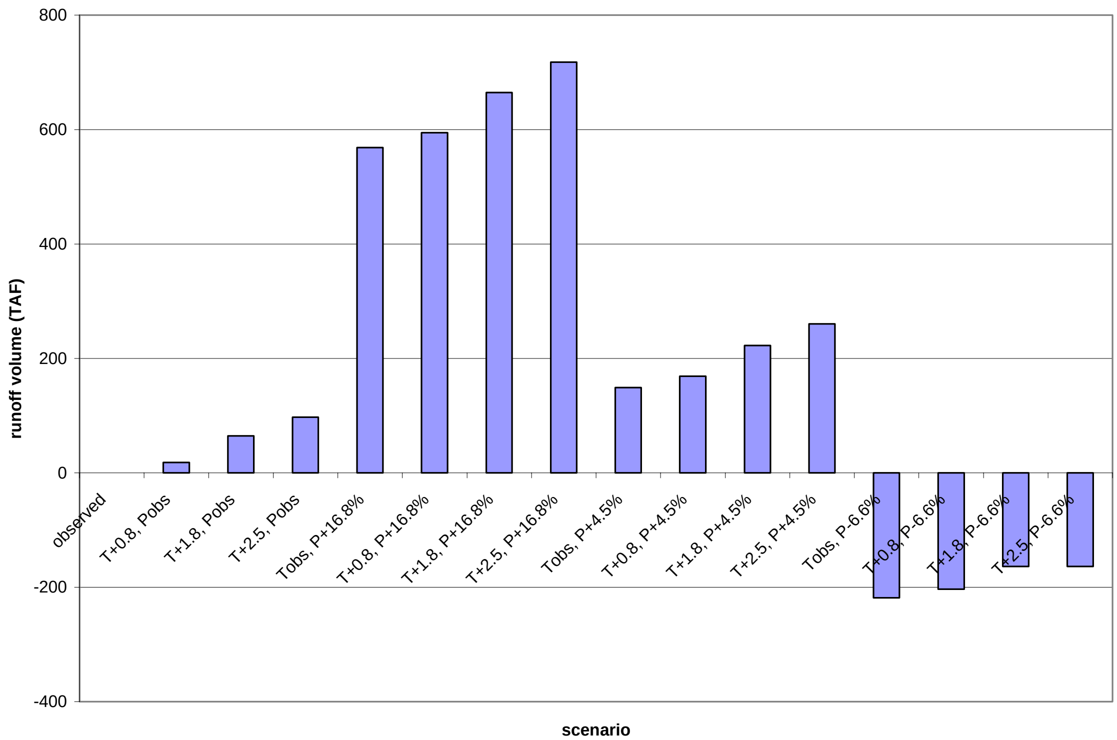


**Figure 100. Changes in runoff volumes from the observed March 1983 snow event.** Temperature has a small effect on overall flood volumes, indicating that as the temperature continues to fall as the flood event progresses, small temperature increases have less effect on inflow volumes. The basin is dry preceding this flood event, though the previous water year is wet.

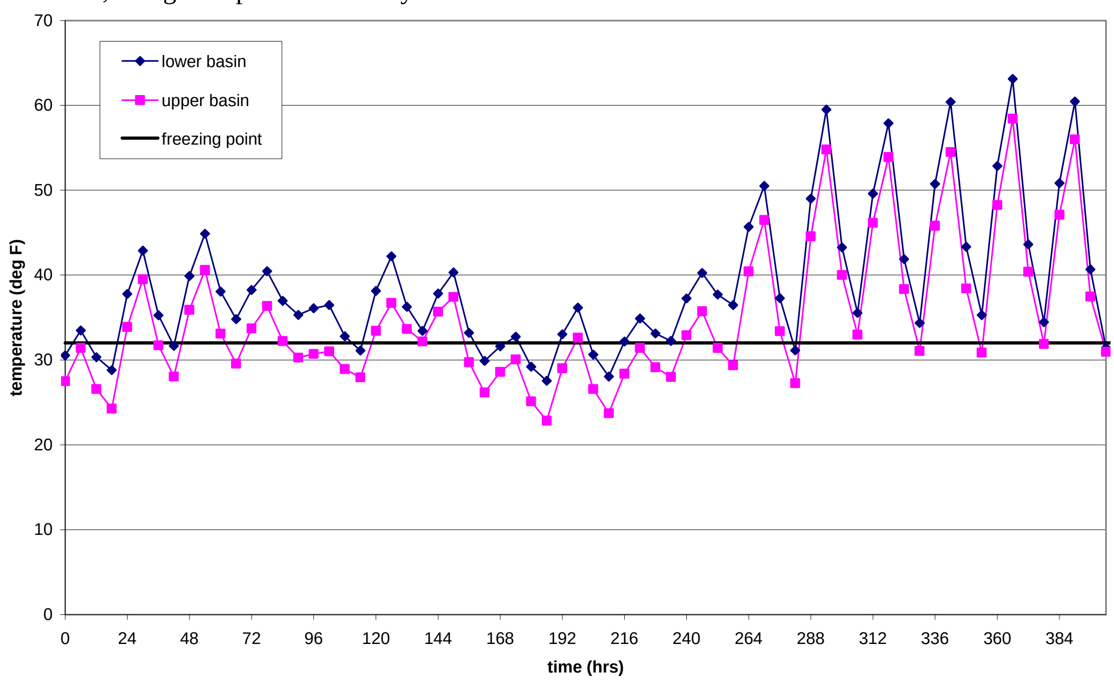


**Figure 301. Temperature trends during the February 1986 rain event.** Temperatures are at and above freezing during this rain event, indicating that increasing temperatures have little effect on the composition of the storm's precipitation.

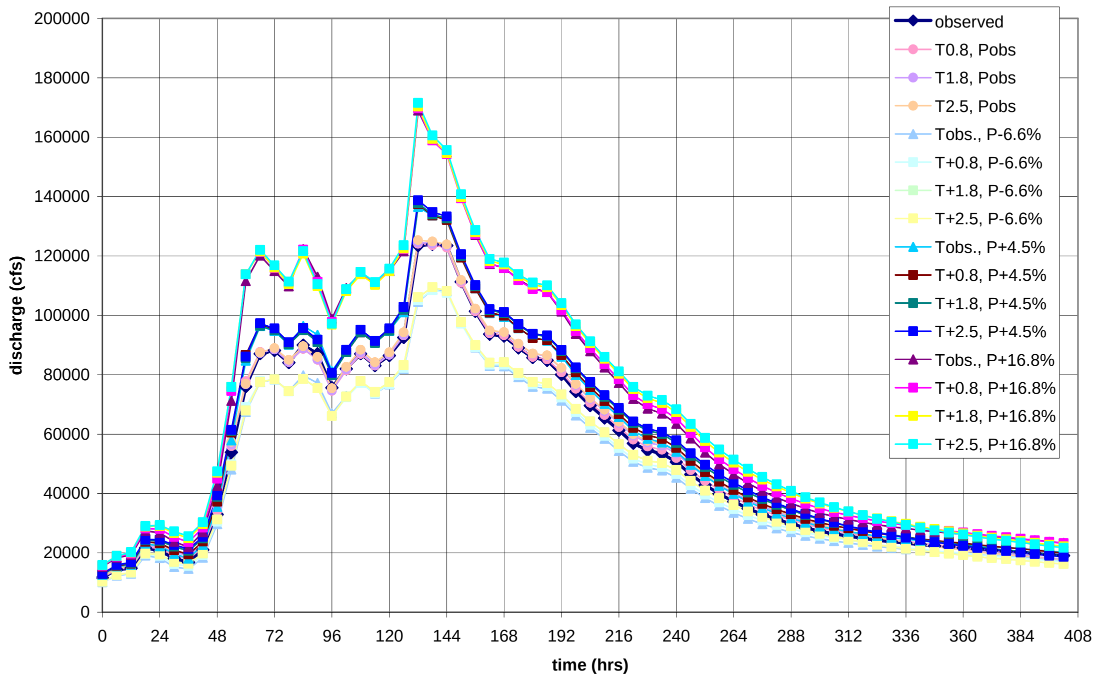


**Figure 102. Climate change inflows for the February 1986 event.** Inflows show little sensitivity to changing temperature regimes. This is illustrated by the lack of variability in climate scenarios that simulate identical precipitation intensities and increasing temperatures. This lack of variability supports the observation that the original event is mostly rain, which is unaffected by temperature increases.

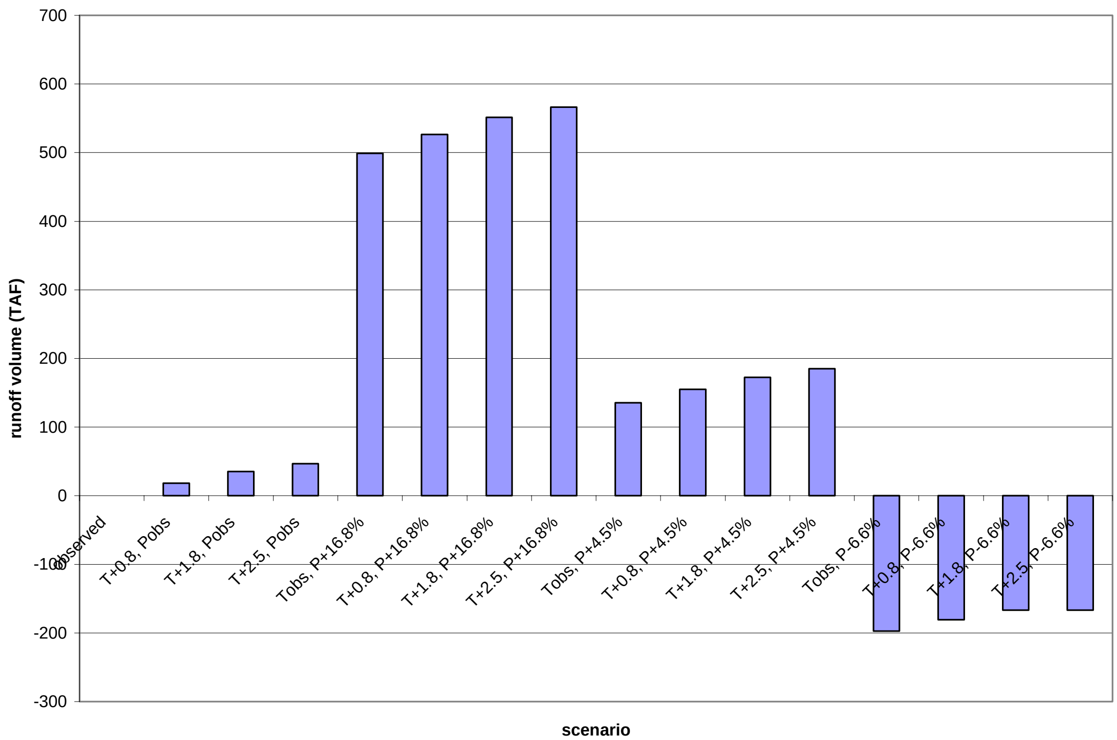


**Figure 103. Changes in runoff volume from the February 1986 event.** Inflow volumes show little response to increasing temperatures. Large volume shifts are due to changes in precipitation intensities. Basin conditions preceding this event are dry, indicating that basin saturation is not present to force inflows to the surface rather than infiltrate.

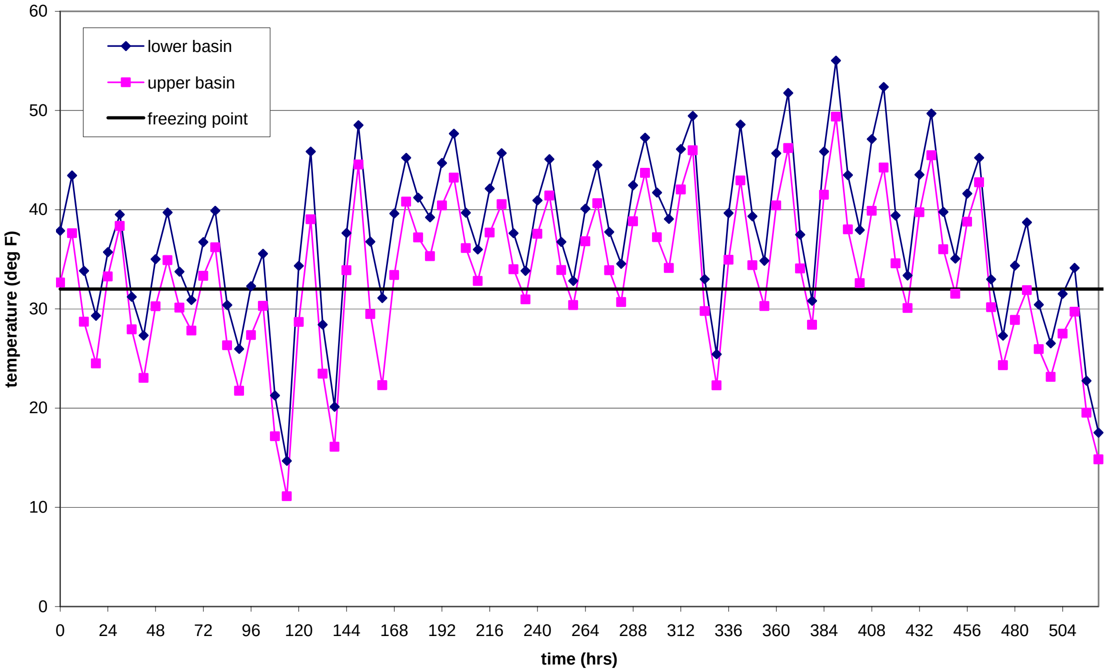


**Figure 104. Temperature trends during the March 1995 snow event.** Temperatures are mostly above the freezing point during the storm event (hours 168-384). Little change in inflows occurs due to increasing temperature scenarios. Smaller events occur before and after the flood event, when temperatures are at and below the freezing point. These smaller events are more sensitive to increased temperatures.

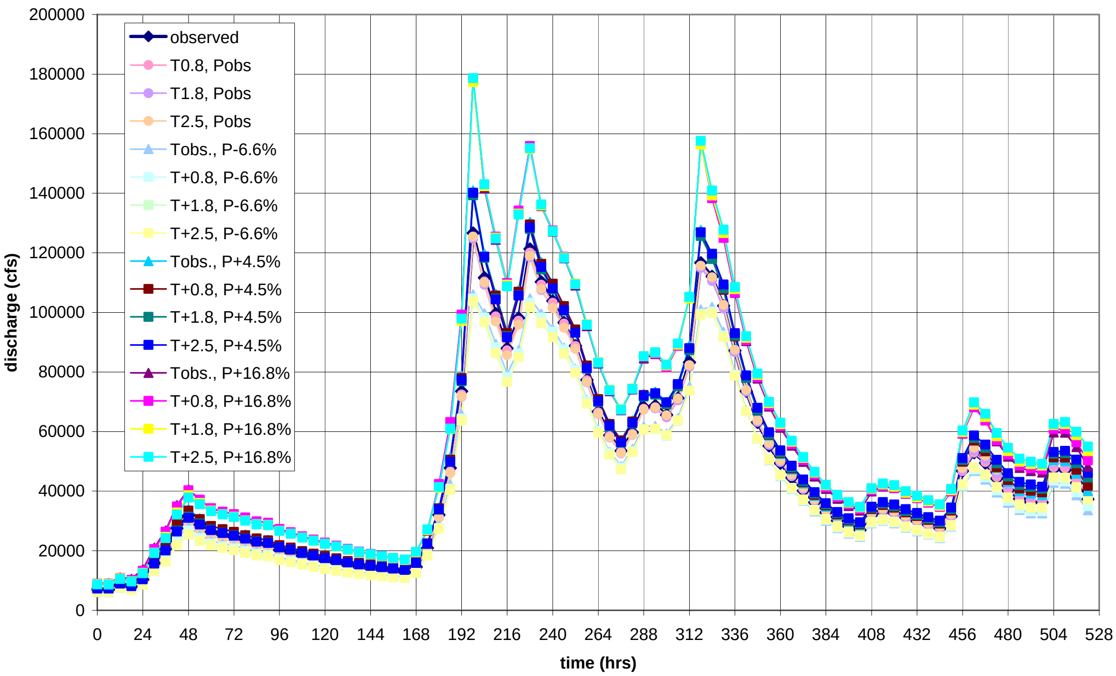


**Figure 105. Climate change inflows for the March 1995 event.** This event shows little sensitivity to increasing temperature changes. As temperatures during the flood event are above the freezing point, little change is expected. The runoff patterns are more consistent with a rain event than with a snow event. During snow events, small temperature increases affect the rain-snow composition of the event and more variability is observed due to temperature increases.

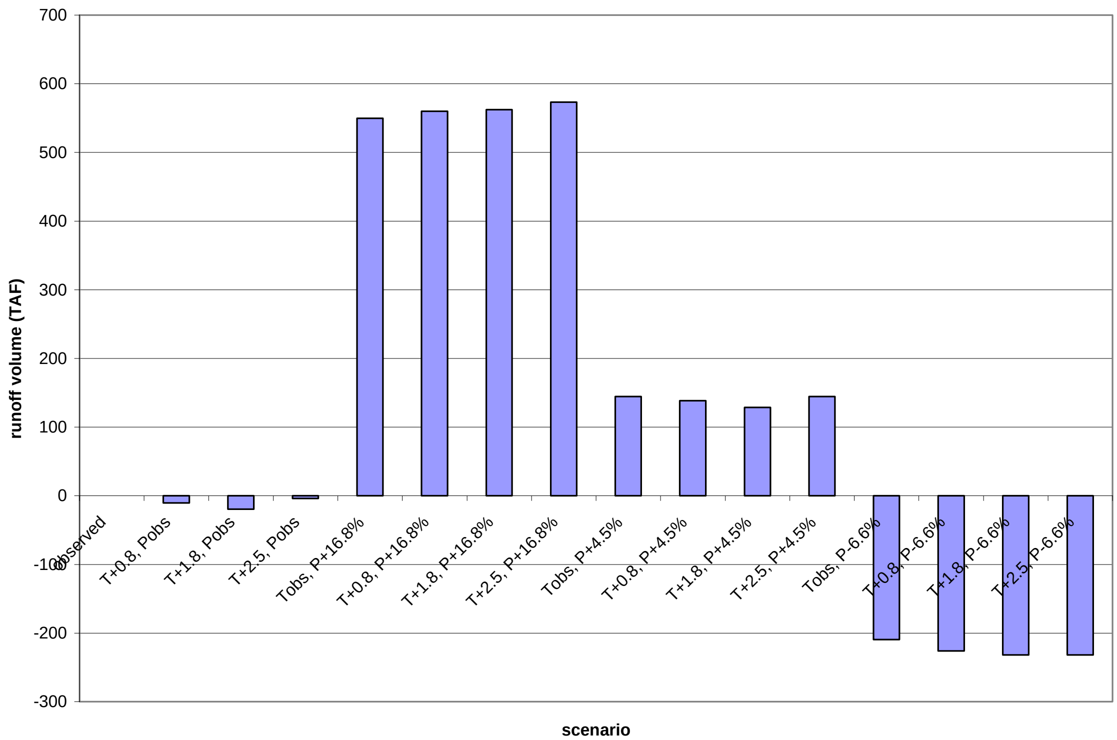


**Figure 106. Changes in runoff volume for the March 1995 snow event.** Little change in inflow volumes are observed due to temperature increases. Large inflow volume changes are due to changes in precipitation intensities.

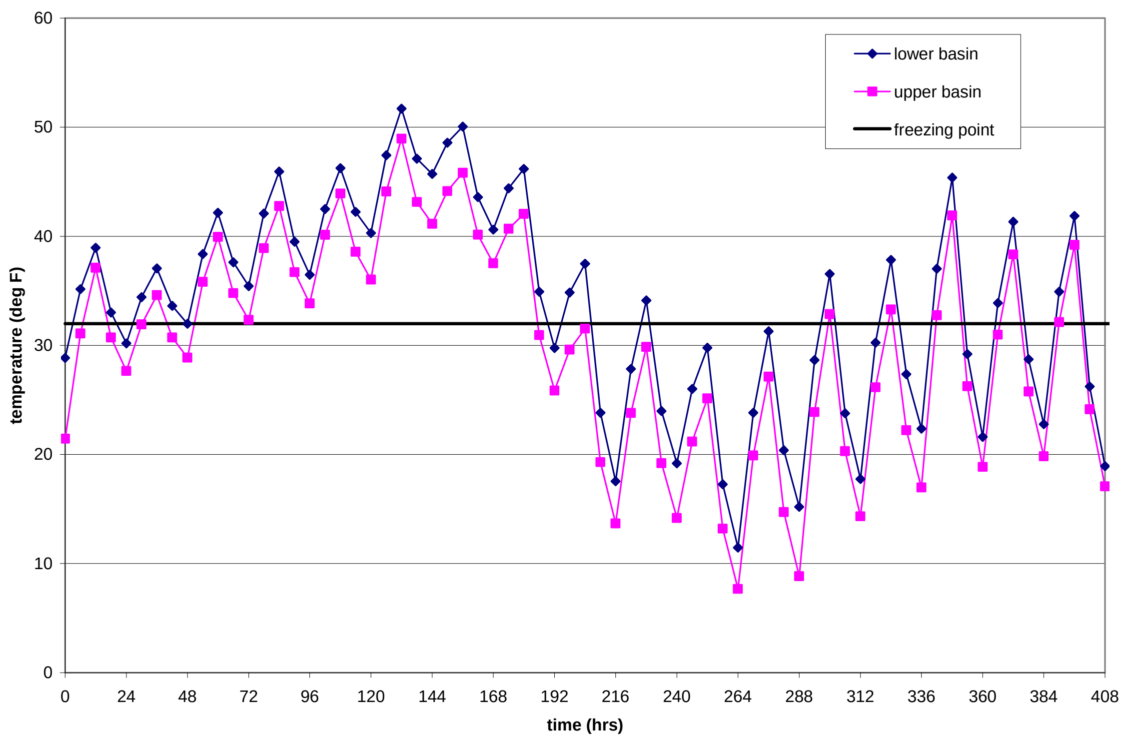


**Figure 107. Temperature trends during the January 1997 event.** Temperatures are well above freezing during the storm event (hours 72-192), indicating that this storm is composed of mostly rain. Increasing the temperature regime does not significantly impact the storm's precipitation composition.

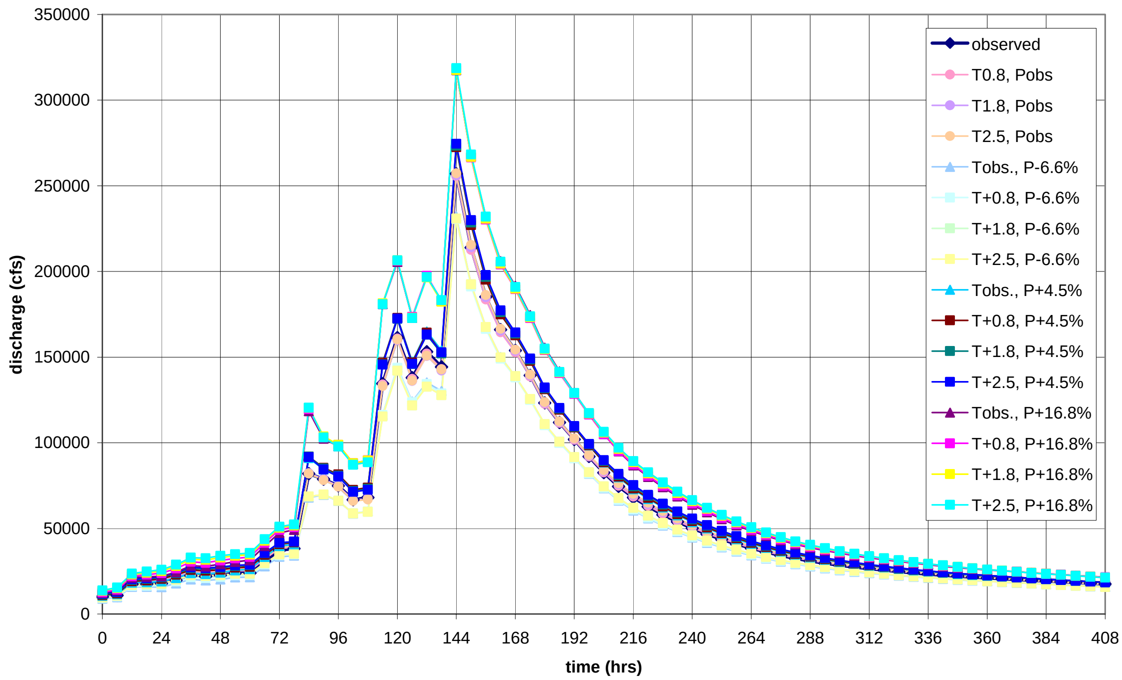


**Figure 108. Climate change inflows for the January 1997 event.** As the observed event is already a rain event, increasing the temperature regime has little effect on the storm's precipitation composition. This is illustrated by the close groupings of climate scenarios that simulate identical precipitation intensities and increasing temperature regimes. Large inflow shifts are due to precipitation intensity changes.

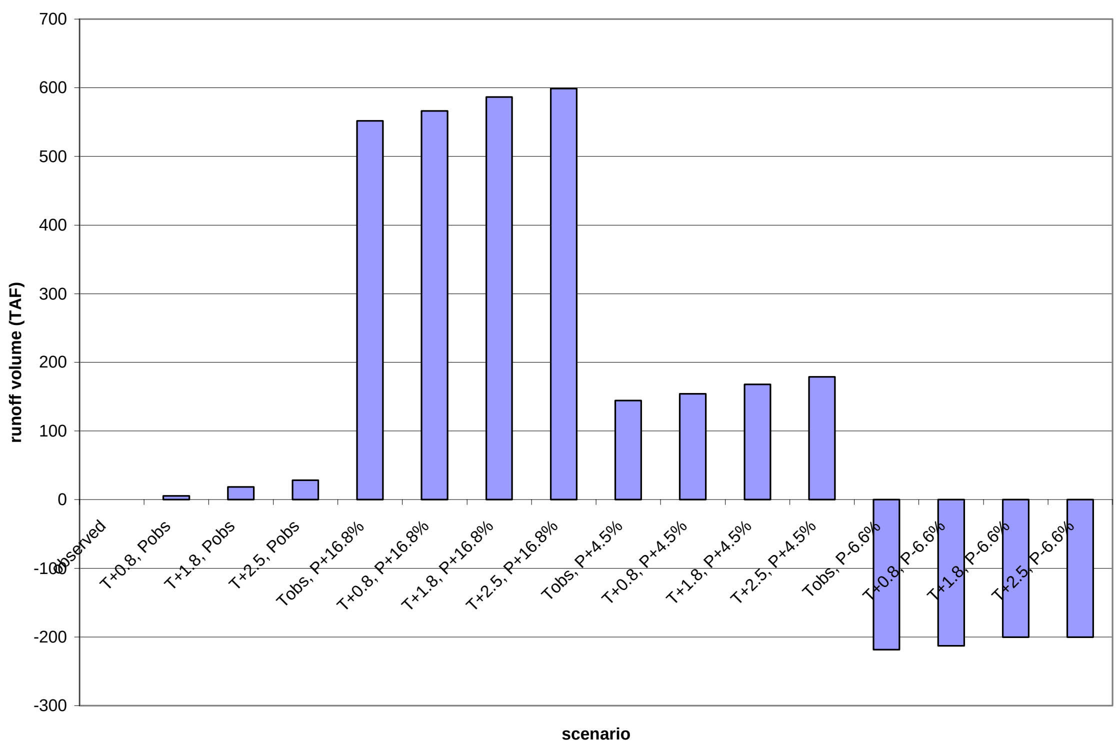


**Figure 109. Changes in runoff volume for the January 1997 rain event.** Inflow volumes do not respond strongly to temperature changes. Basin conditions prior to this storm event are dry, though the previous water year is wet. Large shifts in inflow volumes are due to precipitation intensity changes.

# Appendix D: Reservoir operations results for Shasta, Oroville and New Bullards Bar dams

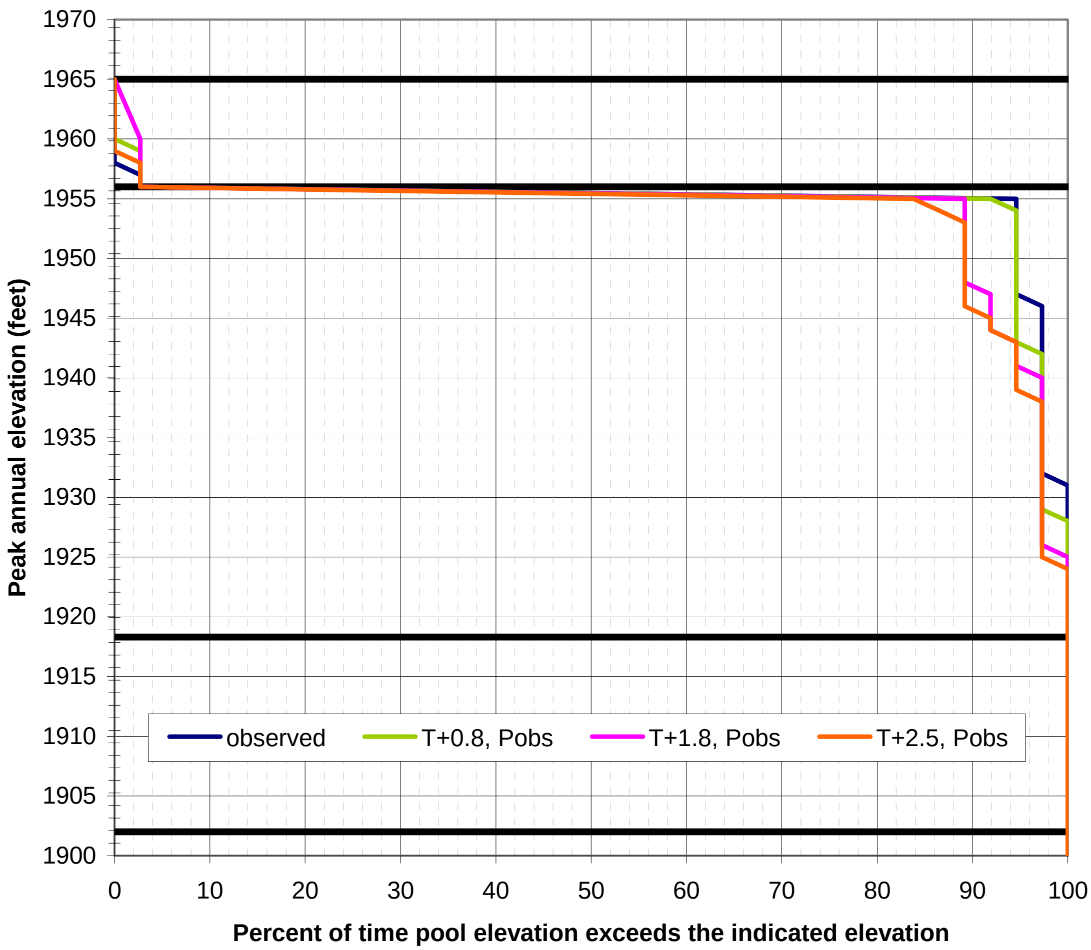


**Figure 110. The reservoir pool elevation exceedence curve for New Bullards Bar Dam given precipitation changes.** As precipitation intensities increase, the curve shifts to the right, indicating that the reservoir pool reaches higher elevations more often. As precipitation intensities decrease, the reservoir pool does not fill to the same elevations as often as when precipitation intensities are higher. The shape of this curve is based on ResSim output and shows that the model performs well at keeping the reservoir pool at elevations defined by the flood control rule curve. Gross pool elevation (1956 ft.) is the target elevation at the end of the flood season. The bottom of the flood control pool between November and April is 1918 ft. With few exceptions, the model can maintain the maximum pool elevation required by the flood control curve.

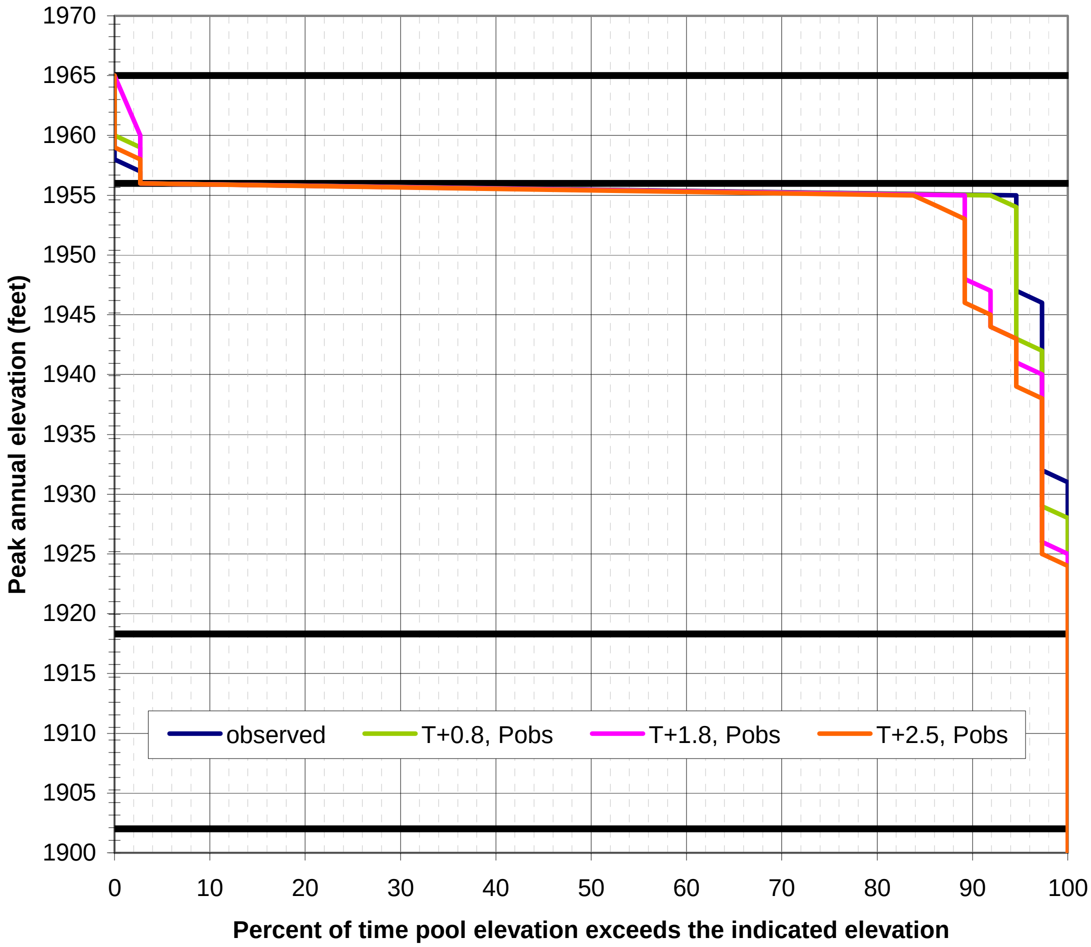


**Figure 111. The reservoir pool elevation exceedence curve for New Bullards Bar Dam given temperature changes.** As temperatures increase, the curve shifts to the left, indicating that the reservoir pool reaches higher elevations less often. As temperatures decrease, the reservoir pool reaches higher elevations more often. The shape of this curve is based on ResSim output and shows that the model performs well at keeping the reservoir pool at elevations defined by the flood control rule curve. Gross pool elevation (1956 ft.) is the target elevation at the end of the flood season. The bottom of the flood control pool between November and April is 1918 ft. With few exceptions, the model can maintain the maximum pool elevation required by the flood control curve.

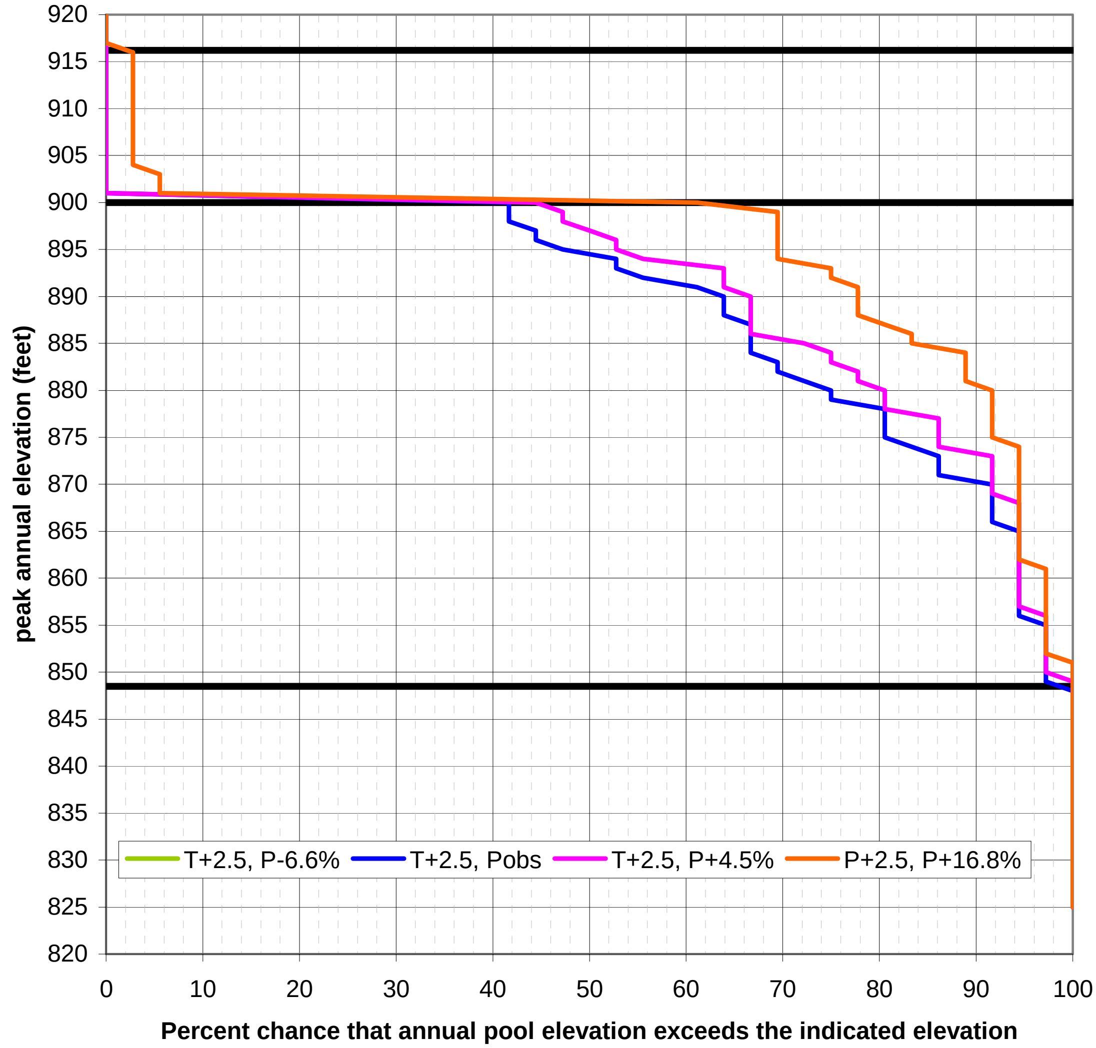


**Figure 112. The reservoir pool elevation exceedence curve for Oroville Dam given precipitation changes.** As precipitation intensities increase, the curve shifts to the right, indicating that the reservoir pool reaches higher elevations more often. As precipitation intensities decrease, the reservoir pool does not fill to the same elevations as often as when precipitation intensities are higher. The shape of this curve is based on ResSim output and shows that the model performs well at keeping the reservoir pool at elevations defined by the flood control rule curve. Gross pool elevation (900.0 ft.) is the target elevation at the end of the flood season. The bottom of the flood control pool between November and April is 848.5 ft. With few exceptions, the model can maintain the maximum pool elevation required by the flood control curve**.**

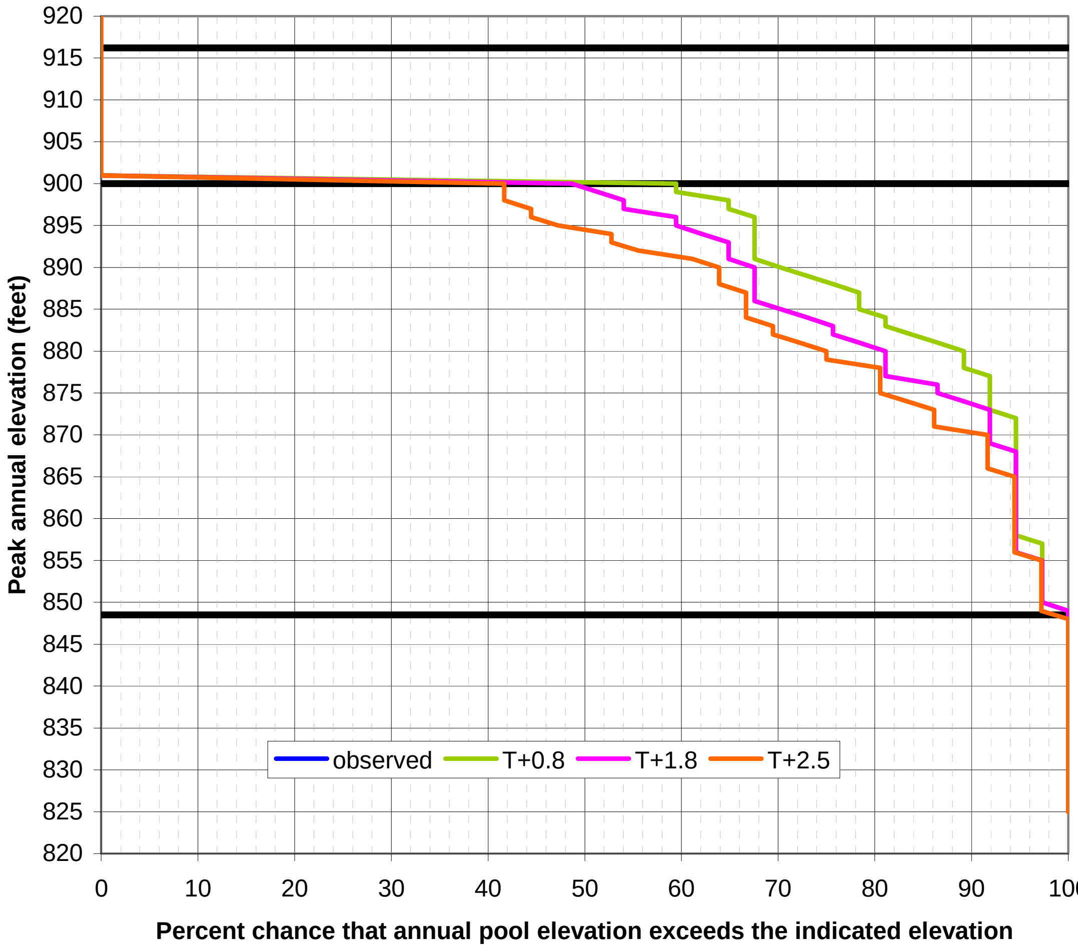


**Figure 113. The reservoir pool elevation exceedence curve for New Bullards Bar Dam given temperature changes.** As temperatures increase, the curve shifts to the left, indicating that the reservoir pool reaches higher elevations less often. As temperatures decrease, the reservoir pool reaches higher elevations more often. The shape of this curve is based on ResSim output and shows that the model performs well at keeping the reservoir pool at elevations defined by the flood control rule curve. Gross pool elevation (900.0 ft.) is the target elevation at the end of the flood season. The bottom of the flood control pool between November and April is 848.5 ft. With few exceptions, the model can maintain the maximum pool elevation required by the flood control curve.

Tables 17-22 identify which reservoir zone the pool peaks in for each flood event and climate scenario. Elevation zones include the buffer, conservation, flood, surcharge pools; top of dam; and overtop. Events during which the reservoir pool peaks above the flood control poll are highlighted.

| Shasta Dam: Zone location of peak pool elevation for sampled flood events, March refill | | | | | | | | |
|---|---|---|---|---|---|---|---|---|
| event | scenario | | | | | | | |
| | observed | TOBS, P-6.6% | TOBS, P+4.5% | TOBS, P+16.8% | T+0.8, P-6.6% | T+0.8, POBS | T+0.8, P+16.8% | T+0.8, P+4.5% |
| Jan-63 | Flood | Flood | Flood | Flood | Flood | Flood | Flood | Flood |
| Dec-64 | Flood | Flood | Flood | Flood | Flood | Flood | Flood | Flood |
| Jan-69 | Flood | Flood | Flood | Flood | Flood | Flood | Flood | Flood |
| Jan-80 | Flood | Flood | Flood | Flood | Flood | Flood | Flood | Flood |
| Dec-82 | Flood | Flood | Flood | Flood | Flood | Flood | Flood | Flood |
| Mar-83 | Flood | Flood | Flood | Flood | Flood | Flood | Flood | Flood |
| Feb-86 | Flood | Flood | Flood | Flood | Flood | Flood | Flood | Flood |
| Mar-95 | Flood | Flood | Flood | Flood | Flood | Flood | Flood | Flood |
| Jan-97 | Flood | Flood | Flood | Flood | Flood | Flood | Flood | Flood |

**Table 17. Location of peak pool elevations for the sampled events in the Shasta Basin.** Scenarios included in this table are the observed temperature regime and T+0.8$^{o}$F regime combined with the observed and perturbed precipitation records.

| Shasta Dam: Zone location of peak pool elevation for sampled flood events, March refill | | | | | | | | |
|---|---|---|---|---|---|---|---|---|
| event | scenario | | | | | | | |
| | T+1.8, P-6.6% | T+1.8, POBS | T+1.8, P+4.5% | T+1.8, P+16.8% | T+2.5, P-6.6% | T+2.5, POBS | T+2.5, P+16.8% | T+2.5, P+4.5% |
| Jan-63 | Flood | Flood | Flood | Flood | Flood | Flood | Flood | Flood |
| Dec-64 | Flood | Flood | Flood | Flood | Flood | Flood | Flood | Flood |
| Jan-69 | Flood | Flood | Flood | Flood | Flood | Flood | Flood | Flood |
| Jan-80 | Flood | Flood | Flood | Flood | Flood | Flood | Flood | Flood |
| Dec-82 | Flood | Flood | Flood | Flood | Flood | Flood | Flood | Flood |
| Mar-83 | Flood | Flood | Flood | Flood | Flood | Flood | Flood | Flood |
| Feb-86 | Flood | Flood | Flood | Flood | Flood | Flood | Flood | Flood |
| Mar-95 | Flood | Flood | Flood | Flood | Flood | Flood | Flood | Flood |
| Jan-97 | Flood | Flood | Flood | Flood | Flood | Flood | Flood | Flood |

**Table 18. Location of peak pool elevations for sampled flood events in the Shasta basin.** Scenarios included in this table are the T+1.8$^{o}$F and T+2.5$^{o}$F temperature regimes combined with the observed and perturbed precipitation records.

| Oroville Dam: Zone location of peak pool elevation for sampled flood events | | | | | | | | |
|---|---|---|---|---|---|---|---|---|
| event | scenario | | | | | | | |
| | observed | TOBS, P-6.6% | TOBS, P+4.5% | TOBS, P+16.8% | T+0.8, P-6.6% | T+0.8, POBS | T+0.8, P+4.5% | T+0.8, P+16.8% |
| Jan-63 | Flood | Flood | Flood | Flood | Flood | Flood | Flood | Flood |
| Dec-64 | Flood | Flood | Flood | Flood | Flood | Flood | Flood | Flood |
| Jan-69 | Flood | Flood | Flood | Flood | Flood | Flood | Flood | Flood |
| Jan-80 | Flood | Flood | Flood | Flood | Flood | Flood | Flood | Flood |
| Dec-82 | Flood | Flood | Flood | Flood | Flood | Flood | Flood | Flood |
| Mar-83 | Flood | Flood | Flood | Flood | Flood | Flood | Flood | Flood |
| Feb-86 | Flood | Flood | Flood | Top of Surcharge | Flood | Flood | Flood | Top of Surcharge |
| Mar-95 | Flood | Flood | Flood | Flood | Flood | Flood | Flood | Flood |
| Jan-97 | Flood | Flood | Flood | Flood | Flood | Flood | Flood | Flood |

**Table 19. Location of peak pool elevations for sampled flood events in the Oroville basin.** Scenarios included in this table are the observed temperature regime and T+0.8°F regime combined with the observed and perturbed precipitation records. Highlighted areas indicate that the peak pool elevation exceeds the flood pool elevation.

| Oroville Dam: Location of peak pool elevation for sampled flood events | | | | | | | | |
|---|---|---|---|---|---|---|---|---|
| event | scenario | | | | | | | |
| | T+1.8, P-6.6% | T+1.8, POBS | T+1.8, P+4.5% | T+1.8, P+16.8% | T+2.5, P-6.6% | T+2.5, POBS | T+2.5, P+4.5% | T+2.5, P+16.8% |
| Jan-63 | Flood | Flood | Flood | Flood | Flood | Flood | Flood | Flood |
| Dec-64 | Flood | Flood | Flood | Flood | Flood | Flood | Flood | Flood |
| Jan-69 | Flood | Flood | Flood | Flood | Flood | Flood | Flood | Flood |
| Jan-80 | Flood | Flood | Flood | Flood | Flood | Flood | Flood | Flood |
| Dec-82 | Flood | Flood | Flood | Flood | Flood | Flood | Flood | Flood |
| Mar-83 | Flood | Flood | Flood | Flood | Flood | Flood | Flood | Flood |
| Feb-86 | Flood | Flood | Flood | Top of Surcharge | Flood | Flood | Top of Surcharge | Top of Surcharge |
| Mar-95 | Flood | Flood | Flood | Flood | Flood | Flood | Flood | Top of Surcharge |
| Jan-97 | Flood | Flood | Flood | Flood | Flood | Flood | Flood | Flood |

**Table 20. Location of peak pool elevations for sampled flood events in the Oroville basin.** Scenarios included in this table are the T+1.8°F and T+2.5°F temperature regimes combined with the observed and perturbed precipitation records. Highlighted areas indication that the peak pool elevation exceeds the flood pool elevation.

| New Bullards Bar Dam: Zone location of peak pool elevation for sampled flood events | | | | | | | | |
|---|---|---|---|---|---|---|---|---|
| event | scenario | | | | | | | |
| | observed | TOBS, P-6.6% | TOBS, P+4.5% | TOBS, P+16.8% | T+0.8, P-6.6% | T+0.8, POBS | T+0.8, P+4.5% | T+0.8, P+16.8% |
| Jan-63 | Flood | Flood | Flood | Flood | Flood | Flood | Flood | Flood |
| Dec-64 | Top of Surcharge | Flood | Top of Dam | Overtop | Flood | Top of Dam | Overtop | Overtop |
| Jan-69 | Flood | Flood | Flood | Flood | Flood | Flood | Flood | Flood |
| Jan-80 | Flood | Flood | Flood | Flood | Flood | Flood | Flood | Flood |
| Dec-82 | Flood | Flood | Flood | Flood | Flood | Flood | Flood | Flood |
| Mar-83 | Flood | Flood | Flood | Flood | Flood | Flood | Flood | Flood |
| Feb-86 | Flood | Flood | Flood | Flood | Flood | Flood | Flood | Flood |
| Mar-95 | Flood | Flood | Flood | Flood | Flood | Flood | Flood | Flood |
| Jan-97 | Flood | Flood | Flood | Top of Dam | Flood | Flood | Top of Surcharge | Top of Dam |

**Table 21. Location of peak pool elevations for sampled flood events in the New Bullards Bar basin.** Scenarios included in this table are the observed temperature regime and T+0.8°F regime combined with the observed and perturbed precipitation records. Highlighted areas indicate that the peak pool elevation exceeds the flood pool elevation.

| New Bullards Bar Dam: Zone location of peak pool elevation for sampled flood events | | | | | | | | |
|---|---|---|---|---|---|---|---|---|
| event | scenario | | | | | | | |
| | T+1.8, P-6.6% | T+1.8, POBS | T+1.8, P+4.5% | T+1.8, P+16.8% | T+2.5, P-6.6% | T+2.5, POBS | T+2.5, P+4.5% | T+2.5, P+16.8% |
| Jan-63 | Flood | Flood | Flood | Flood | Flood | Flood | Flood | Flood |
| Dec-64 | Flood | Top of Dam | Overtop | Overtop | Flood | Top of Surcharge | Overtop | Overtop |
| Jan-69 | Flood | Flood | Flood | Flood | Flood | Flood | Flood | Flood |
| Jan-80 | Flood | Flood | Flood | Flood | Flood | Flood | Flood | Flood |
| Dec-82 | Flood | Flood | Flood | Flood | Flood | Flood | Flood | Flood |
| Mar-83 | Flood | Flood | Flood | Flood | Flood | Flood | Flood | Flood |
| Feb-86 | Flood | Flood | Flood | Top of Dam | Flood | Flood | Flood | Overtop |
| Mar-95 | Flood | Flood | Flood | Flood | Flood | Flood | Flood | Flood |
| Jan-97 | Flood | Flood | Top of Surcharge | Overtop | Flood | Flood | Top of Surcharge | Top of Dam |

**Table 22. Location of peak pool elevations for sampled flood events in the New Bullards Bar basin.** Scenarios included in this table are the T+1.8°F and T+2.5°F temperature regimes combined with the observed and perturbed precipitation records. Highlighted areas indicate that the peak pool elevation exceeds the flood pool elevation.